Conceptual Design of a HMF Process

A comparison between TBP and MIBK as organic solvents for Reactive Extraction

J.W. Keizers

Transport Phenomena
Applied Sciences

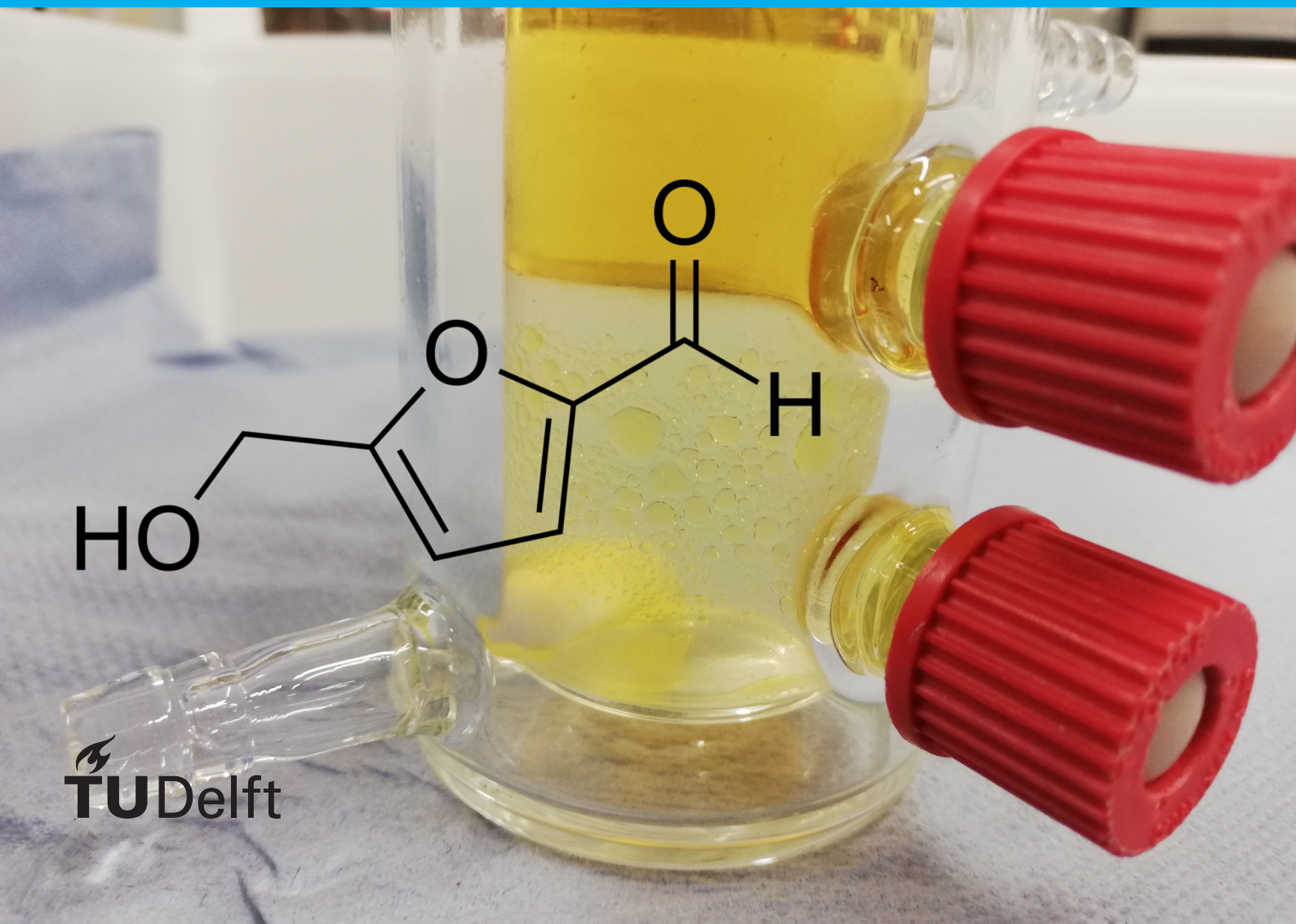

TU Delft

Conceptual Design of a HMF Process

A comparison between TBP and MIBK as organic solvents for Reactive Extraction

by

J.W. Keizers

to obtain the degree of
MSc Chemical Engineering
at the Delft University of Technology.

To be defended publicly on
Friday January 31, 2020 at 09:30 AM.

Faculty of Applied Sciences
Department of Chemical Engineering
Section of Transport Phenomena

Student number: 4385284
Project duration: February 4, 2019 – January 31, 2020
Thesis committee:
Prof. dr. ir. A. B. de Haan, TU Delft (AS), supervisor
Prof. dr. A. E. D. M. van der Heijden, TU Delft (3mE)
Dr. A. J. J. Straathof, TU Delft (AS)

TU Delft

Preface

During a project, there are always going to be ups and downs. One day you make a calculation and you feel like you are on top of the world, only to realize the next morning that you forgot to include an effect somewhere. I would like to thank André de Haan for always having a positive attitude during meetings and providing me with the very welcome perspectives, reminding me to see the bigger picture when I got stuck in my own models. I would also like Saidah Altway, for providing all the data to base this project upon and for her support along the way.

On a certain occasion, while preparing for experimental work, the analysis equipment decided not to cooperate, but instead go for an early retirement. The following weeks I had the opportunity to improve my fitness, by cycling between Applied Sciences and 3mE on a daily basis to ask Michel van den Brink for updates on the HPLC an GC. I would like to thank him for his patience, and hope that the new equipment will perform as expected. In the end, this malfunction did switch the focus to the creation of a process design model, which I am proud to present to anyone interested.

On a personal note, I would like to thank my girlfriend, Ciska, my parents, Huub and Mary, my brothers, Hidde and Tijme, my room mates, Mark and Nick, and my other friends for trying to understand what was going on in my life for almost a year, as well as supporting me even if they did not understand the issues I was having.

J.W. Keizers
Delft, January 2020

Abstract

5-hydroxymethylfurfural (HMF) is a versatile renewable base chemical, which can be produced by the acid-catalyzed dehydration of fructose. At this time HMF cannot yet compete with oil-based analogues, such as p-xylene, due to the high costs of production. Future incentives to encourage the transition to a bio-based economy may increase the feasibility of investing in a HMF production process, but only if an efficient and cost-effective production method is designed. Previous research showed promising results using a reactive extraction unit. However, the selection of the organic solvent has a large influence on both the overall yield, as well as on the energy requirements in the final recovery of the HMF in a subsequent separation step. In this work, an intrinsically better, but hard to separate solvent, tri-butyl phosphate (TBP), was compared to methyl isobutyl ketone (MIBK), a solvent which is easy to separate from the HMF by distillation. The chosen method of separation for the TBP-HMF reaction mixture is back-extraction, using an anti-solvent to transfer the HMF back to an aqueous phase. By using back-extraction, it was possible to lower the energy (steam) requirements of a TBP-based process under the benchmark calculated for a MIBK-based process by 18%. A drawback of the TBP-based process is its increased complexity, leading to higher capital costs. A model was developed to assess the balance between reduced steam demands and increased capital and operational costs. It was found that even if an optimistic scenario for the effectiveness of the anti-solvent was used, the MIBK-based process was superior across nearly all key performance indicators. Most indicative of the relative feasibility is the minimum selling price of HMF (at a production of 20 kton/year), which is €1.85/kg or €1.64/kg, for a TBP- and MIBK-based process respectively. The only area where the TBP-based process performs slightly better is sustainability, with calculated emissions of 1.90 $kgCO_2eq/kg$ HMF compared to 1.97 $kgCO_2eq/kg$ HMF for a MIBK-based process.

Nomenclature

Symbols

[]	Concentration	M
ΔH_{vap}	Heat of vaporization	$\frac{kJ}{kg}$
ρ	Density	$\frac{kg}{m^3}$
τ	Non-dimensional residence time	–
C	Cost	€
D_i	Distribution coefficient of component i	–
E	Energy	J
F	Factor	–
m	Mass	kg
N	Number of stages	–
P	Pressure	bar
Q	Production rate	$\frac{kton}{year}$
S	Selectivity	–
S	Separation factor	–
SF_{ratio}	Solvent-to-feed ratio	–
T	Temperature	$^{\circ}C$
t	Time	s
T_{boil}	Boiling temperature	$^{\circ}C$
X	Conversion	–
x	Mass fraction	–
Y	Yield	–

Abbreviations

ACM	Aspen custom modeler
$CAPEX$	Capital expenditure
CCF	Cumulative cash flow
$CEPCI$	Chemical engineering plant cost index
$DCCF$	Discounted cumulative cash flow
DPI	Direct permanent investment
$EUETS$	European Union emissions trading system

GHG	Greenhouse gas
HMF	5-Hydroxymethyl furfural
$ISBL$	Inside battery limit
KPI	Key performance indicator
LCA	Life cycle analysis
$MIBK$	Methyl isobutyl ketone
MS	Marshall and Swift
MSP	Minimum selling price
$OPEX$	Operational expenditure
$OSBL$	Outside battery limit
PBT	Pay-back time
RE	Reactive extraction
ROI	Return on investment
SHE	Safety, health and environment
TBM	Total bare module
TBP	Tri-butyl phosphate
TPI	Total permanent investment

Contents

1

Introduction

5-hydroxymethylfurfural (HMF) is widely described as a versatile renewable (*green*) base chemical ([1],[2],[3],[4],[5]). As with every chemical, an efficient and cost-effective production method is needed to realize the full potential of HMF. HMF can be produced by the acid-catalyzed dehydration of fructose, using water as a reaction medium.

$$\underset{\text{Fructose}}{C_6H_{12}O_6} \xrightarrow[-3\ H_2O]{H^+} \underset{\text{HMF}}{C_6H_6O_3}$$

However, by-products (most notably humins, levulinic acid and formic acid) tend to be formed irreversibly in an aqueous environment, which is highly undesirable ([1],[3]). To mitigate this problem, the HMF can be simultaneously extracted (using an organic solvent) from the reaction medium, in a reactive extraction unit (schematically shown in Figure 1.1).

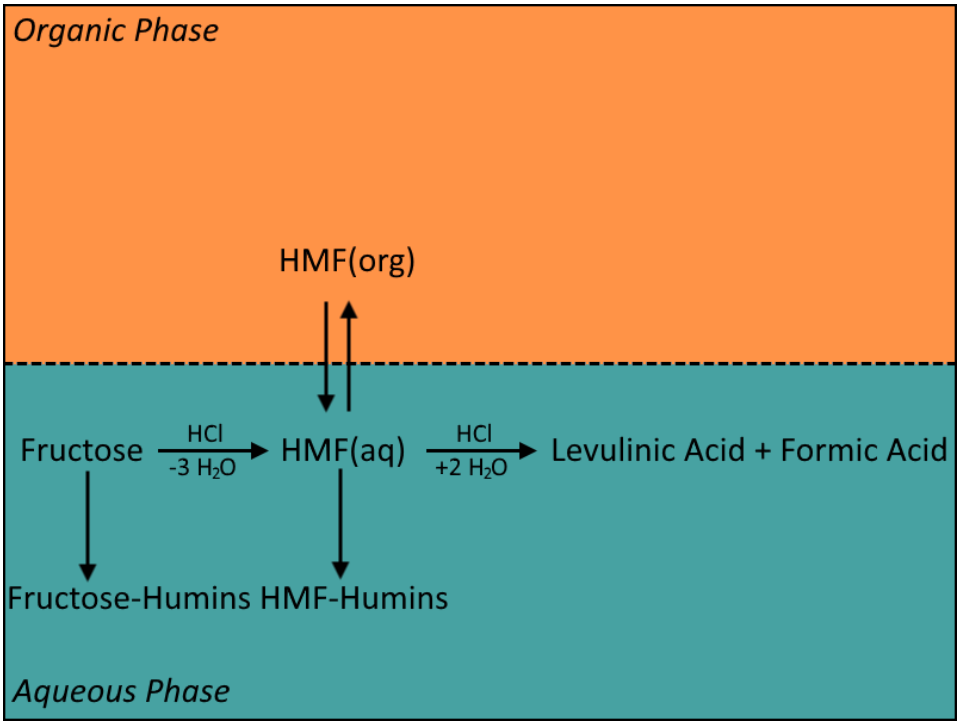

Figure 1.1: Schematic overview of HMF production using reactive extraction, where HMF is transferred to the organic phase after reaction according to the favourable equilibrium. By using reactive extraction, higher yields can be achieved by the prevention of excessive by-product formation.

Previous conceptual design studies at the TU Delft, by Matteo Ottocento [6], Rahul Ravindran [7] and Niels van den Burg [8] indicated that reactive extraction using either MIBK (methyl isobutyl ketone) or 2-pentanol (Figure 1.2) could provide a viable option, although both have their respective drawbacks. Following reactive extraction with MIBK or 2-pentanol, the organic solvent-HMF mixture can be separated without too much difficulty using distillation.

More recent experimental research by Saidah Altway, suggests that using TBP (tri-butyl phosphate, Figure 1.2) as the organic solvent may be an interesting option, as TBP has superior extraction properties to both MIBK and 2-pentanol in terms of selectivity and HMF distribution coefficient ([9], Appendix A). The experimental data on the liquid-liquid equilibria of the different organic solvents in the biphasic reaction system for HMF production provided by Saidah forms the foundation on which to model the extraction of HMF, which is needed to obtain a quantitative model on which process-related and economic decisions can be based.

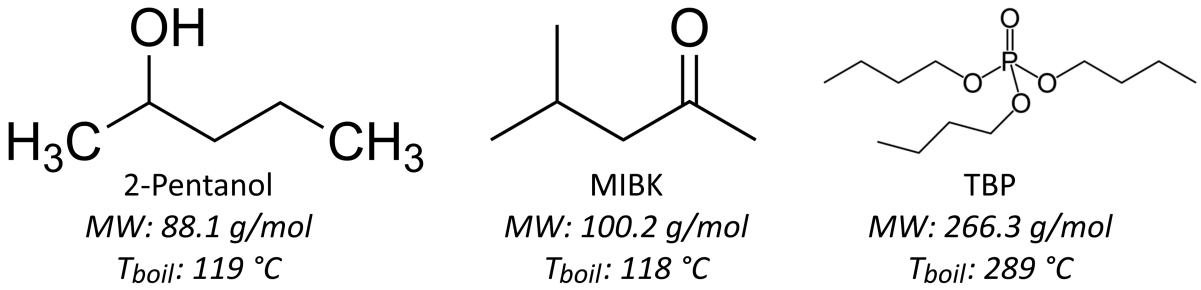

Figure 1.2: Structure formulas, molecular mass and normal boiling points of the solvents under investigation.

The drawback of TBP is that the low volatility prevents the use of distillation as a viable option for the separation of the final product. Therefore, in order to make use of the superior extraction properties of TBP, a separation system, including the recovery (recycle) of TBP and the production of HMF at the required purity, has to be designed and evaluated.

1.1. Research goals

The main objective of the project is to find the most viable method of producing HMF by making use of reactive extraction and an adequate solvent recovery system. An important assumption in this project formulation is that a process (for HMF production) based on reactive extraction will always perform better overall than a process in which reaction and extraction are carried out in individual units. A main interest is, to see whether it is more economically feasible to use a intrinsically better extractive solvent (TBP), which cannot be recovered through distillation under standard conditions or a solvent (MIBK or 2-pentanol) with lower performance indicators (selectivity and distribution coefficient), which can easily be recovered by distillation. Currently, three main knowledge gaps can be identified:

1. The ideal operating conditions for reactive extraction unit using TBP.
2. The benchmark figures for a distillation based recovery system for a process using MIBK or 2-pentanol.
3. The ideal recovery structure for a HMF process using TBP.

In the context of this project *ideal* describes the optimal economic performance of a system.

To fill gaps in the current knowledge, the previous models, developed by M. Ottocento [6], for reactive extraction will be adjusted to gain insight in the ideal operating conditions using TBP as the organic phase. This will be done by adjusting the appropriate parameters such as the selectivity and distribution coefficients as found by experimental work on the liquid-liquid equilibria. The operating conditions will then be selected and compared to the previous work, to ensure reproducability before continuing the project.

The benchmark figures for a distillation recovery system for a process using a volatile organic solvent (such as MIBK) will be analyzed on a conceptual basis, resulting in simple calculations with reasonable accuracy.

The design of an effective and efficient recovery structure for a TBP-HMF mixture requires multiple aspects. Initially, a simple back-extraction method is explored. Throughout the research, this idea will be built upon step-by-step to reduce the energy demands of a TBP based process below the benchmark figures for a MIBK based process, before continuing to the final phase of the project, where the two options are evaluated in their totality.

Once the most optimal process configuration is found for both a process using TBP and a process using a volatile organic solvent a cost estimation will be performed to compare both options (both initial investment (CAPEX) and operational cost (OPEX)). An estimation will be made for the minimum selling price of HMF and compared between the different process option to assess feasibility.

At the end of the project, knowledge has been gained on the ideal operating conditions and unit operations for a HMF production process using either TBP or MIBK as an organic solvent. More specifically, the assessment will enable a verdict on the feasibility of such processes and put forward a recommendation based on documented decision-making, conceptual calculations and process simulations in combination with systematic financial estimations. The focus of this assessment will ultimately be a balancing act of the reduced utility demands of using a better solvent versus the increased process complexity of using a non-volatile organic solvent.

To conclude, the essence of this research project can be captured by the following sentence:

"A systematic comparison, on a basis of economics and sustainability, between TBP and MIBK as an organic solvent for a process using reactive extraction to produce HMF."

2

Optimization

The first research goal: to find the ideal operating conditions for the reactive extraction (RE) unit, was targeted by optimization of model variables to meet specifications. To provide insight in the optimization of the RE unit previously modeled in Aspen Custom Modeler (ACM) by Matteo Ottocento (adapted ACM code given in Appendix B), seven key concepts will first be discussed. Secondly, the methodology is set out. Lastly, results are presented and discussed.

2.1. Concepts

Solvent characteristics

Key concepts to understand in the assessment of solvent characteristics are: solvent-to-feed ratio, distribution coefficients and separation factors.

Solvent-to-feed ratio (Equation 2.1) is a term to describe the relative amount of organic solvent needed compared to the aqueous feed in order to obtain the specified performance. As more solvent increases energy requirement during separation, a low SF_{ratio} is wanted.

$$SF_{ratio} = \frac{m_{org,in}}{m_{aq,in}} \tag{2.1}$$

The distribution coefficient of compound i, is given by Equation 2.2. A higher value indicates a higher ratio of a compound in the organic phase compared to the aqueous phase. In the context of solvent selection for a HMF process, a high D_{HMF} is desirable, as this will decrease the required SF_{ratio}

$$D_i = \frac{w_i^{Org}}{w_i^{H2O}} \tag{2.2}$$

An ideal solvent selectively extracts HMF from the aqueous phase. In reality, solvents are not perfectly selective, and a small amount of water will be co-extracted with the HMF. This is undesirable, since this additional water will have to be removed in following separation steps, increasing the energy demands of the process. The extent to which a solvent is able to selectively extract HMF is given by the separation factor (S) of the organic solvent (Equation 2.3), the ratio of the distribution factors of HMF and water.

$$S = \frac{D_{HMF}}{D_{H2O}} \tag{2.3}$$

Unit performance

Different solvent characteristics lead to varying performance in the reactive extraction unit. Key concepts to understand in the assessment of the unit performance are: conversion, selectivity and yield.

Conversion (X) is the measure for how much fructose has reacted, expressed as the ratio of reacted

fructose and total fructose before the reaction was started (Equation 2.4). A high conversion is often desirable, unless this strongly interferes with selectivity.

$$X = \frac{Fructose_{Reacted}}{Fructose_{Total}} \tag{2.4}$$

The selectivity (S, Equations 2.5-2.8) is an indication of the fraction of fructose which gets converted to the desired product. The overall selectivity for fructose to HMF is given by,

$$S = \frac{HMF_{Out}}{HMF_{Theoretical}} \tag{2.5}$$

Here, $HMF_{Theoretical}$ is the maximum amount of HMF which could be formed, if all converted fructose forms HMF. As multiple reactions occur within the system, a selectivity is also introduced for the dehydration of the fructose to HMF and for the degradation of HMF.

$$S_{Dehydration} = \frac{HMF_{Produced}}{HMF_{Theoretical}} \tag{2.6}$$

$$S_{HMF} = \frac{HMF_{Out}}{HMF_{Produced}} \tag{2.7}$$

Note that $HMF_{Out} \leq HMF_{Produced}$, as the HMF partially gets converted to by-products before being extracted to the organic phase. Naturally, since the overall selectivity is comprised of these two individual factors, it can also be expressed by,

$$S = S_{Dehydration} S_{HMF} \tag{2.8}$$

The final performance indicator is the yield (Y), which is used to compare the final amount of HMF leaving the reactive extraction unit to the theoretical maximum amount of HMF which could be formed (Equations 2.9 and 2.10).

$$Y = \frac{HMF_{Out}}{HMF_{Theoretical}} \tag{2.9}$$

This equation looks very similar to Equation 2.5 for selectivity, however, this time the value $HMF_{Theoretical}$ is computed for all fructose in the system instead of only the reacted fraction of fructose. The yield is a result of the amount of fructose converted and the selectivity of the conversion of the fructose and can, therefore, also be expressed by,

$$Y = XS \tag{2.10}$$

Residence time

Residence time, defined as the average time a molecule stays in the reactive extraction unit can be used to compare different configurations. However, this is not very useful, as temperature and catalyst concentration both enormously affect the reaction rate. Therefore, it is more useful to use a residence time expressed in units of the characteristic time of reaction.The characteristic time of reaction, defined as the time at given conditions (temperature and catalyst concentration) at which the concentration of HMF reaches a maximum value in the reaction mixture, can aid in selecting the proper residence time in the RE unit. Therefore, it is useful to compute these values in the possible operational range. Characteristic times of reaction were computed for temperatures between 80 and 200°C, at 20°C intervals and catalyst concentrations between 0.5 and 2 mol/L HCl, at 0.25 mol/L intervals. The results are presented in Table 2.1. These values are used for the analysis in Section 2.3.

Table 2.1: Characteristic times of reaction, given in minutes, for a wide range of temperatures and catalyst concentrations.

T (°C) \ [HCl] (M)	0.5	0.75	1	1.25	1.5	1.75	2
80	1.28E+03	6.85E+02	4.38E+02	3.09E+02	2.31E+02	1.81E+02	1.48E+02
100	1.35E+02	7.16E+01	4.53E+01	3.17E+01	2.39E+01	1.87E+01	1.52E+01
120	1.68E+01	8.82E+00	5.53E+00	3.90E+00	2.92E+00	2.28E+00	1.84E+00
140	2.43E+00	1.27E+00	7.98E-01	5.56E-01	4.13E-01	3.21E-01	2.59E-01
160	4.05E-01	2.08E-01	1.31E-01	9.11E-02	6.76E-02	5.25E-02	4.22E-02
180	7.55E-02	3.82E-02	2.36E-02	1.79E-02	1.32E-02	1.01E-02	8.05E-03
200	1.66E-02	8.37E-03	5.14E-03	3.52E-03	2.58E-03	1.99E-03	1.73E-03

2.2. Methodology

Table 2.2: Process variables.

Parameter	Variable type	Lower boundary	Upper boundary	Note
S/F ratio	Fixed	1	15	Minimize
τ (s)	Fixed	-	-	-
$C_{Fructose,0}$ (M)	Fixed	0.37	1	Validity range
$C_{HCl,0}$ (M)	Fixed	0.045	2	Validity range
T (°C)	Fixed	88	140	Validity range
P (bar)	Free	-	-	Safety
N_{Stages}	Fixed	-	-	Minimize
Conversion	Free	-	1	Maximize
$S_{reaction}$	Free	0.9	1	Requirement[1]
$S_{Dehydration}$	Free	-	1	Maximize
S_{HMF}	Free	-	1	Maximize
Yield	Free	0.85	1	Requirement
$w_{H_2O}^{Org}$	Free	0	1	Minimize

[1] It will be shown in the Analysis subsection that this requirement cannot be met realistically, yield will be the main performance indicator of the system.

Since this optimization problem has many variables and equations describing the system, an attempt to solve the problem analytically has not proven to be an effective approach. However, this problem lends itself perfectly to an informed decision, after considering all the individual effects of parameter changes, which is what was focused on during the initial stage of the project. The set requirements and evaluated process parameters are given in Table 2.2. The main differences between the three solvents are the distribution coefficient and separation factor. Average values (experimentally determined by Saidah Altway) were used and are given in Table 2.3.

Table 2.3: Solvent characteristics.

	TBP	MIBK	2-pentanol
$\overline{D_{HMF}}$	3.15	2.16	2.45
$\overline{S}$	53.31	55.03	21.28

The evaluated parameters in the model are independent of the feed flow rate, since the volume is set as a free variable and the system is at equilibrium at all times. Nevertheless, an estimate for the feed flow rate was made, to increase the resemblance with the final process and to hopefully prevent any computational (convergence) problems at a later stage. This estimate is based on an annual HMF production of 20 kton at 8000 operational hours.

$$\phi_{n,Fructose} = \frac{m_{HMF,Out}}{M_{HMF} t_{operational} Yield} \tag{2.11}$$

$$\phi_{n,Fructose} = 2.3 \cdot 10^4 \frac{mol}{hour} \tag{2.12}$$

$$\phi_{m,Feed} = \frac{\phi_{n,Fructose} \cdot \rho_{Feed}}{C_{Fructose,Feed} \cdot 10^3} \tag{2.13}$$

$$\rho_{Feed} \approx \rho_{H_2O} = 1 \cdot 10^3 \frac{kg}{m^3} \tag{2.14}$$

$$C_{Fructose,Feed} = 0.5M \tag{2.15}$$

$$\phi_{m,Feed} = 4.6 \cdot 10^4 \frac{kg}{hour} \tag{2.16}$$

2.3. Results and discussion

Residence time

As can be expected conversion increases with residence time, as the reaction mixture can simply react for a longer period of time. This positively influences the amount of fructose which is dehydrated to HMF. An opposite effect is seen for the HMF selectivity, as the HMF has more time to degrade at longer residence times. These competing effects, result in a optimal residence time in which the function of conversion and overall selectivity attains its maximum value. This optimal residence time was determined empirically,

$$\tau_{Optimum} = \frac{5}{8} t_{characteristic} \tag{2.17}$$

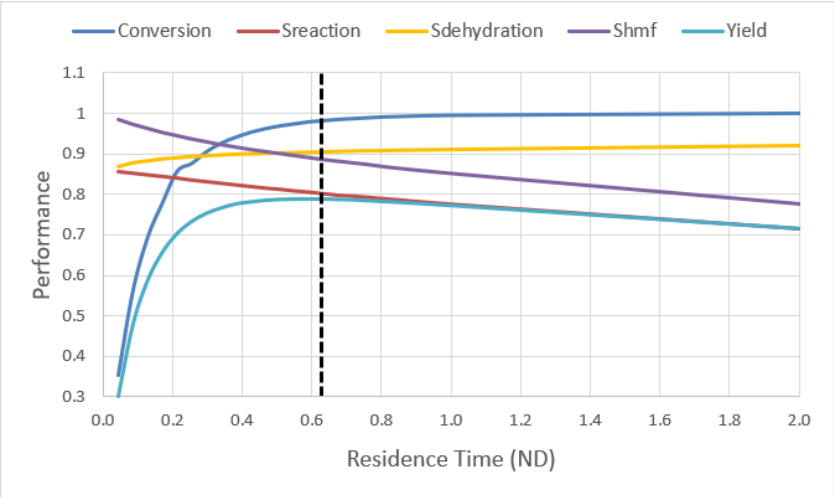

Figure 2.1: RE unit performance at different residence times, made non-dimensional using the characteristic time of reaction ($t_{characteristic}$). $S/F = 2$, $C_{Fructose,0} = 0.5M$, $T = 140°C$, $C_{HCl,0} = 0.5M$, $N_{Stages} = 5$.

This value can be visually confirmed by examining Figure 2.1. In the final process design, recycle of unreacted fructose is also considered. Therefore, it might be beneficial to operate at a lower residence time, as overall conversion is higher than single-pass conversion.

Catalyst (HCl) concentration

At first glance from Figure 2.2 it seems that a high HCl concentration is better across the board for all performance indicators. While this is theoretically true, it does not show any drawbacks for using a more corrosive reactive medium. At this point the use of a high catalyst concentration can unfortunately not been pushed aside for that qualitative line of reasoning, especially since it will otherwise be nearly impossible to fulfill the requirements of the current project within the validity limits of the system.

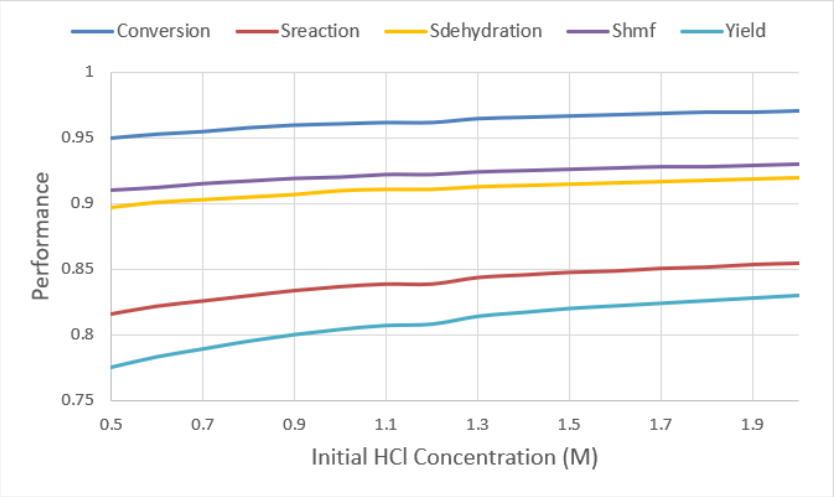

Figure 2.2: RE unit performance as a function of $C_{HCl,0}$. $S/F = 2$, $C_{Fructose,0} = 0.5M$, $T = 140°C$, $\tau = 0.5t_{characteristic}$, $N_{Stages} = 5$.

To further study the effect of catalyst concentration, temperature was set constant (140°C). The results are shown in Figure 2.3. As previously known, higher catalyst concentration leads to a decrease in minimum S/F ratio. What this new analysis does show, is that the optimum residence time is not constant (as previously assumed), but is correlated with the inverse catalyst concentration, as indicated by the white dashed line in Figure 2.4. It also unveils that operations need to be carried out at high ($[HCl] > 1.75M$) catalyst concentrations to achieve feasible S/F ratios (indicated by red dashed outline in Figure 2.4).

Temperature

To study the effect of temperature, catalyst concentration was set constant ($2M$). The results are shown in Figure 2.5. As expected, operating at higher temperatures decrease the minimum S/F ratio required. Interesting to note is that residence time does not seem to influence the S/F ratio greatly across the full temperature range, as can be seen clearly in Figure 2.6. Initially, at low residence times (red dashed region), conversion is the main limiting factor, although at high temperatures this already results in a very decent S/F ratio. In the second region (green dashed), selectivity is still high, while conversion increases steadily. In the last region (blue dashed), selectivity is decreasing while conversion eventually reaches the maximum value. Considering that the final design may very well incorporate a recycle to reduce the importance of single-pass conversion, while reducing by-product formation will always be a priority, lower residence times are preferred over higher residence times at all temperatures.

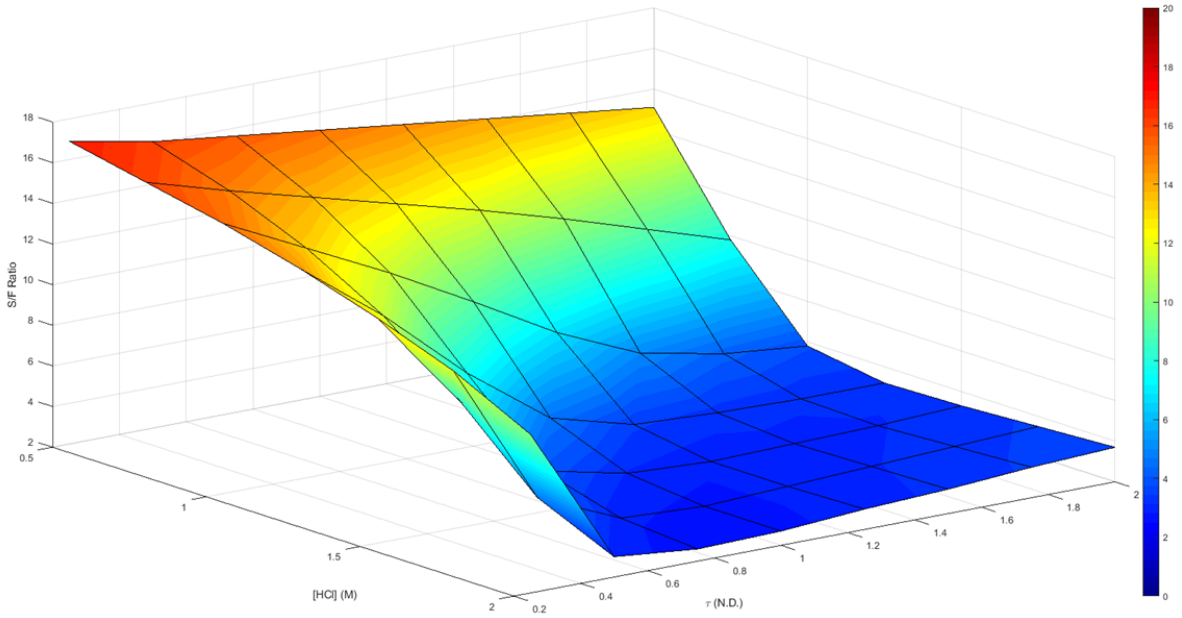

Figure 2.3: S/F ratio (water saturated TBP as organic phase) at 85% yield and specified temperature of 140°C. Manipulated variables: catalyst concentration and non-dimensional residence time. 3-D plot.

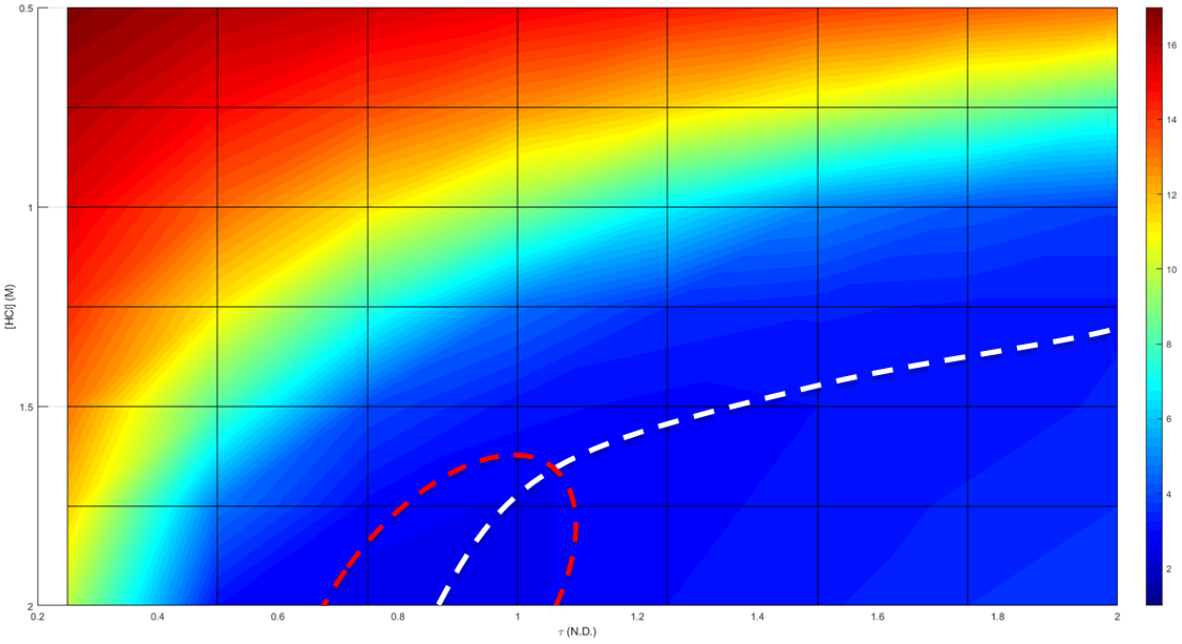

Figure 2.4: S/F ratio (water saturated TBP as organic phase) at 85% yield and specified temperature of 140°C. Manipulated variables: catalyst concentration and non-dimensional residence time. 2-D plot ($\tau, [HCl]$-plane). Minima are found along the dashed white line, while the feasible region is indicated by the red dashed outline.

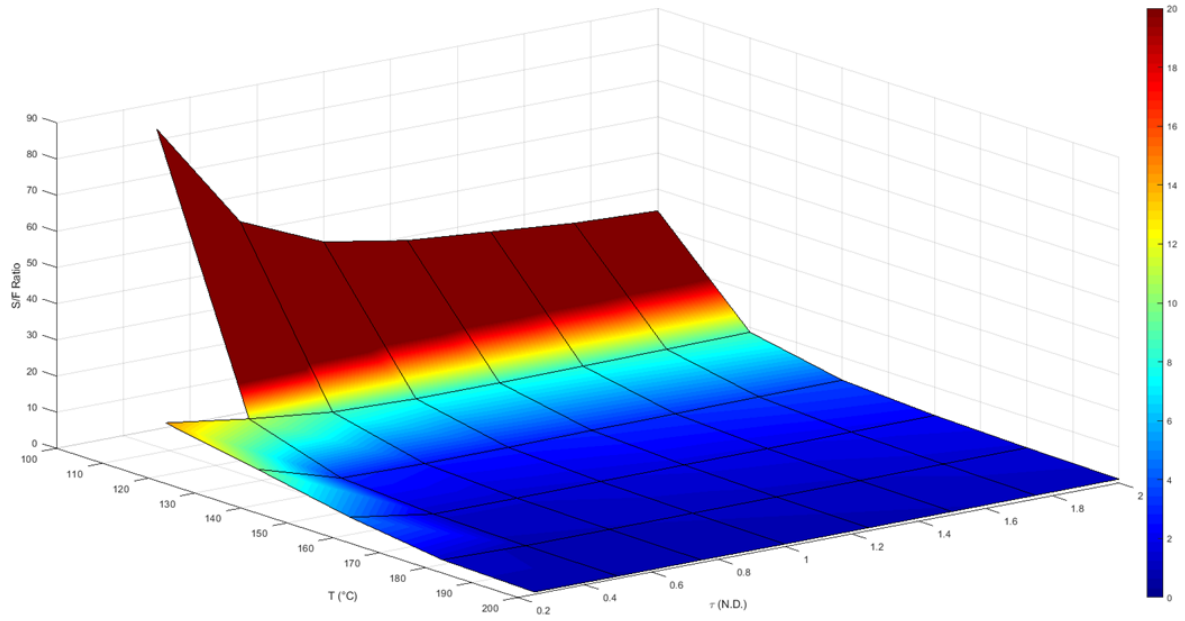

Figure 2.5: S/F ratio (water saturated TBP as organic phase) at 85% yield and specified catalyst concentration of $2M$. Manipulated variables: temperature and non-dimensional residence time. 3-D plot.

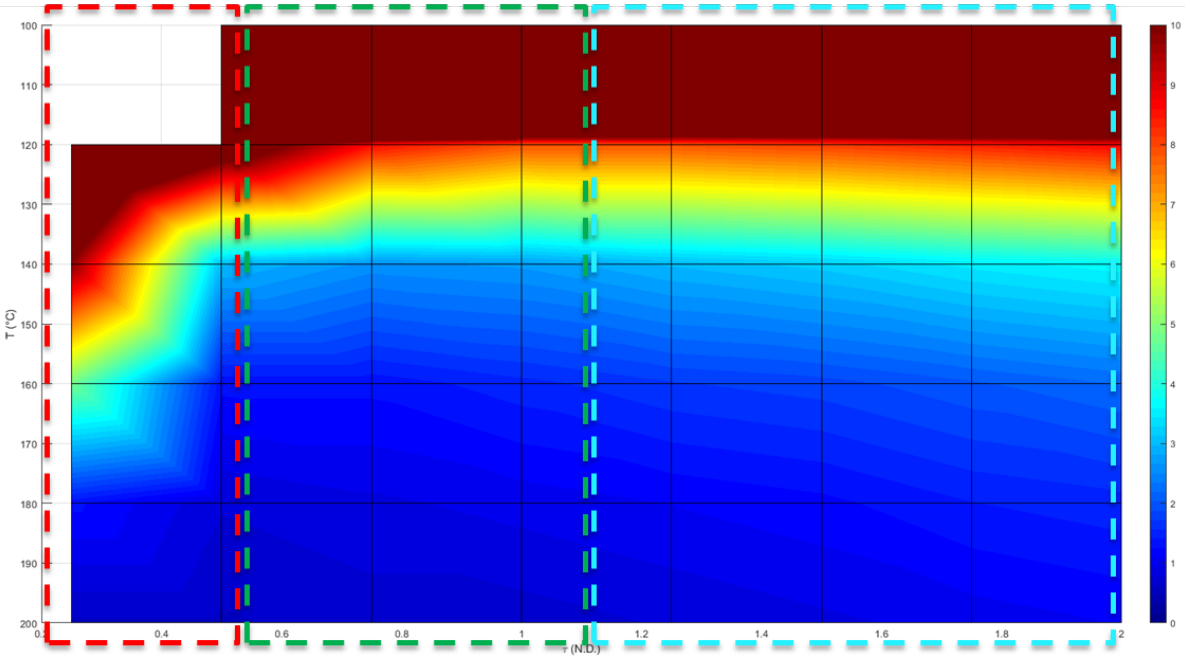

Figure 2.6: S/F ratio (water saturated TBP as organic phase) at 85% yield and specified catalyst concentration of $2M$. Manipulated variables: temperature and non-dimensional residence time. 2-D plot (τ, T-plane). Three distinct regimes are indicated, showing a competing effect of conversion and selectivity. Red: Low conversion. Green: Conversion limited. Blue: Selectivity limited.

S/F ratio

An increased S/F ratio ensures a higher selectivity as the HMF is extracted faster from the aqueous reaction mixture, the HMF has less time to degrade to HMF-Humins, levulinic acid and formic acid. The yield as a function of S/F ratio seems to follow a logarithmic trend, approaching a limit induced by the dehydration selectivity, which is independent of the S/F ratio (only a function of catalyst concentration).

The conversion is positively affected by an increased solvent amount, although this effect is marginal (+0.5% from S/F=1 to S/F=3).

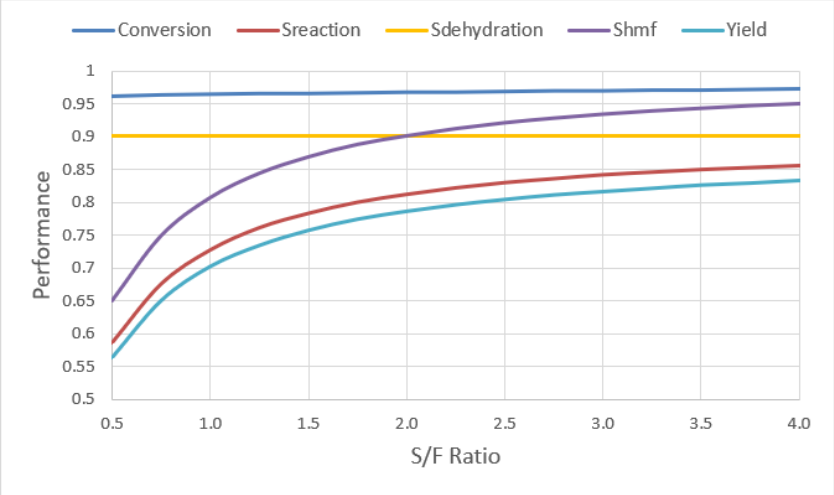

Figure 2.7: RE unit performance at different S/F ratios. $C_{Fructose,0} = 0.5M$, $T = 140°C$, $C_{HCl,0} = 0.5M$, $\tau = 0.5t_{characteristic}$, $N_{Stages} = 5$.

Although more solvent leads to a better performance, it is still a main interest to keep the amount of solvent to a minimum for the given process requirements, as less solvent means less energy needed in downstream processing of the organic phase. The result of the simulations showing these effects is given in Figure 2.7

Number of stages

Increasing the number of stages has the benefit of increased conversion at the cost of a larger unit. Since the trade-off is hard to quantitatively assess at this stage, the number of stages was kept constant at 5 stages. In this way, at least an honest comparison can be made between the three solvents, considering a higher/lower intrinsic conversion characteristics.

Operating conditions

In the following section the optimal operating conditions are given for two requirement sets (Tables 2.4 and 2.5). The procedure was constant, using optimal settings, while increasing S/F ratio until requirements were met (illustrated by Figure 2.8).

Yield above 85%

Table 2.4: Operating conditions at 85% yield.

	TBP	MIBK	2-pentanol
S/F ratio	2.6	3.7	3.2
τ (s)	10.3	10.3	10.3
$C_{Fructose,0}$ (M)	0.5	0.5	0.5
$C_{HCl,0}$ (M)	2	2	2
T (°C)	140	140	140
P (bar)	19.2	19.2	19.2
N_{Stages}	5	5	5
Conversion	0.984	0.984	0.989
$S_{reaction}$	0.865	0.865	0.861
$S_{Dehydration}$	0.922	0.922	0.922
S_{HMF}	0.938	0.938	0.934
Yield	0.851	0.851	0.851
$w_{H_2O}^{Org}$	0.046	0.030	0.071

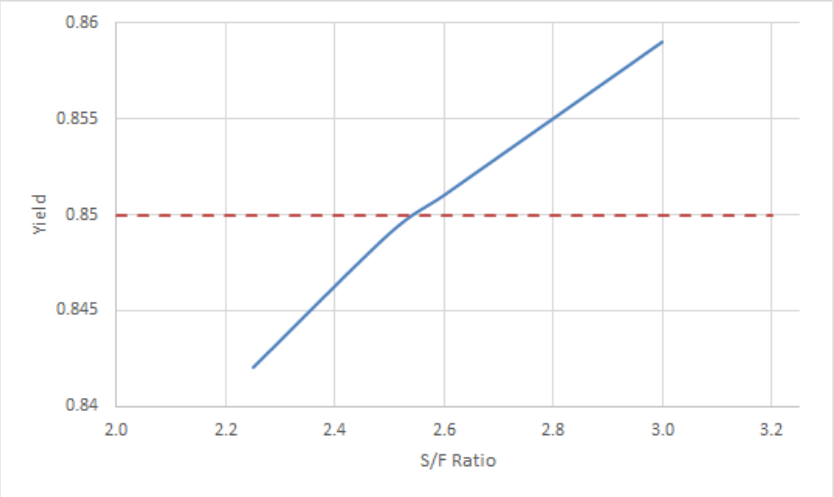

Figure 2.8: Analysis of feasible S/F region (meeting requirements).

Yield at 90% and $S_{Reaction}$ above 90%

Table 2.5: Operating conditions at 90% yield and above 90% overall selectivity.

	TBP	MIBK	2-pentanol
S/F ratio	9.5	13.4	8.1
τ (s)	10.3	10.3	10.3
$C_{Fructose,0}$ (M)	0.5	0.5	0.5
$C_{HCl,0}$ (M)	2	2	2
T (°C)	140	140	140
P (bar)	19.2	19.2	19.2
N_{Stages}	5	5	5
Conversion	0.994	0.993	0.999
$S_{reaction}$	0.906	0.906	0.901
$S_{Dehydration}$	0.921	0.921	0.921
S_{HMF}	0.983	0.984	0.979
Yield	0.900	0.900	0.900
$w_{H_2O}^{Org}$	0.046	0.031	0.066

Analysis

Since the two sets of process requirement produce distinctly different results, they will be discussed individually, as this will naturally lead to the drawn conclusions.

Yield above 85%

At a yield of 85% results of the simulation point to expected results. Since TBP has a higher affinity for HMF than MIBK or 2-pentanol, the amount of solvent employed is lowest. Furthermore, it can be noted that TBP performance across the board matches MIBK performance closely, except for a higher water content of the organic phase. However, the total amount of water extracted is balanced out by the lower amount of solvent. On the other hand, 2-pentanol has some interesting characteristics, with the conversion being slightly higher at comparable yield, due to the reduced selectivity of the solvent, due to a lower separation factor. The lower separation factor also leads to a higher amount of water being extracted.

Yield at 90% and $S_{Reaction}$ above 90%

Unexpectedly, at a yield of 90% it seems less 2-pentanol would be needed than TBP, although both the distribution coefficient and separation factor of 2-pentanol indicate poorer solvent performance. Although the fraction of water in the organic phase is still higher in 2-pentanol ($w_{H_2O}{}^{Org}$ is not strongly affected by S/F ratio), which increases downstream energy cost, this does not justify the use of TBP in itself.

Investigation of the simulation results unveiled a probable culprit for these deviating results, namely the catalyst concentration along the stages. The catalyst concentration in the final stage is given in Table 2.7.

Table 2.6: Catalyst concentration in final stage. $N_{Stages} = 5$, $C_{HCl,0} = 2M$, $S/F = 8$

	TBP	**MIBK**	**2-pentanol**
C_{HCl}	3.8	2.9	6.0

Clearly, the increase in catalyst concentration is substantial, especially for 2-pentanol. This drives conversion up to nearly 100% at lower S/F ratios. This yields the results invalid, as the range of validity for the reaction model is limited to a HCl concentration of 2M. Furthermore, a H_3O^+ concentration of 6M would indicate a theoretical pH of -0.8, which would be highly acidic (corrosive). It is proposed that the increase in catalyst concentration is purely an effect of water being transported into the organic phase, under the model assumption that HCl cannot transfer to the organic phase. An analysis of the final catalyst concentration was carried out to quantify this effect. First a crude mass balance on the water is implemented, neglecting the minor contribution of the dehydration of fructose,

$$m_{H_2O,Out}^{Org} = F\frac{S}{F}\frac{w_{H_2O}^{Org}}{w_{Org}^{Org}} \tag{2.18}$$

$$m_{H_2O,Out}^{Aq} = F w_{H_2O,In}^{Aq} - m_{H_2O,Out}^{Org} \tag{2.19}$$

$$m_{H_2O,Out}^{Aq} = F\left[w_{H_2O,In}^{Aq} - R_{SF}\frac{w_{H_2O}^{Org}}{w_{Org}^{Org}}\right] \qquad with \qquad R_{SF} = \frac{S}{F} \tag{2.20}$$

This is then used to describe the final HCl concentration in terms of the initial concentration,

$$[HCl]_{Out} = [HCl]_0\frac{m_{H_2O,In}^{Aq}}{m_{H_2O,Out}^{Aq}} \tag{2.21}$$

$$[HCl]_{Out} = [HCl]_0\frac{w_{H_2O,In}^{Aq}}{w_{H_2O,In}^{Aq} - R_{SF}\frac{w_{H_2O}^{Org}}{w_{Org}^{Org}}} \tag{2.22}$$

All that is needed are the relations defining the weight fractions, which are approximated by,

$$w_{H_2O,In}^{Aq} = 1 - w_{Fructose,In}^{Aq} - w_{HCl,In}^{Aq} \tag{2.23}$$

$$w_{Org,Out}^{Org} = 1 - w_{H_2O,Out}^{Org} - w_{HMF,Out}^{Org} \tag{2.24}$$

$$w_{HMF,Out} = \frac{1}{Yield[Fructose]_0\rho_{Aq}R_{SF}} \tag{2.25}$$

Combining the relations above yields,

$$[HCl]_{Out}(R_{SF}, w_{H_2O}^{Org}) = \frac{1.68}{0.84 - R_{SF}\left[w_{H_2O}^{Org} - \frac{0.05}{R_{SF}}\right]} \tag{2.26}$$

This equation is plotted in Figure 2.9, which shows the increase in HCl concentration with increasing S/F ratios. All constants and assumptions for this calculation are given in Table 2.7.

Table 2.7: Parameters and assumptions in predicting $[HCL]_{Out}$.

Parameter	Value	Assumption
$w^{Aq}_{H_2O,In}$	0.84	-
ρ_{Aq} $(\frac{kg}{m^3})$	1000	Constant
$w^{Org}_{H_2O,Out}$	-	Constant, effect of dehydration negligible
$w^{Org}_{Org,Out}$	-	$f(R_{SF})$, all HMF in organic phase
$[HCl]_0$	2	-
Yield	0.9	Theoretical

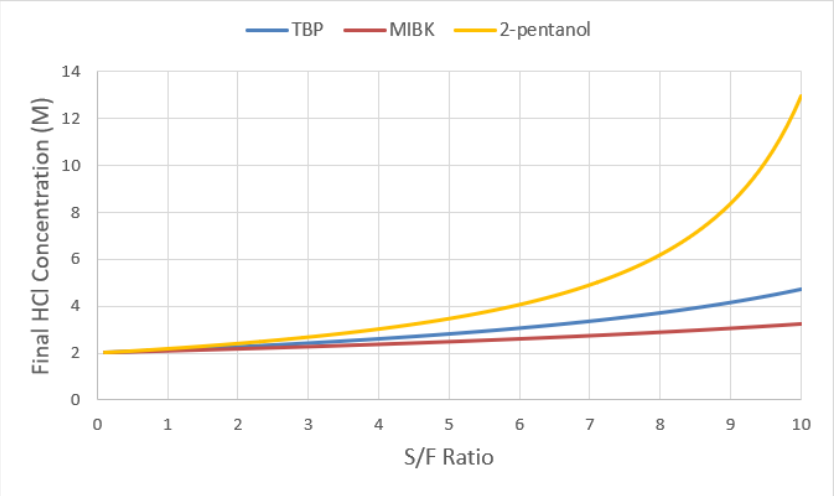

Figure 2.9: Expected final catalyst concentration for the solvents at a yield of 90%.

Since the transfer of water from the aqueous to the organic phase is responsible for the increasing HCl concentration, the problem can possibly be prevented by using a organic feed which is saturated with water (based on the final composition, $w^{Org}_{H_2O,In} = w^{Org}_{H_2O,Out}$). As can be expected, by feeding the organic phase to the RE unit, with an amount of water corresponding to the final equilibrium value, no additional water is co-extracted in the unit, ensuring that the catalyst concentration remains constant along the stages. This solution will not greatly affect the performance of the system, since a similar amount of water and solvent is leaving the system for further separation compared to using a pure organic feed. The water which would normally get extracted to the organic phase, will leave the system in the depleted aqueous phase leaving the RE unit. When this is considered, different operating conditions are found. These are given in Table 2.8. These results are more in line with both the expectation and the given validity limits of the kinetic model.

Table 2.8: Operating conditions at 90% yield and above 90% overall selectivity, saturated organic feed.

	TBP	**MIBK**	**2-pentanol**
S/F ratio	34	50	39
τ (s)	11	11	11
$C_{Fructose,0}$ (M)	0.5	0.5	0.5
$C_{HCl,0}$ (M)	2	2	2
T (°C)	140	140	140
P (bar)	19.2	19.2	19.2
N_{Stages}	5	5	5
Conversion	0.980	0.980	0.981
$S_{reaction}$	0.918	0.918	0.916
$S_{Dehydration}$	0.922	0.923	0.922
S_{HMF}	0.994	0.995	0.994
Yield	0.900	0.899	0.900
$w_{H_2O}^{Org}$	0.048	0.031	0.073

Conclusion

Since the goal of the project is to find an optimal process, in which the least amount of energy is employed per unit of HMF produced, the produced data must be interpreted in a wider context than only the RE unit. As separation of HMF from MIBK or 2-pentanol can be achieved using distillation, while HMF and TBP cannot due to close relative volatility, it is of key importance that RE performance of TBP is distinctly better than the MIBK or 2-pentanol performance, to allow for extra unit operations in downstream processing of the TBP-HMF product stream.

For a yield of 85% it can be concluded that TBP may indeed be a feasible solvent, justifying any further examination of the proposed system. However, for a yield of 90%, it was found that non of the three solvents can realistically meet the target at a low S/F ratio. Furthermore, the used model introduces a clear problem at these high S/F ratios as previously described, leading to the false conclusion that 2-pentanol may actually perform better than TBP. To mitigate this limitation a (water) saturated organic feed can be introduced, to prevent any significant changes in the aqueous phase volume. Once this was taken into account TBP was indeed found to have the best performance.

Considering the results of the initial investigation it was needed to reconsider some of the choices made in the optimal operating conditions for the MIBK and 2-pentanol systems. It will benefit the accuracy of the results to either redesign the Aspen Custom Modeler unit or to set the process requirement to a yield of 85%. Since the former will be too time consuming and defer progress to the final objective, it is chosen to adjust the process requirement accordingly, as to adhere to a more reliable regime of the model.

Newly simulated data supports many of the previously drawn conclusions, especially the need of high catalyst concentration. Increasing the temperature beyond 140 °C may lead to even better performance of the RE unit in terms of S/F ratio, although this will lead to very short residence times, which may bring into question whether it is valid to assume that all stages immediately reach their equilibrium position. Lastly, considering the ideal residence time, it was found that this is not a constant fraction of the characteristic time for all catalyst concentrations. The trend for the ideal residence time was described and can be used going forward.

3

Separation

Since separation of HMF and TBP by distillation is not a possibility, due to a small difference in relative volatilities and the risk of degrading the final product at high temperatures, a different option had to be explored. To this extent back-extraction was selected.

3.1. Back-extraction

The recovery of TBP from the product mixture can be achieved by back-extraction of HMF into an aqueous phase. Doing so mitigates the difficulty of separation of HMF and TBP based on relative volatilities. First, the principles behind back-extraction are explained, after which the complexity will be increased from an equilibrium stage, to a continuous column, finally resulting in a conceptual approach to close the gap between energy consumption for a MIBK and a TBP based process.

Principles

As for extraction, the driving force for back-extraction is the chemical equilibrium of the solute distributed between the two phases. The mixture coming from the RE unit is a stable single phase, but subsequent phase separation can be achieved by adding a co-solvent or varying the temperature of the mixture. In the context of this project, the option of back-extracting the HMF to an aqueous phase, from which it can be separated by distillation, is investigated.

An analogy to a different process shows that the back-extraction principle can be very effective. Lactic acid for example can be back-extracted with single stage recoveries up to 80% ([10],[11],[12]). It should be noted that these high values are only obtained once a proper anti-solvent is selected, which decreases the affinity of the solute for the organic phase. Furthermore, the back-extraction is carried out at an elevated temperature to promote the effective back-extraction.

Co-solvent

To make an initial assessment of suitable anti-solvents, a list of eleven solvents was compiled (Table 3.1). The main selection criteria were: polarity, boiling point and density. Apolar solvents should be good candidates, since they are likely to have low solubility in water and negatively impact the affinity of HMF for the organic phase. The performance of these solvents were then analysed using Aspen Plus (Section 3.1).

Table 3.1: Solvents selected for screening.

Solvent	T_{boil} (°C)	ρ (kg/m^3)
Pentane	36	626
Hexane	68	655
Heptane	98	684
Benzene	80	876
Cyclohexane	81	779
Cyclopentane	49	751
Cyclohexene	83	811
2-methylpentane	60	653
3-methylpentane	63	664
1,4-cyclohexadiene	88	847
Methylcyclopentane	72	749

Simulation

Since screening all potential co-solvents in a lab environment would take too much time, simulations (Aspen Plus) were used to assess all candidates. The first step in generating meaningful results is setting up the properties database. All co-solvents, along with water, HMF and TBP were loaded. Binary interaction (NRTL) parameters were given as an input for the regressed TBP-HMF-water system. Further binary parameters were either taken from the Aspen database when available or estimated by a UNIFAC group contribution method.

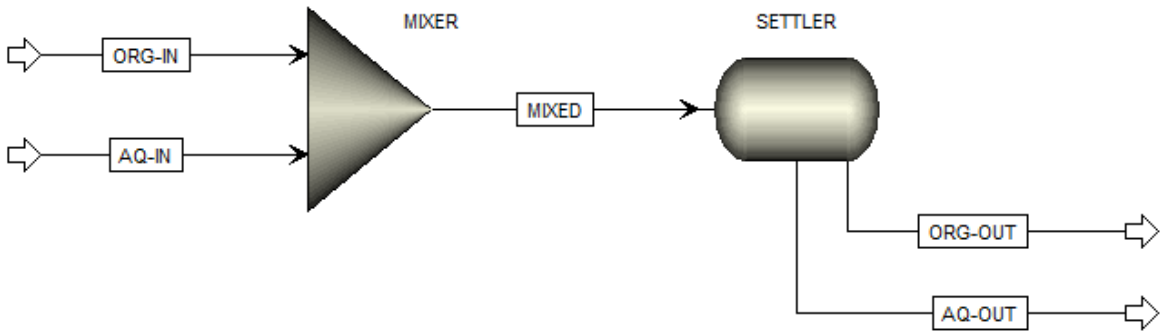

Figure 3.1: Aspen Plus setup for liquid-liquid equilibrium (LLE) simulation.

Secondly, the flowsheet was set up to imitate a single stage equilibrium experiment, as seen in Figure 3.1. Since all organic solvents have a lower density than water, the organic phase will leave the decanter model in the top stream. To validate the setup, the lab experiment for a TBP-HMF-water system was reproduced. As can be seen in Figure 3.2, the experiment and simulation show good agreement, although the performance at lower initial HMF concentration (right-hand side of the graph, corresponding to higher D_{HMF} values) does slightly deviate, resulting in a simultaneous over-prediction of separation factor and slight under-prediction in distribution coefficient, which indicates less water and less HMF are extracted to the organic phase in the simulation.

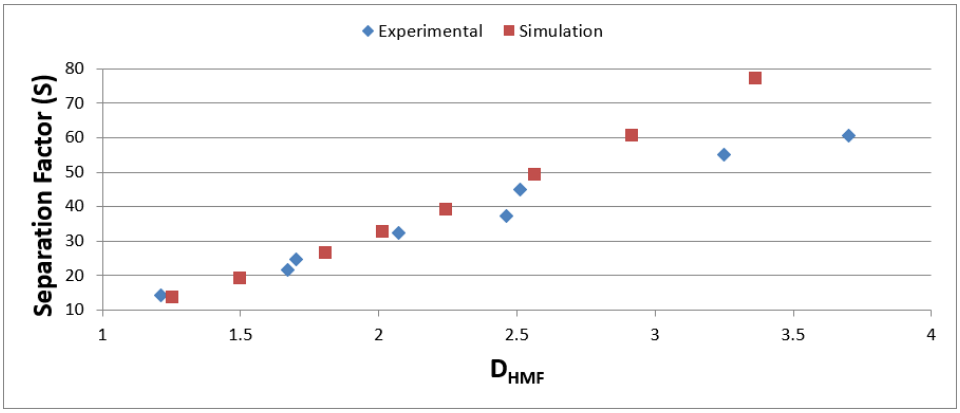

Figure 3.2: Comparison of experimental and simulation results of the TBP-HMF-water.

To check for distinct differences between the potential anti-solvents a relatively simple procedure was followed. First, the solvents were mixed in varying mass ratios (wash to feed, W/F, ratios of 0.5, 1 and 2) to a stream with the composition similar to the organic phase coming from the RE unit ($x_{TBP} = 0.93$, $x_{HMF} = 0.02$ and $x_{H2O} = 0.05$). These results are given in Figure 3.3 and show three key aspects:

1. Benzene exhibits superior anti-solvent properties.
2. All candidates (except) benzene perform approximately equally well.
3. Back-extraction yields aqueous solutions of 0.5wt% HMF at given specifications.

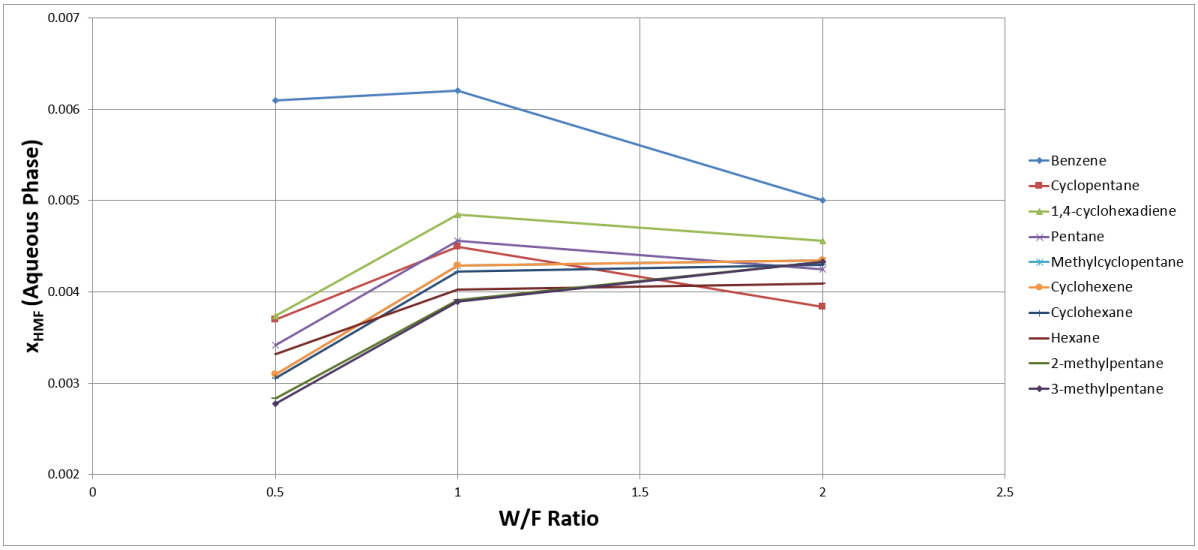

Figure 3.3: HMF content in the aqueous phase (equilibrium composition) for different anti-solvents. Feed is given by the TBP-HMF-water mixture from RE unit. W/F ratios given on a mass basis.

Building on these insights, benzene is the most promising candidate, which will be further investigated. Other solvents perform very similarly, so secondary considerations, such as SHE aspects and availability, should be taken into account in selecting the next best option. For the purpose of deeper analysis, 2-methylpentane, which seems to achieve its maximum aqueous HMF concentration at a higher W/F ratio, and hexane, which was found to separate the least amount of water into the aqueous phase, were selected.

Subsequently, the simulation setup was used to find equilibrium compositions for systems with a 1:1 ratio of organic phase (TBP + anti-solvent) and aqueous phase (water + HMF), with a initial HMF content

varying from 5 to 50 wt%. From these compositions, distribution coefficients were derived, according to:

$$D_{HMF}^{Aq} = \frac{x_{HMF}^{Aq}}{x_{HMF}^{Org}} \tag{3.1}$$

The results for an organic phase of anti-solvent with TBP (1:1) and a purely anti-solvent organic phase are given in Figures 3.4 and 3.5 respectively. In both cases pure TBP is included as a benchmark. As expected the pure anti-solvents do a relatively better job at removing the HMF from the organic phase, with distribution coefficients close to 1, whereas the TBP + anti-solvent mixtures perform poorly, especially at higher initial HMF concentrations. Poor performance at high HMF concentrations does, however, not necessarily prevent the use of the anti-solvent, as the final process will only have low HMF concentrations, due to the amount of solvent used in the RE unit.

Lastly, the effect of temperature on the distribution coefficient (D_{HMF}^{Org}), was studied. As seen in Figure 3.6, increasing the temperature leads to a decrease in distribution coefficient, implying a higher HMF concentration in the organic phase. Interestingly, pure TBP seems to exhibit this effect even more strongly than the mixed organic solvents at high temperatures, which is in contradiction with a previous assumption that the distribution coefficient of HMF in TBP would remain stable in the temperature range of the RE unit.

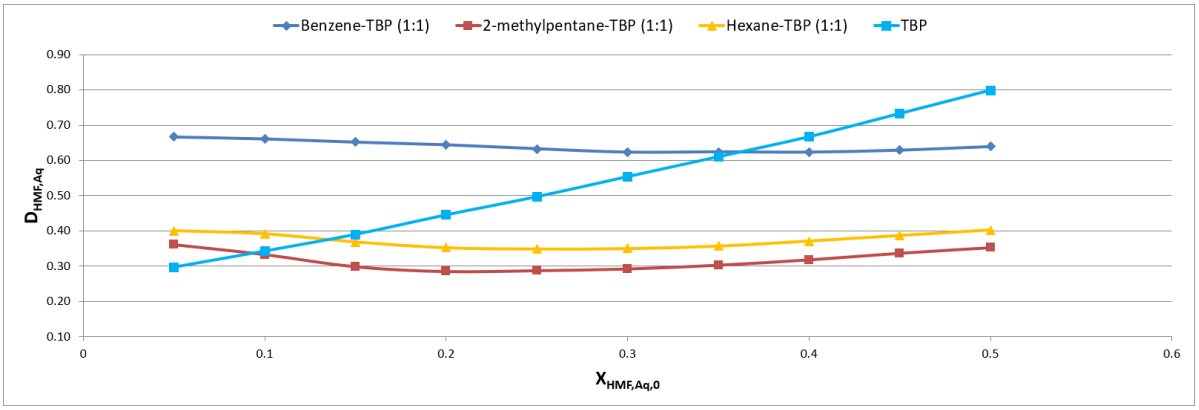

Figure 3.4: Comparison of the distribution coefficient (D_{HMF}^{Aq}) between different TBP + anti-solvent mixtures.

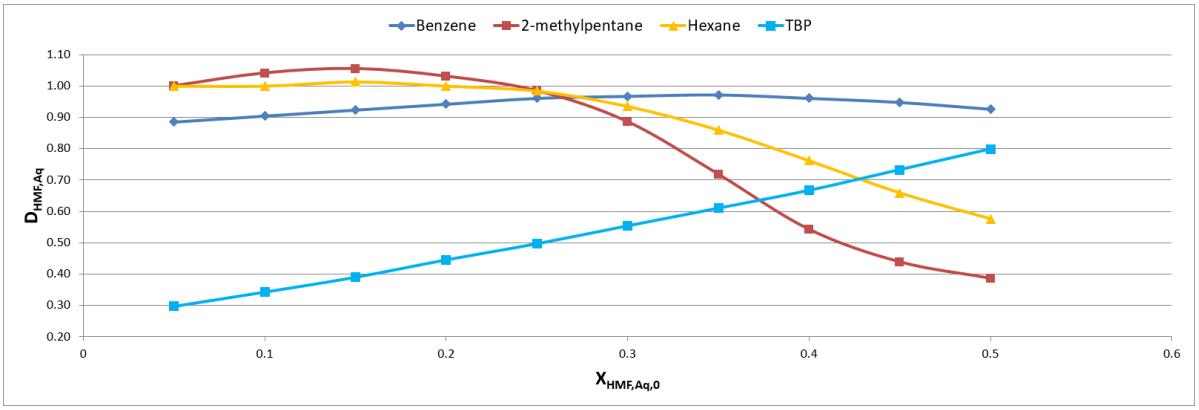

Figure 3.5: Comparison of the distribution coefficient (D_{HMF}^{Aq}) between different (pure) anti-solvents.

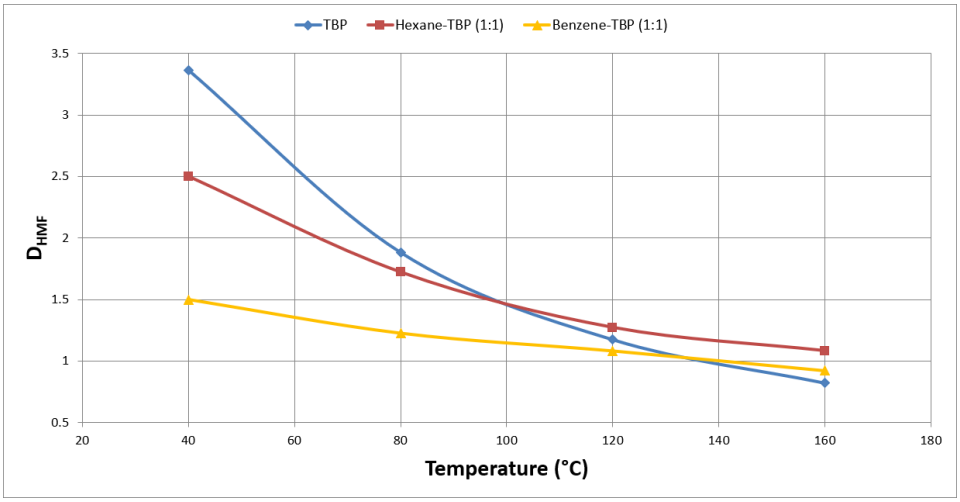

Figure 3.6: The effect of temperature on the distribution coefficient (D_{HMF}^{Org}). The distribution coefficient is inversely proportional to temperature.

Aspen Plus difficulties

On closer inspection of the ternary diagrams, data for 2-methylpentane (and possibly hexane), proves to be unreliable. As can be seen in Figure 3.7, tie lines cross, which should not be possible, since this implies that there are compositions at which the system will not go to two equilibrium compositions. To check whether the simulation does produce results of the expected order of magnitude, a simple mass balance calculation was performed, based on literature solubility data for a hexane-HMF-water assuming a weighted average mixing law for the solubilities ([13],[14]). This confirms a mass fraction of around 0.5 wt% HMF in the aqueous phase at a W/F ratio of 1.

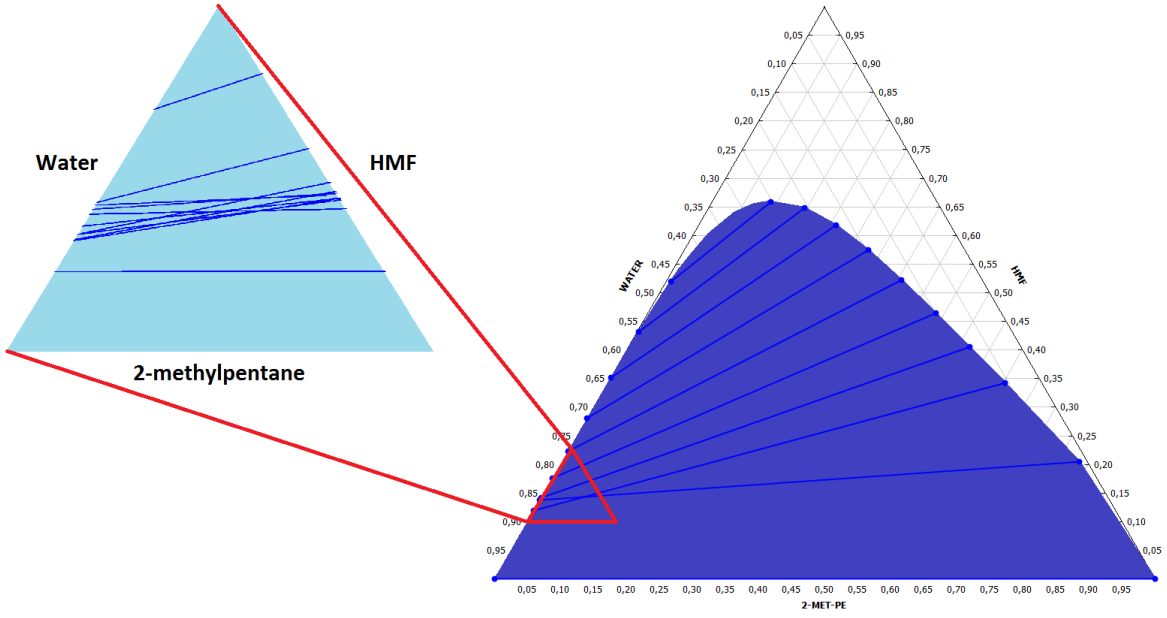

Figure 3.7: Ternary diagram 2-methylpentane-HMF-water. Magnified section shows crossing of tie-lines. Tie-line density was increased in this area to magnify this effect.

3.2. Single equilibrium stage

Up to this point, effectively a single equilibrium stage setup was studied. Simulations showed that it is possible to decrease the distribution factor for HMF with respect to the organic phase by adding an anti-solvent, or by increasing the temperature. However, resulting aqueous solutions of HMF still have a very low HMF concentration, leading to infeasible subsequent process designs, as relatively large quantities of water have to be evaporated to obtain a small amount of HMF. At this point, the possibility of using back-extracting for the separation of a TBP-HMF-water mixture does not yet look very promising. Therefore, a next step had to be made away from a single stage model to a continuous column, which provides the opportunity of recovering a larger fraction of HMF.

3.3. Continuous column

Building on the simulations and insights of the single stage model, it was simulated whether continuous back-extraction could be competitive with a MIBK distillation-based process. The composition of the input stream for the counter-current column was given by the RE model (Table 3.2).

Table 3.2: Composition of feed streams for TBP and MIBK (benchmark) process.

	TBP	**MIBK**
x_{HMF}	0.02	0.01
x_{H2O}	0.05	0.03
x_{Org}	0.93	0.96

Matlab was then used to compute what fraction of HMF was extracted (Appendix C) and used as an input for a minimization problem of two variables in which hexane to feed ratio and water to feed ratio, were adjusted to find the minimum energy requirement based on heat of vaporization (Table 3.3). The number of stages was fixed at 10. The extracted fraction of HMF is plotted in Figure 3.8

Table 3.3: ΔH_{vap} values used in calculations.

	ΔH_{vap} (kJ/kg)
Water	2257
MIBK	405
Hexane	335
Heptane	320

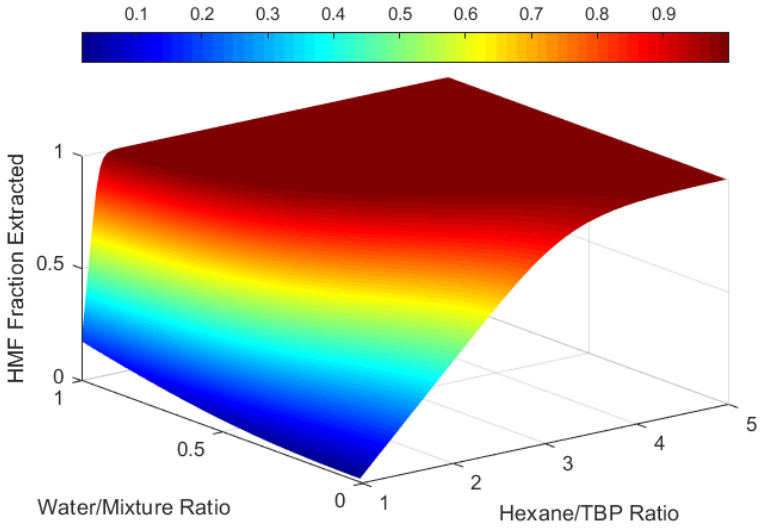

Figure 3.8: Fractional extraction of HMF as a function of hexane and water to feed ratio.

The simulation provides an insight in the combination of variables resulting in the lowest energy requirement (Figure 3.9).

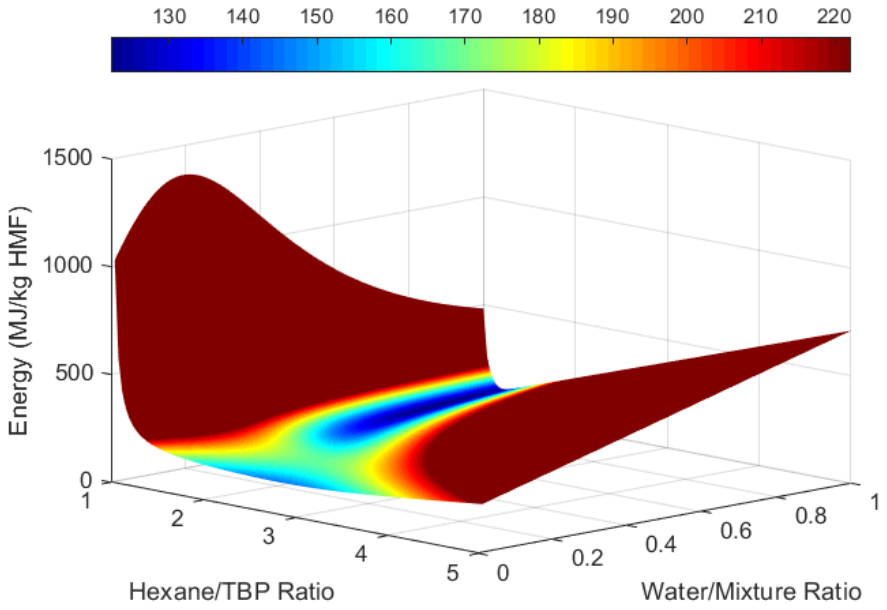

Figure 3.9: Energy landscape as a function of the hexane/TBP and water/feed ratios.

In Figure 3.10 the results are plotted against the MIBK benchmark figure, which shows that by using a single stage at the given inlet composition the minimum energy requirement is around 3 times that of the benchmark.

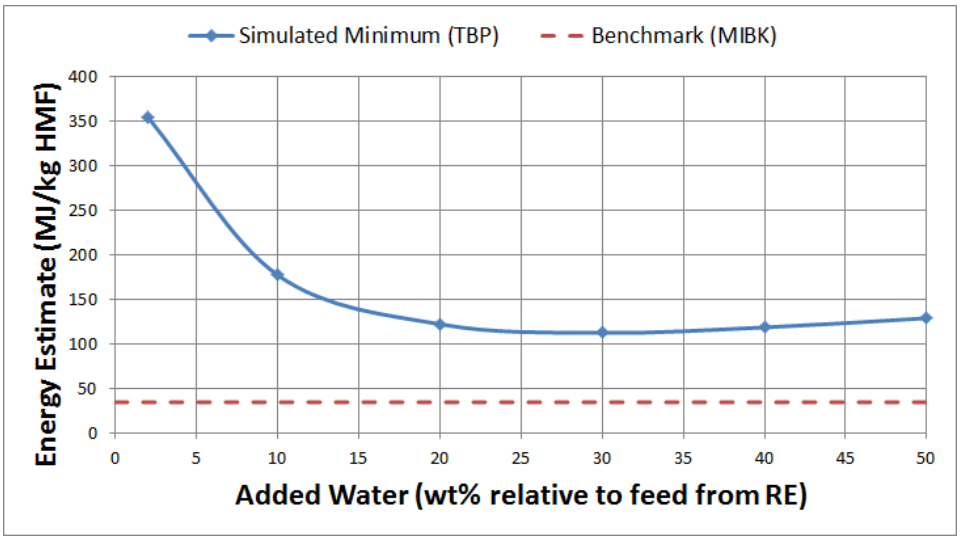

Figure 3.10: Estimated energy demand on a HMF mass basis, showing the influence of additional water.

A possible explanation is, that to extract a decent quantity of HMF too much water needs to be added, tremendously increasing the overall energy demand of the process. This idea is reinforced by looking at the relative contributions from energy use for either the recovery of organic solvent, or water, across the three processes (Figure 3.11). This negates any positive performance effects TBP has in the RE unit.

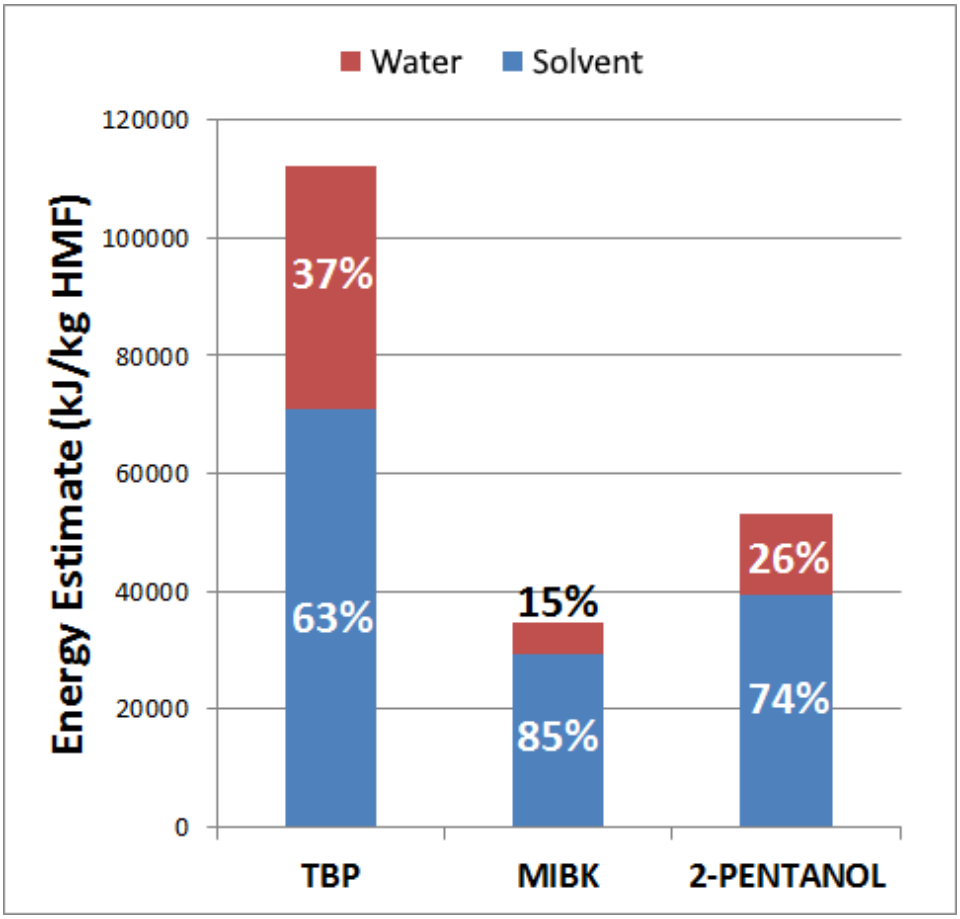

Figure 3.11: Comparison between the different organic solvents. Energy demand is split in two categories: evaporation of solvent and evaporation of water.

Another aspect to note is, that while the MIBK-based process outperforms the TBP-based process, the energy demand is still high for both in terms of HMF produced. Therefore, an idea worth exploring is, if lower energy requirements can be achieved by increasing the HMF fraction in the reaction mixture. In turn, this will provide the added benefit of reducing the amount of water needed for reasonable extraction.

3.4. Conceptual design approach

Examining the problem in a more conceptual manner, the task at hand is split in two sub-problems. First, it was shown that back-extraction is not feasible at low HMF concentrations. In order to circumvent this issue, the maximum HMF concentration in the reaction mixture was determined to improve performance. This was done numerically, with the highest concentration (20.0 wt%) being found at a high temperature (200°C), high catalyst concentration (2M) and high initial fructose concentration (2M) (Figure 3.12). From these concentrations the maximum achievable concentration after the RE unit was calculated considering an extraction factor of 1 in an infinite length extraction column. Minimum S/F ratio followed from this, since,

$$E = \frac{S}{F}_{min} D_{HMF} \tag{3.2}$$

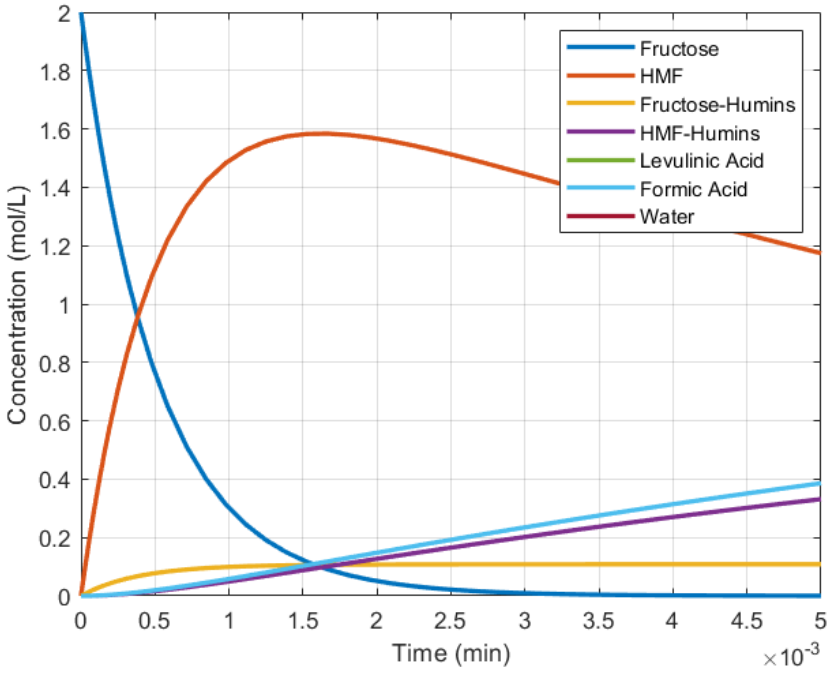

Figure 3.12: Concentration profile of the reaction mixture. T=200 °C, [HCl]=2M, [Fructose]=2M.

Additionally, the minimum S/F ratio for the RE model was also reevaluated, with a focus on high final concentration, while keeping yield at a minimum of 85%. This was possible by increasing the temperature and initial fructose concentration. The compositions used in further calculations are given in Table 3.4

Table 3.4: Composition of streams after first extraction stage (reactive extraction) for TBP and MIBK (benchmark) process. Parameters used in calculation for back-extraction.

	TBP		**MIBK**	
	RE model	***Reaction model***	***RE model***	***Reaction model***
x_{HMF}	0.29	0.54	0.23	0.38
x_{H2O}	0.04	0.03	0.02	0.02
x_{Org}	0.67	0.43	0.75	0.60
S/F ratio	0.50	0.26	0.70	0.49
Yield (%)	85.1	79.2	85.1	79.2

Second, the question remains whether Aspen properly predicts what happens when an anti-solvent is introduced to the system to aid the back-extraction. Since it cannot be said with certainty until experimental work takes place, several scenarios were considered (Figure 3.13). It is apparent that reality should be somewhere between the best-case (pure exponential curve) and most-likely case (Aspen prediction, base case), for the back-extraction to be a success. From here on calculations were done with ΔH_{vap} values for heptane, since this was available in the lab at 3mE were any potential experiments to take place. This should not influence the results drastically in comparison to previous sections, since heptane and hexane are predicted to have similar anti-solvent performance and have comparable heat of evaporation.

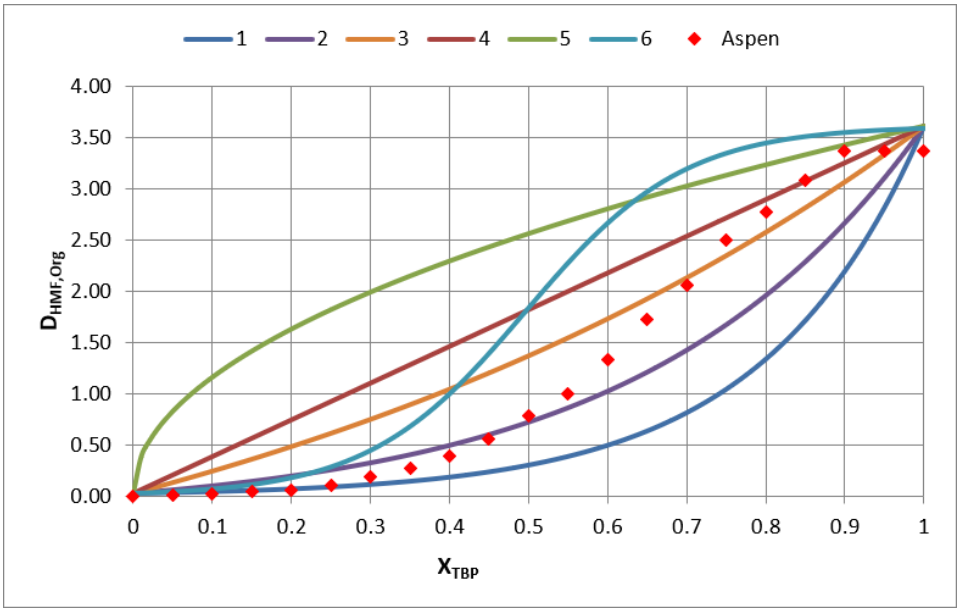

Figure 3.13: Possible scenarios for the distribution coefficient as a function of heptane to TBP ratio. Note: scenario curves are given for a set mass fraction of HMF.

The blue-print of the calculations is shown in Figure 3.14, in which three main steps can be described,

1. Transfer of HMF from the aqueous reaction mixture to the organic phase. Typical D_{HMF} values are high, around 4, due to the influence of salt in the reaction mixture.
2. The HMF-water-organic mixture is diluted with heptane before back-extraction, reducing the HMF fraction depending on the heptane to TBP ratio.
3. Transfer of HMF back into an aqueous phase. As an effect of the anti-solvent, supplemented by the lack of salt, further lowering the D_{HMF} (below 1, depending on heptane to TBP ratio), HMF can be recovered.

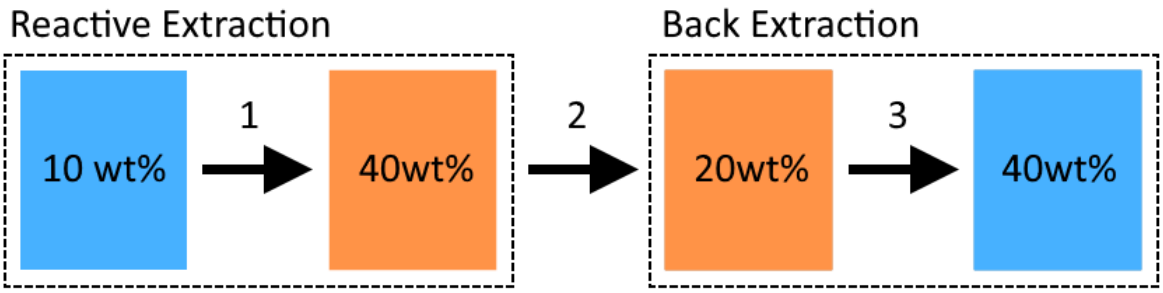

Figure 3.14: Schematic blue-print of the conceptual calculations. An example of the HMF mass fraction in various phases is shown to give a indication of what happens throughout the system.

D_{HMF} = constant

To keep calculations more simple at first, the back-extraction was considered at a constant distribution coefficient. Constant here indicates no additional deviation as a result of dilution by the anti-solvent, meaning a single scenario curve, generated for a fixed mass fraction of HMF (set at 20 wt% in the organic phase after addition of heptane) in the mixture, can be used over the entire range of heptane to TBP ratios. From the results (Figure 3.15), it follows that there is still a gap between the performance of both solvents.

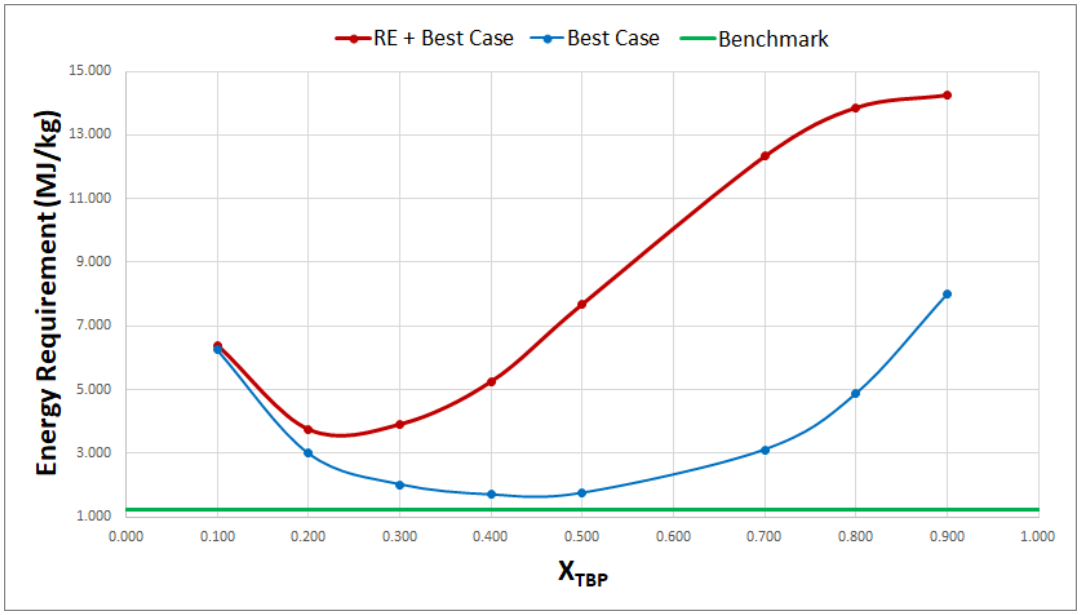

Figure 3.15: Calculated energy demand based on constant D_{HMF}.

D_{HMF} = *f*(x_{HMF})

Experimental data indicates that at high HMF fraction the distribution coefficient is lower than at low HMF fractions, and not constant. To incorporate this effect in the calculations, the scenario curves can be rescaled using the value of the distribution coefficient at the point of pure TBP (right-hand side of Figure 3.13, $D_{HMF,0}$), according to the values in Table 3.5.

Table 3.5: Distribution coefficients as a function of HMF mass fraction in organic phase.

TBP fraction	x_{HMF}	$D_{HMF,0}$
0.1	0.054	4.1
0.2	0.107	2.8
0.3	0.161	2.2
0.4	0.215	1.9
0.5	0.268	1.7
0.6	0.322	1.5
0.7	0.376	1.4
0.8	0.430	1.3
0.9	0.483	1.2

Taking this into account results in a more accurate estimation for energy requirement across the board. Results for the best-case scenario (exponential curve to $D_{HMF,0}$) for both the RE model and the reaction model as input are presented in Figure 3.16.

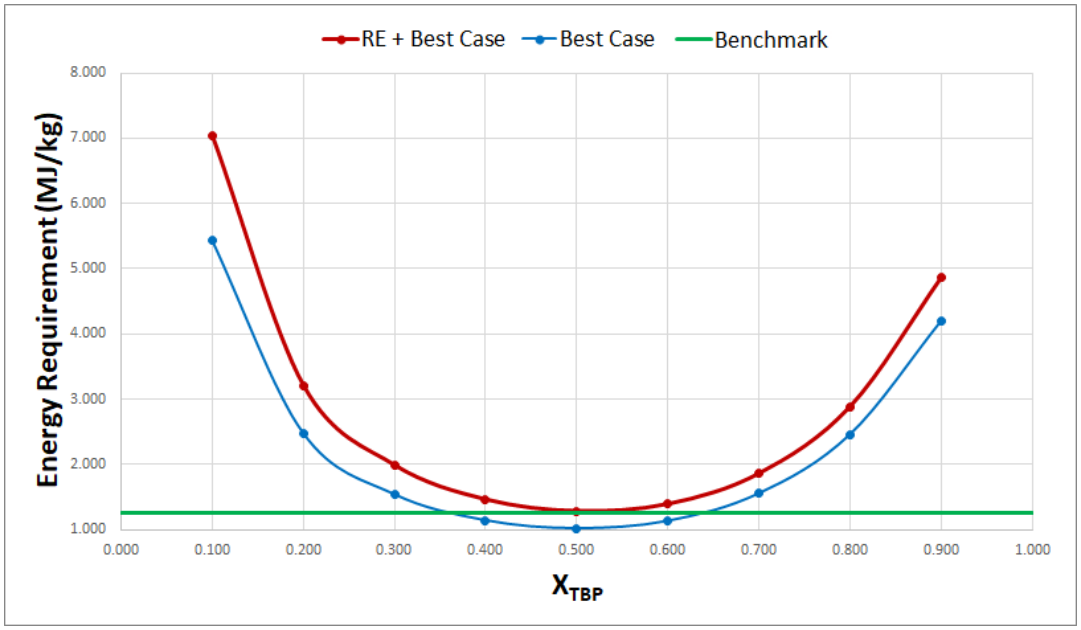

Figure 3.16: Calculated energy demand based on variable D_{HMF}.

This looks promising, since the estimated energy requirement is now only 80-90% of the benchmark.

3.5. Additional remarks

Two aspects considered have not yet received attention: other anti-solvents and varying the extraction factor. These will be discussed briefly in the following sections.

Anti-solvent selection

To reduce the distribution coefficient as effectively as possible a anti-solvent should be chosen to have very low affinity with HMF. It may be the case, that hydrocarbons with a longer carbon chain length do a better job than those with a shorter chain length. Initial assessment of hexane (C6), heptane (C7) and octane (C8) in Aspen was inconclusive (Figure 3.17), and not useful without further experimental work, which is why choosing a specific anti-solvent was not looked into in much detail.

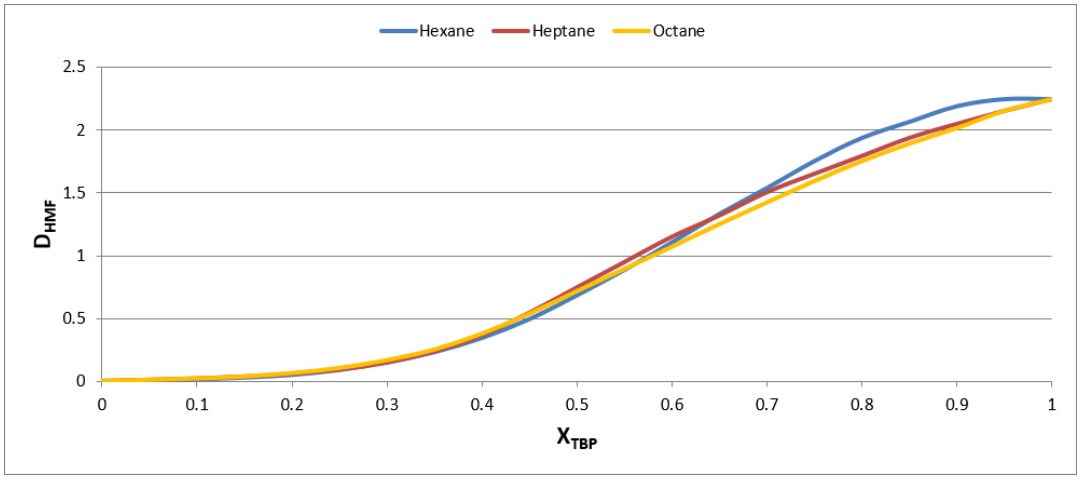

Figure 3.17: Comparison of different anti-solvents as simulated by Aspen.

Extraction factor

It may be interesting to look at the effect of lowering the extraction factor, thus leaving some of the HMF in the organic stream leaving the system or elevating the extraction factor to reduce the number of stages needed. For the option of a back-extraction process the extraction factor can be varied for both the reactive extraction and the back-extraction. As can be seen in Figure 3.18, the optimum performance relative to the benchmark is achieved by calculating both extraction steps at a extraction factor of 1.

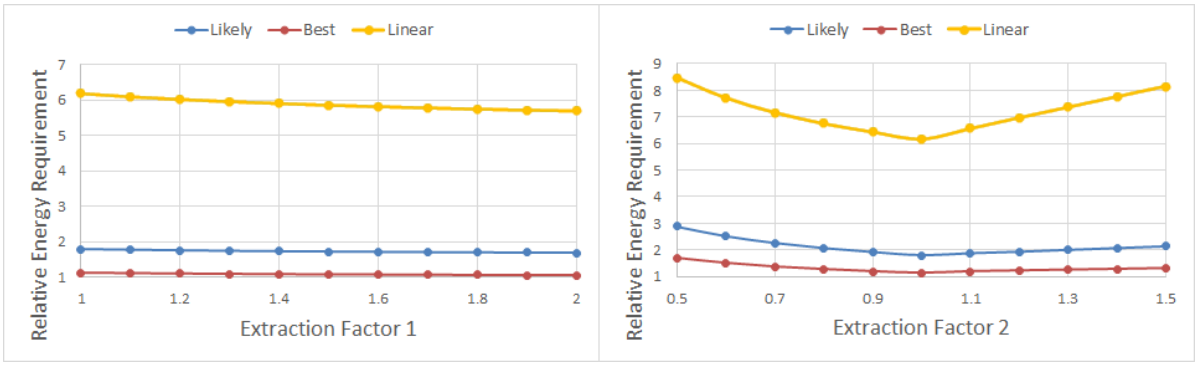

Figure 3.18: Calculated relative energy demand as a function of extraction factor. Left: Reactive extraction. Right: Back-extraction.

3.6. Conclusion

By taking a step-by-step approach it was possible to close the gap between a TBP-based process and a MIBK-based process for the production of HMF. It has to be noted however, that this statement relies heavily on specific assumptions, which will have to be confirmed by experimental work if the model predicts that a TBP based process might be feasible depending on the exact distribution values. To justify experimental work the model should show at least a good margin compared to the benchmark (MIBK-based) process.

4

Process modeling

This chapter aims to provide an overview of the comparative analysis between an HMF production process using either MIBK or TBP as the solvent in a reactive extraction setup, to investigate the need for further experimental work and to draw preliminary conclusions. The processes will be compared on the basis of economics, as well as sustainability. The full model is available digitally and an in-depth user-guide of the model is provided in Appendix D.

4.1. Flowsheet and main assumptions

Principally, the choice for using MIBK or TBP comes down to the balance between energy usage and process complexity (i.e. capital and operational cost). So far, the main focus was the reduction of energy requirements, to increase the feasibility of using the intrinsically better solvent, TBP. To illustrate the increased complexity of using a high-boiling point solvent, simplified flowsheets of the processes is shown in Figure 4.1. To keep the economical model simple, yet realistic, four assumptions were made:

1. For initial estimates the number of main unit operations are two and four, for the MIBK and TBP based process respectively. These values will be used in Section 4.2. The assumption is that these units will contribute most to the overall capital cost, ensuring an adequate level of accuracy, without the need for a detailed analysis of additional equipment between the main units and for recycling purposes.

2. The volume reduction effect when using TBP instead of MIBK has a minor effect on the contribution of the reactive extraction unit on the overall cost. This can be shown by the following calculation:

$$\frac{Cost_{RE,TBP}}{Cost_{RE,MIBK}} \approx \left(\frac{V_{RE,TBP}}{V_{RE,MIBK}}\right)^{0.6} \tag{4.1}$$

   First, the volume of the reactive extraction units is approximated by the sum of solvent volumes, assuming dissolved salts, fructose and HMF have a negligible effect on the total volume.

$$\frac{Cost_{RE,TBP}}{Cost_{RE,MIBK}} \approx \left(\frac{V_{TBP} + V_{Water}}{V_{MIBK} + V_{Water}}\right)^{0.6} \tag{4.2}$$

   Substituting in the values from the reactive extraction unit model yields,

$$\frac{Cost_{RE,TBP}}{Cost_{RE,MIBK}} \approx 0.9 \tag{4.3}$$

   Since the effect on this individual unit is around 10%, the overall effect on the process with 4 units is around 3%. This is well below the overall accuracy of the used estimation methods and including the factor may lead to more uncertainties. However, it can be reconsidered if the two processes are shown to perform very similarly under the current calculation methods.

3. Design pressure (factor in Hill estimation method) of the reactive extraction unit was taken at 20 bar, to prevent the development of water vapor at the design temperature of 200°C.

4. For economic estimation purposes, the process location is taken as Western Europe, resulting in an Investment Site Factor (F_{ISF}) of 1.25.

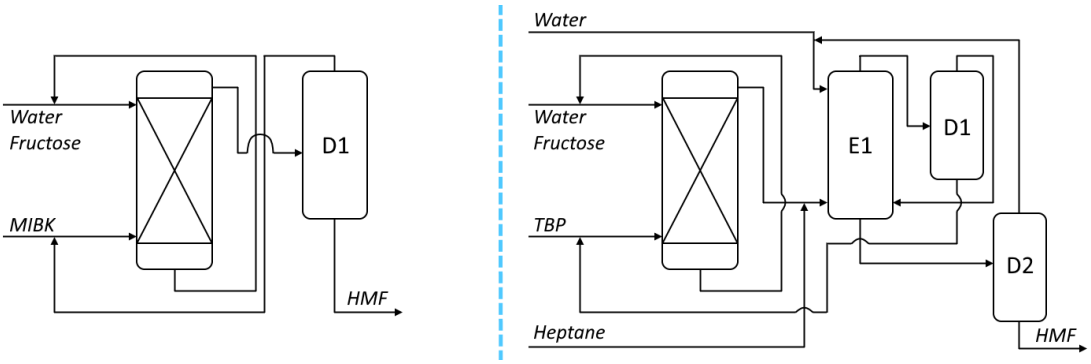

Figure 4.1: Simplified flowsheet of the processes. Only main components of inlet and outlet streams are indicated, purge streams not indicated. Left: MIBK based process. Right: TBP based process.

4.2. Economics

Arguably, the main driver behind all business decisions is the possibility for financial gains. In this scenario specifically, the question boils down to whether the reduction in energy requirements for a TBP based process, can offset the increased capital and operational cost incurred by the more complex process setup. To assess the financial aspect an estimation was made for both the capital and operational cost, as a function of number of main units, raw material cost and plant capacity.

Methods

Capital costs

Two relatively simple functional unit estimation methods were used to approximate the total permanent investment cost (C_{TPI}) of the process facilities. Both methods have an accuracy of $\pm$25% at best [15]. Estimated values as a function of plant capacity are shown in Figure 4.2. From the C_{TPI}, the capital expenditure (CAPEX) is calculated by including an additional 15% for working capital [16].

Hill

The Hill order-of-magnitude estimate is based on the production rate and the basic process flowsheet, including design pressures of the units. First the production rate factor (F_{PR}) is computed.

$$F_{PR} = (\frac{2.205Q}{10})^{0.6} \tag{4.4}$$

Where Q is the annual HMF production in kton. Subsequently the module costs C_M of all units are computed as a function of production rate factor, material factor (F_M) and design pressure (P, in bar).

$$C_M = F_{PR}F_M \quad if \quad P \leq 7bar \tag{4.5}$$

$$C_M = F_{PR}F_M(\frac{14.5P}{100}) \quad if \quad P > 7bar \tag{4.6}$$

The material factors are given in Table 4.1. In the following calculations, stainless steel was chosen, considering the higher corrosion resistance to elevated operating temperatures and low pH levels than carbon steel. A nickel alloy, may be the optimum choice for the reactive extraction unit specifically, given its superior to stainless steel with regards to withstanding acid induced corrosion [17].

Table 4.1: Material factors used in Equations 4.5 and 4.6.

Material	F_M
Carbon steel	1.0
Copper	1.2
Stainless steel	2.0
Nickel alloy	2.5
Titanium clad	3.0

The total bare module investment (C_{TBM}) is then computed using the sum of module costs and the piping and instrumentation factor (F_{PI}, 2.15 for fluids handling) and updated with the current Marshall and Swift Process Industries Average Cost Index (MS index, estimated at 1800 for 2018 based on Marshall Swift Valuation Services index average for all sectors [18]).

$$C_{TBM} = F_{PI}(\frac{MSindex}{1365})\sum C_M \tag{4.7}$$

The direct permanent investment is obtained by accounting for construction factors F_1 and F_2 (Table 4.2).

$$C_{DPI} = (1 + F_1 + F_2)C_{TBM} \tag{4.8}$$

Table 4.2: Construction factors used in Equation 4.8.

	F_1
Outdoor construction	0.15
Mixed indoor and outdoor construction	0.4
Indoor construction	0.8
	F_2
Minor additions to existing facilities	0.1
Major additions to existing facilities	0.3
Grass-roots plant	0.8

To reduce the complexity of the model, all calculations are based on the assumption of an outdoor construction which is a major addition to existing facilities, in line with a scenario that a company in Western Europe would build the process facilities near existing operations. The final step of the estimation process is computing the total permanent investment (C_{TPI}).

$$C_{TPI} = 1.5C_{DPI} \tag{4.9}$$

Bridgewater

The Bridgewater estimation is based on production rate, conversion of raw material to product and the number of functional units. Furthermore, the principle of economies of scales in introduced not only by exponents of less than 1, but also by a non-continuous function set (around 60 kton/year) describing the cost. At production rates above 60 kton/year, costs are initially lower than those estimated by the equation dictating production rates below 60 kton/year. However, costs rise more quickly with increased production, taking into account the increased complexity of building a larger facility. The function set is given by Equations 4.10 and 4.11.

$$C_{ISBL,2000} = 209700N(\frac{Q}{s})^{0.3} \quad if \quad Q \leq 60000\frac{ton}{year} \tag{4.10}$$

$$C_{ISBL,2000} = 2610N(\frac{Q}{s})^{0.675} \quad if \quad Q > 60000\frac{ton}{year} \tag{4.11}$$

Where N is the number of functional units, Q is annual production of HMF and s is the overall yield (in this case, fructose to HMF yield). Using the Chemical Engineering Plant Cost Index (CEPCI), the previous estimate is adjusted to represent the current economy. The current model uses the 2017 value of 567.5 [19].

$$C_{ISBL,Current} = C_{ISBL,2000}\frac{CEPCI_{Current}}{CEPCI_{2000}} \tag{4.12}$$

After factoring in the site location the Inside Battery Limit (ISBL) costs are converted to a total permanent investment cost by using a factor of 1.2 for a fluid processing plant [16].

$$C_{TPI} = F_{ISF}(C_{ISBL} + C_{OSBL}) \tag{4.13}$$

$$C_{TPI} \approx 1.2 F_{ISF} C_{ISBL} \tag{4.14}$$

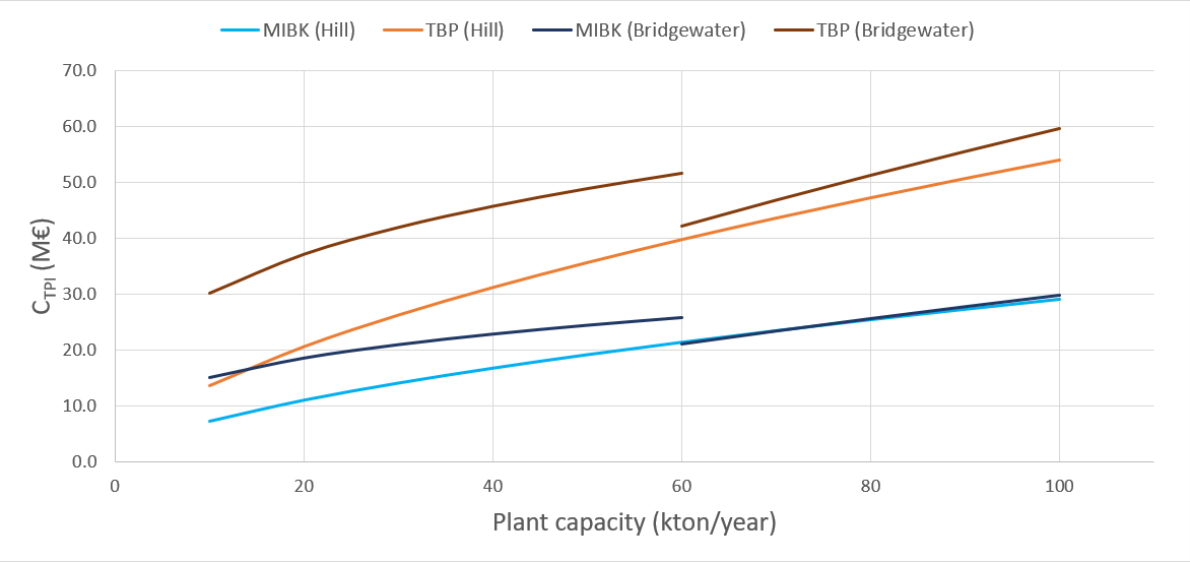

Figure 4.2: Estimated total permanent investment cost of both processes using the Hill and Bridgewater estimation methods.

Operational costs

The operational expenditure (OPEX) consist of three main factors: the raw materials, utilities and other business related costs, such as labor and indirect costs. The raw material costs are calculated using the mass balance over the process automatically calculated in the model as a function of plant capacity and the yield as predicted by the reactive extraction model. This also accounts for the recycling efficiency.

The model simultaneously calculates the utility demands based on a rudimentary energy balance over the process units, taking into account heating and cooling of streams between units and any phase changes that occur in distillation units. The unit costs of the main raw materials and steam are given in Table 4.3.

Table 4.3: Main material and utility costs.

Material/Utility	**€/ton**	
Fructose	700	[20]
MIBK	1500	[21]
TBP	2500	[22]
Heptane	1500	[23]
Steam	27	[24],[25]

Labor and indirect costs are calculated based on typical values as expressed in percentages of either the total permanent investment or sales and are given in Table 4.4 [16].

Table 4.4: Constants used for labor and indirect cost calculations.

Operating cost	
Labor	€70000 x number of shifts (4 or 5 depending on operational hours)
Supervision	15% of operating labor
Supplies	15% of maintenance supplies
Maintenance cost	
Supplies	3.5% of C_{TPI}
Labor, supervision	130% of maintenance supplies
Laboratory charges	15% of operating labor
Royalties	4% of total production costs without depreciation
Indirect cost	
Plant overhead	22% of operating and maintenance labor and supervision costs
Depreciation	Fraction of C_{TPI} depending on depreciation period
Other	3% of C_{TPI}
General cost	
Administration	2% of sales
Marketing and sales	3% of sales
Research and development	5% of sales

Key performance indicators

To keep the economic analysis consistent, proper key performance indicators (KPIs) had to be selected to compare the two processes. Pay-back time (PBT) and return on investment (ROI) were selected, as they are familiar indicators for potential investors. Minimum selling price (MSP) was selected as the least complex indicator to compare both processes.

Pay-back time

The PBT is defined as the time required for the discounted cumulative cash flow (DCCF) to become positive (i.e. when an investor would be better of investing instead of simply collecting rent without investing). Naturally, a lower PBT is more interesting for an investor, since the money is recouped faster. Additionally, a low PBT is favourable when raw material costs for a process tend to fluctuate heavily, as the initial PBT estimation involves less long-term speculation.

Return on investment

The ROI is an annual measure defined by the ratio between the profits (or losses) [26]. The ROI is based on the first year and does therefore not consider the changing value of money, due to inflation, over time. The ROI is calculated by:

$$ROI = \frac{Profits/Losses}{CAPEX} 100\% \tag{4.15}$$

The ROI can be negative or positive, depending on whether the process is profitable or not. A high ROI does not only indicate an opportunity to quickly recover the invested money, but also points towards a lower risk investment.

Minimum selling price

The minimum selling price, defined as the price HMF has to be sold at to break even (i.e. no annual profits or losses, Equation 4.16), is an interesting KPI for two reasons.

$$MSP = \frac{OPEX}{Q} \tag{4.16}$$

First, it is a very tangible indicator to compare both processes, as everyone is familiar with the concept of prices for goods. Simply put, a lower price for the same product is a better price. Secondly, this value can be used to easily compare to both other HMF processes in the future (described in literature or new research), as well as the theoretical minimum price for an ideal process, based solely on the

raw material price and yield (Y) (Equation 4.17).

$$MSP_{Theoretical} = Cost_{Fructose} \frac{M_{HMF}}{M_{Fructose}} \frac{1}{Y} \tag{4.17}$$

Using this equation, benchmark values can be computed. These are presented in Table 4.5. Since the model is based on a yield between 80 and 85%, depending on which calculation method is chosen, and a base fructose price of 700 €/ton, the lowest achievable HMF price is therefore around 1200 €/ton, before considering any costs beside raw materials.

Table 4.5: Theoretical minimum selling prices for an ideal process, with no energy requirements, perfect recycles and no other costs.

		Yield (%)					
		75	***80***	***85***	***90***	***95***	***100***
Cost (€/ton)	***500***	952	893	840	794	752	714
	600	1143	1071	1008	952	902	857
	700	1333	1250	1176	1111	1053	1000
	800	1524	1429	1345	1270	1203	1143
	900	1714	1607	1513	1429	1353	1286
	1000	1905	1786	1681	1587	1504	1429

Analysis

As the model can accommodate many configurations, the first step in analysing the respective economic performances of a MIBK or TBP based process is determining the effect of calculation methods and which factors are most influencial on the minimum selling price. Finally, different scenarios and settings are explored to conclude the comparison between the two process options. Basic inputs used for analysis are given in Table 4.6.

Table 4.6: Model setting used for analysis.

Business options	
Desired HMF selling price	€2.0/kg
Operational hours	8000 hours
Inflation rate	3%
Current fructose price	€0.7/kg
Process options	
Capacity	20 kton/year
Recycling efficiency	98%
Heat exchanger efficiency	95%
Pump efficiency	85%
Scenario options	
Cost scenario	Stable
Solvent scenario	Exp1
Fructose source	HFCS (Import)
Calculation options	
Base model	ACM RE Model
Economic approximation method	Mixed
Include pre-heating and product cooling	Yes

Calculation methods

The calculation methods which can be varied are twofold. The base model can be chosen and the economic estimation method can be selected.

The main differences between the two base models, the ACM RE model and the kinetic model, are the achieved yield (85% and 79% respectively) and the maximum HMF concentration in the reaction mixture (higher for the kinetic model). Theoretically, a high yield is more important if the raw material

costs are high in comparison to the utility costs, while a high HMF concentration is more important if the utility costs are high, as less energy will be needed to separate the final product from the reaction mixture. As can be seen in Table 4.7, the ACM model predicts lower possible selling prices, which indicates a high contribution of raw materials on the cost of HMF. This will be confirmed in the next section. However, no large anomalies are seen in selecting either of the two methods, with a maximum deviation of 5.6% (Hill estimation, MIBK).

Table 4.7: Effect of calculation settings on minimum selling price in €/kg. Input: Varying calculation options.

	Hill		**Bridgewater**		**Mixed**	
	MIBK	***TBP***	***MIBK***	***TBP***	***MIBK***	***TBP***
Kinetic Model	1.69	1.84	1.76	2.00	1.73	1.92
ACM RE Model	1.60	1.78	1.67	1.93	1.64	1.85

In addition to the Hill and Bridgewater estimators, an average value can also be selected. This can be especially interesting if the two estimators vary greatly (at low plant capacities) and a less extreme estimate is desired. Also note, that for plant capacities above 60 kton/year both methods estimate very similar values (Figure 4.2). When reviewing the minimum selling prices at 20 kton/year (Table 4.7), using the Hill method results in a more optimistic MSP, due to the lower CAPEX, which was to be expected. Furthermore, the Hill method consistently estimates a smaller percentual difference between the MSP of a MIBK or TBP based process compared to the Bridgewater estimator.

In conclusion, the selection of calculation methods comes down to how optimistic the user wants to present the results. The most optimistic estimates are found using the ACM RE Model with a Hill estimator. Opposed to this, the Kinetic Model with a Bridgewater estimator produces the most pessimistic results, which may be more interesting for potential investors.

Main contributors

The examination of the main cost contributor of the processes can be approached from different angles. The first aspect to look at is the main unknown in all calculations, the effectiveness of the anti-solvent heptane in the back-extraction of HMF in the second stage of the TBP based process. The second aspect to review is the balance between raw material, utility and other costs associated with the process options.

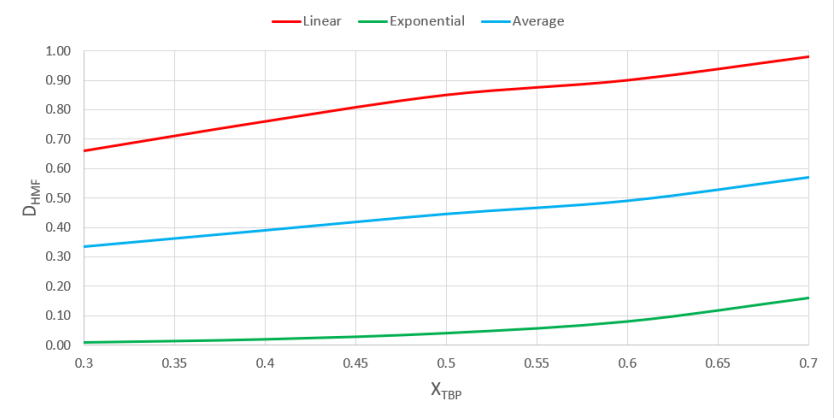

Figure 4.3: A selection of the solvent scenarios present in the model.

To bridge the CAPEX gap created by the additional units in a TBP based process, the anti-solvent should be as effective as possible in transferring the HMF from the reaction mixture back to an aqueous phase. The model includes various scenarios for this effectiveness and automatically selects the optimal ratio of heptane to TBP on the basis of resulting MSP. Three of these scenarios are presented in Figure 4.3: a linear decrease in the distribution factor, an exponential decrease or the average between the two. The resulting MSPs are given in Table 4.8. As a reference the value for a MIBK based process is included in the table.

Table 4.8: Calculated MSP for different solvent scenarios. Input: Varying solvent scenarios.

Scenario	MSP (€/kg)
Linear	1.94
Average	1.88
Exponential	1.85
Perfect	1.80
MIBK	1.64

Based on this it is very clear that the high effectiveness of an anti-solvent is an absolute necessity for even coming remotely close to the MSP of an MIBK based process. Even if the model is used to evaluate a perfect anti-solvent scenario (Solvent scenario “Zero1”), able to remove all HMF from the reaction mixture at a TBP fraction of 0.7, the MSP would be 9.7% higher than that of a MIBK based process. For further analysis, the exponential model is used, as this is the most interesting, while still being a realistic (although the most optimistic) estimation.

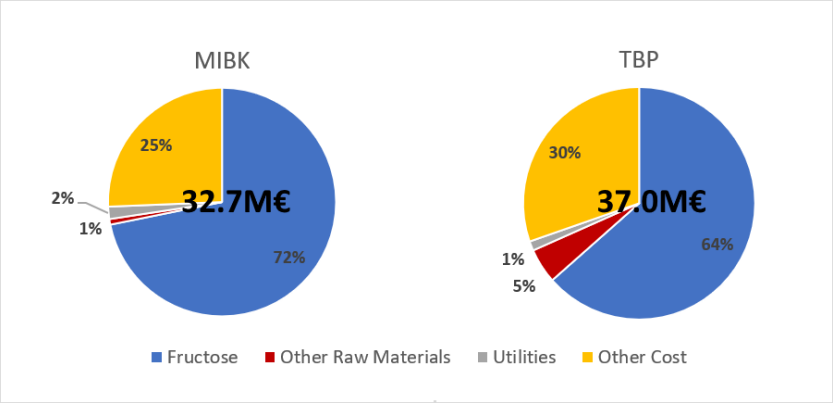

Figure 4.4: Percentual contributions of individual factors on the OPEX of a MIBK and TBP based process. The total OPEX is displayed within each pie chart.

To better grasp why there is such a difference between the resulting MSP of both process options the OPEX can be split in four main fractions as seen in Figure 4.4. Interesting to note is that the absolute contribution of fructose is the same for both processes (23.5 M€) since this is based on yield, which was kept constant between the processes, to enable a direct comparison. The other raw materials contribute more for a TBP based process, to account for additional solvent cost for the back-extraction unit. While the utility contribution (both absolute and relative) decreases slightly when switching from an MIBK to a TBP based process, this is only a small fraction of the overall cost with the current utility prices. On the other hand, the other costs considerably rise as an effect of the increased CAPEX associated with the TBP based process, accounting for two-thirds of the overall rise in operational cost.

Plant capacity

As the sales rise linearly with increased capacity, while the CAPEX (and therefore OPEX) rises exponentially with an exponent of lower than 1, it is expected that the MSP will decrease with higher capacity. This is the case, as can be seen in Figure 4.5, confirming the correct implementation of plant capacity in the model. However, as this is equally true for both processes, this does not influence the choice for one solvent over the other.

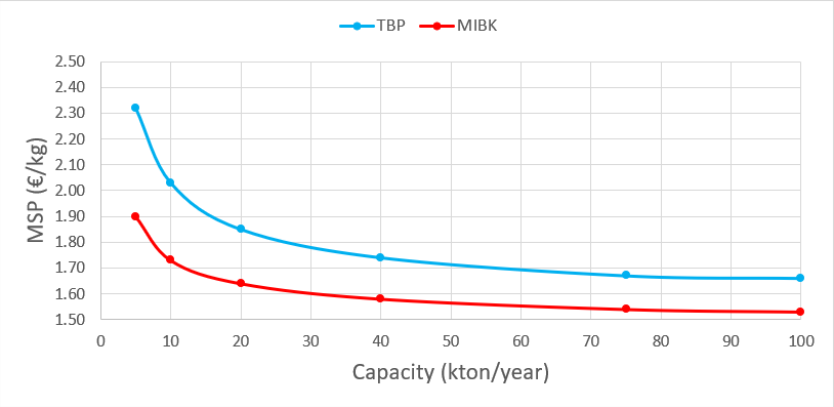

Figure 4.5: Comparison of minimum selling prices over a range of capacities. Furthermore, this shows inverse relationship between plant capacity and minimum selling price. Input: Varying capacity.

Economic scenarios

Economic scenarios can be used to assess the feasibility of both processes in case either fructose or steam prices fall or rise in the next twenty years.

As previously mentioned, fructose prices dictate the overall MSP of HMF. However, this does not create a difference between the two process options, due to the specification of a constant yield. Nevertheless, the model can be used to predict the PBT based on several scenarios, which can give interesting insights for investors. For example, if the current selling price of HMF is set at the theoretical minimum of €1.25/kg and the fructose price falls to €0.30/kg at an exponential rate in the following twenty years, the PBT of an MIBK based process is twenty years, while the TBP process is not profitable in the given time-frame (Figure 4.6). In reality, investors might use this to assess when the process becomes profitable, to plan future investments.

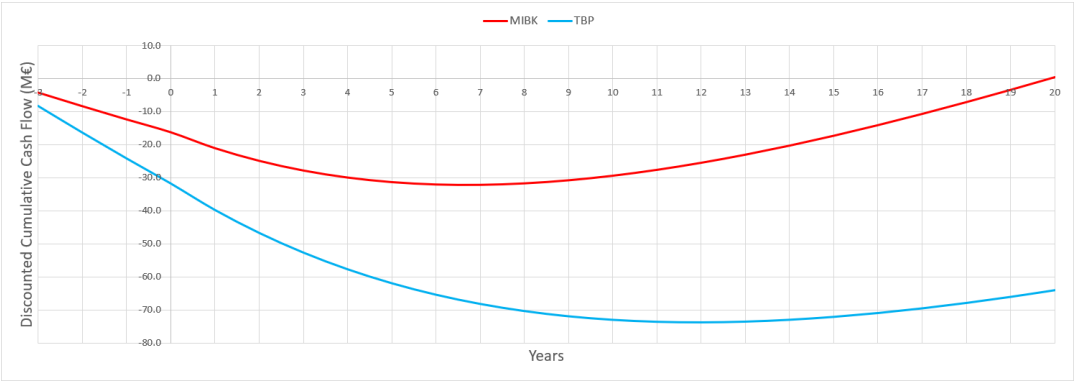

Figure 4.6: Comparison of discounted cumulative cash flows if fructose prices fall to €0.30/kg over the next twenty years.

Since the main benefit of the TBP based process is a lower steam consumption, it is comparatively favourable if steam prices rise. Unfortunately, the contribution of steam on the total cost is very small, which means a large price increase is needed before the more cost-effective process is TBP based. Illustrative of this fact is the scenario in which steam prices quadruple in the next twenty years (Figure 4.7). In this case the MIBK process still heavily outperforms the TBP based process, confirming again that the increase in CAPEX is not warranted by the slight utility benefits.

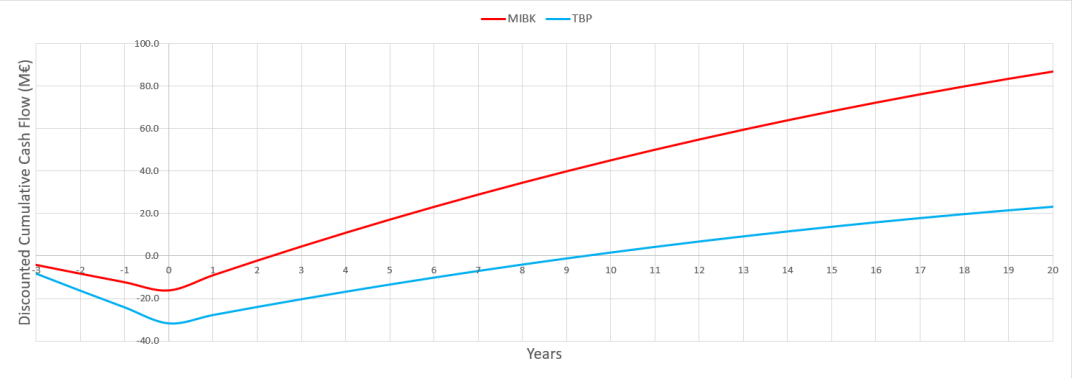

Figure 4.7: Comparison of discounted cumulative cash flows if steam prices quadruple over the next twenty years.

4.3. Sustainability

Designing a sustainable process is considered in addition to purely financial considerations as a driver behind conceptual design. The reasons behind this are both idealistic as required by European law. In the first place, academia should always strive for solutions which reduce the impact of industry on the planet, without compromising quality of life. Secondly, the European Union Emissions Trading System (EU ETS), effectively puts a cap on total greenhouse gas (GHG) emissions, for which rights have to be bought by and traded between companies [27]. If the price of these emission rights rises excessively in the future, a process with lower emissions may become more economically feasible, as a company can either produce more, without acquiring more emission right or has to pay less in order to maintain the same level of production.

Methods

The sustainability of the processes was evaluated using a life-cycle analysis (LCA). The main benefit of using a LCA is that it is simple to use and review, yet able to cover all aspects of the process, by converting all emissions to CO_2 equivalents. A drawback of using a LCA, as with any model, is that it is only as accurate as the inputs. Therefore, a strategy was adopted to find the most accurate and consistent values, by reviewing data sources in the following order:

1. **Preferred source**. Values found in public database “Idemat 2017”, Ecoinvent V3.3. This is preferred, since the calculation method is consistent for all values.

2. **Secondary source**. Values found in literature, calculation methods may vary. Preferred over estimation, especially for highly contributing factors.

3. **Estimation**. Values estimated by either finding values of precursors and taking a (stoichiometrically) weighted average or taking a value of a similar compound.

Analysis

The key results of the LCA are presented in Table 4.9. As expected the carbon footprint of a TBP based process is smaller than that of a MIBK based process, since the raw material contributions are comparable due to the specified yield and the TBP process is specifically designed to reduce the main other contributor, steam.

Table 4.9: Key results from the LCA of both process options.

		MIBK		TBP	
		(kg CO_2eq/ kg HMF)	(% of total)	(kg CO_2eq/ kg HMF)	(% of total)
Factor	Fructose	1.43	(72.3)	1.43	(75.1)
	Other raw materials	0.05	(2.7)	0.05	(2.8)
	Steam	0.47	(23.7)	0.40	(21.1)
	Other	0.03	(1.3)	0.02	(1.1)
	Total	1.97		1.90	

The lion's share of the emissions is due to fructose. To accommodate for different business scenarios, three possible fructose sources are included in the model. The emission factors and resulting emissions are given in Table 4.10.

Table 4.10: Emission values for fructose obtained from three different agricultural sources [28]. Computed HMF emission values are given for both process options.

Source	**Emission factor (kg CO_2eq/ kg fructose)**	**MIBK (kg CO_2eq/ kg HMF)**	**TBP (kg CO_2eq/ kg HMF)**
Beets	0.50	1.39	1.31
Cane	0.70	1.72	1.65
HFCS	0.85	1.97	1.90

Since the LCA is independent of plant capacity, an emission difference of 3.7%, indicates that the theoretical production volume can be 3.7% higher for a TBP based process, under the assumption that the facility is operating at the emission limit posed by the EU ETS. In turn, this has a direct effect on the sales figures, as can be seen in Figure 4.8. The dashed line represents the DCCF without taking the increased production into account. Including this effect only slightly increases the relative performance of the TBP based process, only decreasing the PBT from 9 years to 8 years and 8 months for a plant capacity of 20 kton/year.

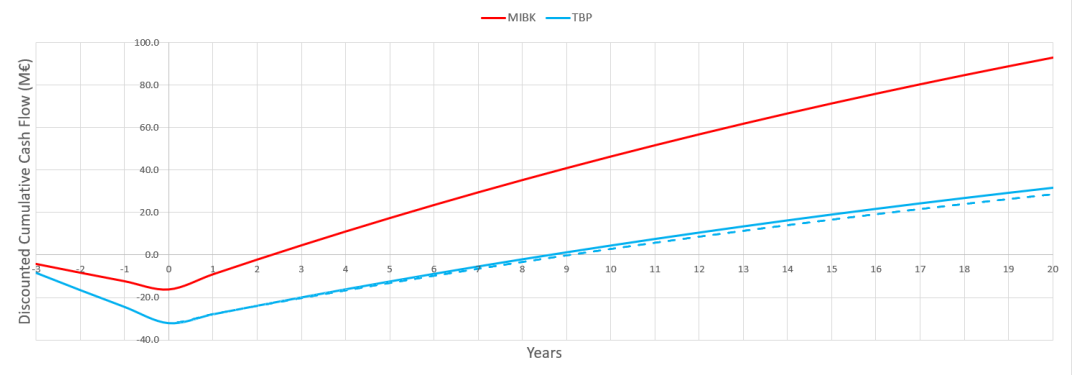

Figure 4.8: The effect of lower emissions on the DCCF for a TBP based process, when operating at the emission limit posed by the EU ETS.

On a final note, the LCA only considers the cradle-to-gate cycle for the product. It can be expected that more GHGs are emitted during the build of a TBP based process facility, due to the increased number of units. This was left out of consideration, due to the one-off nature of these emissions (no additional emissions after commissioning), however it is worth thinking about, considering the small difference in carbon footprint between the two options.

4.4. Conclusion

Based on the analysis of both process options, it is clear that for both the cost associated with the production of HMF, as well as the carbon emissions, fructose is the main contributor. Any energy requirement benefits a TBP based process has over a MIBK based process, are too small to make a definitive impact, compared to the high CAPEX (approximately doubled) and OPEX (around a 15% increase depending on capacity). Furthermore, the carbon emission reductions are too low to justify the TBP based process on a basis of a production limit, since the MIBK process is still the superior option for all KPIs.

Therefore, it is recommended not to pursue the option of using TBP as a solvent for the production of HMF at this moment in time. A more fruitful endeavor could be the further optimisation of a MIBK based process, including detailed design of the reactive extraction unit, as well as heat integration. In future studies, it is recommended to either examine solvents which can be separated by distillation (like MIBK), or have far superior solvent characteristics, such that a larger volume difference can be obtained for the RE unit, substantially lowering the CAPEX of such a process.

To get an idea of how much the CAPEX should be lowered, the theoretical CAPEX for a TBP based process was determined at which the MSP is equal to that of a MIBK based process (Figure 4.9). The assumption was made that the labor cost for operators is only influenced by the number of units in the process and not by production volumes, and material losses in recycle were not taken into account. Even then, it is only above a production of 60 kton/year at which the reduction in utility cost exceed the additional labor cost of operating two more units. This means that at a production rate below 60 kton/year, the CAPEX of a TBP based process should actually be lower than the CAPEX of a MIBK based process to be feasible.

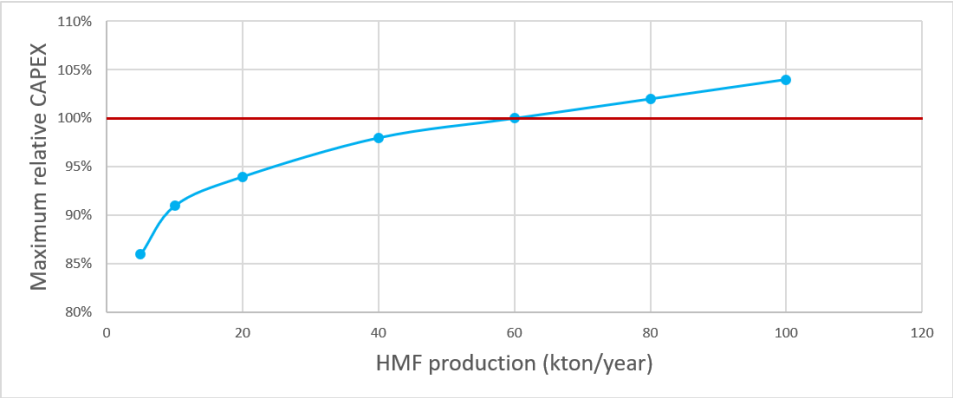

Figure 4.9: Maximum relative CAPEX for a TBP based process as a function of HMF production.

Ideally, a future solvent will also enable a process capable of achieving a yield of at least 90% at low solvent-to-feed ratios, since this will directly lower the overall fructose consumption. MIBK is also not capable of such yields at low solvent-to-feed ratios, as seen in Section 2.3. Interestingly, the current approach of focusing on higher HMF fractions also reduces the MSP of a MIBK based process compared to the previously described operating conditions at low HMF concentrations, as can be seen in Table 4.11, where the MSP has been calculated by adapting the process model to fit the RE operating conditions at low HMF concentration.

Table 4.11: Overview of computed process options.

	TBP		**MIBK**			
HMF concentration	High				Low	
Calculation model	Kinetic	ACM	Kinetic	ACM	ACM	ACM
Yield	0.79	0.85	0.79	0.85	0.85	0.90
x_{HMF}	0.54	0.29	0.38	0.23	0.01	0.001
x_{Water}	0.03	0.04	0.02	0.02	0.97	0.97
$x_{Solvent}$	0.43	0.67	0.60	0.60	0.02	0.03
MSP_{HMF} (€/kg)	1.92	1.85	1.73	1.64	2.31	8.02

5

Conclusion and recommendations

Conclusion

After comparing a TBP-based and a MIBK-based process for the production of HMF by reactive extraction, it can be concluded that a MIBK-based process is most feasible at this point in time, even though the performance of TBP is superior when only assessing the reactive extraction unit, due to the small margins presented by energy reductions.

At a yield of 85% results of the reactive extraction pointed to expected results. Since TBP has the highest affinity for HMF, solvent to feed ratios are below those of the volatile solvents. However, the performance of TBP across the board matches MIBK performance closely, except for a higher water content of the organic phase. Yields of 90% were not attainable at realistic solvent to feed ratios, due to limitations in selectivity. Examining the model at these high yield uncovered an issue with the model, in which the catalyst concentration was allowed to increase tremendously (even by 200% for 2-pentanol) along the stages. This was resolved by not separating the water from the organic reaction mixture before recycling the solvent, resulting in an already saturated organic feed.

Since the goal of the project was to find an optimal process, in which the least amount of energy is employed per unit of HMF produced, all the produced data was interpreted in a wider context than only the RE unit. As separation of HMF from MIBK (or 2-pentanol) can be achieved using distillation, while HMF and TBP cannot due to close relative volatility, it was of key importance that the RE performance of TBP, which is the intrinsically superior solvent, is distinctly better than the MIBK or 2-pentanol performance, to allow for two extra process units in the downstream processing of the TBP-HMF product stream.

A step-by-step approach was taken to close the gap between a TBP-based process, using back-extraction to separate the HMF from the reaction mixture, and a MIBK-based process. By increasing the complexity from a single equilibrium stage, to a continuous column, ending with a more conceptual approach, it was possible to reduce the energy requirement for a TBP-based process to around 90% of that of a MIBK-based one, although the exact change in distribution coefficient due to the addition of an anti-solvent (hexane or heptane) was not known and had to be approximated by different scenarios for purpose of economic calculations.

Based on the analysis of both process options, it is clear that for both the cost associated with the production of HMF, as well as the carbon emissions, fructose is the main contributor. Any energy requirement benefits a TBP based process has over a MIBK based process, are too small to make a definitive impact, compared to the high CAPEX (approximately doubled) and OPEX (around a 15% increase depending on capacity). Furthermore, the carbon emission reductions are too small to justify the TBP based process on a basis of a production limit, since the MIBK process is still the superior option for all economic key performance indicators.

Recommendations

From the outset it was clear, that the margins were small, due to the excessive contribution fructose has on the price of the final product. Therefore, it is worthwhile researching novel solvents which enable a process to be operated at very high selectivities, with a reduced emphasis on high conversion, which can also be achieved by a smart recycle design.

Due to economic and sustainability related reasoning, it is recommended not to pursue the option of using TBP as a solvent for the production of HMF at this moment in time. A more fruitful endeavor could be the further optimisation of an MIBK based process, including detailed design of the reactive extraction unit, as well as heat integration. In future studies, it is recommended to either examine solvents which can be separated by distillation (like MIBK), or have far superior solvent characteristics, such that a larger volume difference can be obtained for the RE unit, substantially lowering the CAPEX of such a process. Ideally, such a solvent will also enable a process capable of achieving a yield of at least 90% at low solvent-to-feed ratios, since this will directly lower the overall fructose consumption.

Furthermore, new studies on organic solvents with a high boiling point such as TBP, should only be undertaken if it is very clear from the beginning that the increase in CAPEX will be offset by the superior solvent characteristics in both the reactive extraction unit, as well as a subsequent separation unit. The model developed for TBP can aide in the initial screening of new solvents, even after acquiring a small set of experimental data points for a novel solvent, which reduces project duration in the future.

List of Figures

List of Tables

Bibliography

[1] I. K. M. Yu and D. C. W. Tsang. Conversion of biomass to hydroxymethylfurfural: A review of catalytic systems and underlying mechanisms. *Biosource Technology*, 238:716–732, 2017.

[2] R.-J. van Putten. Experimental and modelling studies on the synthesis of 5-hydroxymethylfurfural from sugars. *University of Groningen (PhD Thesis)*, 2015.

[3] A. D. Patel. Techno-economic analysis of Di-butyl ketone, Di-methyl furan and Hydroxymethylfurfural production from biomass based resources. *Iowa State University (MSc Thesis)*, 2009.

[4] T. Wang. Catalytic conversion of glucose to 5-hydroxymethylfurfural as potential biorenewable platform chemical. *Iowa State University (PhD Thesis)*, 2014.

[5] Zhang-L. Zhou T. Chen J. Wang, C. and F. Xu. Synergy of Lewis and Brønsted acids on catalytic hydrothermal decomposition of carbohydrates and corncob acid hydrolysis residues to 5-hydroxymethylfurfural. *Scientific Reports*, 7:40908:1–9, 2017.

[6] M. Ottocento. Conceptual Design of HMF production by Reactive Extraction. Using 2-pentanol as the solvent and in the presence of an inorganic salt. *Delft University of Technology (MSc Thesis)*, 2018.

[7] R. Ravindran. Reactive Extraction of HMF. A Conceptual Design Model for higher selectivity of HMF from Fructose. *Delft University of Technology (MSc Thesis)*, 2018.

[8] N. van den Burg. HMF production via Reactive Extraction. Model design and validation for the simultaneous production and separation of 5-hydroxymethyl furfural. *Delft University of Technology (MSc Thesis)*, 2017.

[9] Pujar S. C. Altway, S. and A. B. de Haan. Liquid-liquid equilibria of ternary and quaternary systems involving 5-hydroxymethylfurfural, water, organic solvents, and salts at 313.5 K and atmospheric pressure. *Fluid Phase Equilibria*, 475:100–110, 2018.

[10] Leeman M. Vossebed F. Visser T. J. Schuur B. Krzyzaniak, A. and A. B. de Haan. Novel extractants for the recovery of fermentation derived lactic acid. *Separation and Purification Technology*, 111:82–89, 2013.

[11] Yawalkar A. A. Moulijn J. A. Wasewar, K. L. and V. G. Pangarkar. Fermentation of Glucose to Lactic Acid Coupled with Reactive Extraction: A Review. *Industrial & Engineering Chemistry Research*, 43:5969–5982, 2004.

[12] I. S. Udachan and A. K. Sahoo. A Study of Parameters Affecting the Solvent Extraction of Lactic Acid from Fermentation Broth. *Brazilian Journal of Chemical Engineering*, 31:821–827, 2014.

[13] Wang F. Yu Y. Wang L. Ma, H. and X. Li. Autocatalytic Production of 5-Hydroxymethylfurfural from Fructose Based Carbohydrates in a Biphasic System and Its Purification. *Industrial & Engineering Chemistry Research*, 54:2657–2666, 2015.

[14] Donadieu L. Orlander, D. R. and M. Benedict. The Distribution of Nitric Acid Between Water and Tributyl Phosphate - Hexane Solvents. *American Institute of Chemical Engineers*, 7:152–159, 1961.

[15] G. J. Petley. A method for estimating the capital cost of chemical process plants: fuzzy matching. *Loughborough University*, 1997.

[16] Seader J. D. Lewin D. R. Seider, W. D. and S. Widagdo. *Product and Process Design Principles: Synthesis, Analysis, and Evaluation*. John Wiley Sons, Inc., 2009.

[17] Sherif E.-S. M. Abdo H. S. Alharti, N. and S. Z. El Abedin. Effect of Nickel Content on the Corrosion Resistance of Iron-Nickel Alloys in Concentrated Hydrochloric Acid Pickling Solutions. *Advances in Materials Science and Engineering*, 1893672:1–8, 2017.

[18] Marshall Swift Valuation Services. Report - Inventory Index Factors. pages 1–9, 2018.

[19] Chemengonline. CEPCI. URL: `http://scribd.com/document/410567937/cepci-2019`. Retrieved: December 16, 2019.

[20] Huang-K. Maravelias C. T. Motagamwala, A. H. and J. A. Dumesic. Solvent system for effective near-term production of 5-hydroxymethylfurfural (HMF) with potential for long-term process improvement. *Energy & Environmental Science*, 12:2212–2222, 2019.

[21] ICIS. MIBK prices. URL: `https://www.icis.com/explore/resources/news/2017/02/14/10078953/european-mibk-spot-prices-continue-to-rise-on-feedstocks-tightness/`. Retrieved: December 16, 2019.

[22] TBP prices. URL: `https://www.alibaba.com/showroom/price-tributyl-phosphate.html`. Retrieved: December 16, 2019.

[23] Heptane prices. URL: `https://www.alibaba.com/showroom/industrial-grade-heptane.html`. Retrieved: December 16, 2019.

[24] U.S. Department of Energy. How To Calculate The True Cost of Steam. 2003.

[25] U.S. Department of Energy. Benchmark the Fuel Cost of Steam Generation. 2012.

[26] A. Botchkarev and P. Andru. A Return on Investment as a Metric for Evaluating Information Systems: Taxonomy and Application. *Interdisciplinary Journal of Information, Knowledge, and Management*, 6:245–269, 2011.

[27] European Commission. *EU ETS Handbook*. European Union, 2015.

[28] Landquist B. Klenk, I. and O. R. de Imaña. The Product Carbon Footprint of EU beet sugar. *Sugar Industry*, 137:169–177, 2012.

[29] A. Cesnovar. Modelling the Acid Catalyzed Production of 5-Hydroxymethylfurfural from Fructose and Glucose. *Delft University of Technology (MSc Thesis)*, 2016.

A

Experimental data

The experimental data used during this project was provided by Saidah Altway.

TBP

Table A.1: Data for the TBP-HMF-water system. $T = 40°C$, $P = atmospheric$.

w_{HMF}^{Org}	D_{HMF}	S
0.0508	3.70	60.7
0.1058	3.25	55.1
0.1225	2.51	44.8
0.1741	2.46	37.3
0.2079	2.07	32.3
0.2167	1.70	24.6
0.3188	1.67	21.7
0.3419	1.21	14.1

Table A.2: Data for the TBP-HMF-water-NaCl-DES system. $T = 40°C$, $P = atmospheric$.

w_{HMF}^{Org}	D_{HMF}	S
0.0492	4.43	71.5
0.0857	3.82	65.9
0.1186	3.41	63.1
0.1400	3.14	56.1
0.1503	3.01	52.8
0.1874	2.92	47.9
0.2142	2.37	37.0
0.2291	2.06	32.2

MIBK

Table A.3: Data for the MIBK-HMF-water system. $T = 40°C$, $P = atmospheric$.

w_{HMF}^{Org}	D_{HMF}	S
0.0339	1.47	54.4
0.0587	1.38	43.1
0.0931	1.29	29.3
0.1128	1.24	28.8
0.1272	1.15	26.7
0.1752	1.10	20.4
0.2138	1.05	14.2
0.2601	0.97	8.8

Table A.4: Data for the MIBK-HMF-water-NaCl system. $T = 40°C$, $P = atmospheric$.

w_{HMF}^{Org}	D_{HMF}	S
0.0361	2.24	86.2
0.0855	2.06	64.4
0.1010	2.00	62.5
0.1279	2.19	60.8
0.1953	2.23	49.6
0.1940	2.00	40.8
0.2404	2.22	41.1
0.2953	2.34	34.9

2-pentanol

Table A.5: Data for the 2-pentanol-HMF-water system. $T = 40°C$, $P = atmospheric$.

w_{HMF}^{Org}	D_{HMF}	S
0.0403	1.94	15.6
0.0649	1.92	14.4
0.0898	1.86	12.7
0.1347	1.79	10.5
0.1394	1.78	9.8
0.1852	1.66	9.0
0.2095	1.58	7.5
0.2803	1.32	4.2

Table A.6: Data for the 2-pentanol-HMF-water-NaCl system. $T = 40°C$, $P = atmospheric$.

w_{HMF}^{Org}	D_{HMF}	S
0.0421	2.70	26.0
0.0860	2.39	21.9
0.1242	2.44	21.4
0.1568	2.33	20.3
0.1863	2.32	20.2
0.2305	2.61	22.1
0.2174	2.35	19.6
0.2543	2.45	18.8

B

Aspen Custom Modeler code

Aspen Custom Modeler (Version 8.8) was used to compute the composition of the reaction mixture based on the model developed by M. Ottocento [6]. The available stand-alone ACM model provided the basis for the design so far. However, to use it in a complex process flowsheet it had to be functionalized using ports to specify process variables. Furthermore an icon was created and streams attached for the ports to retrieve data from. The functionalized icon with streams and the input windows are shown in Figures B.1 and B.2 respectively.

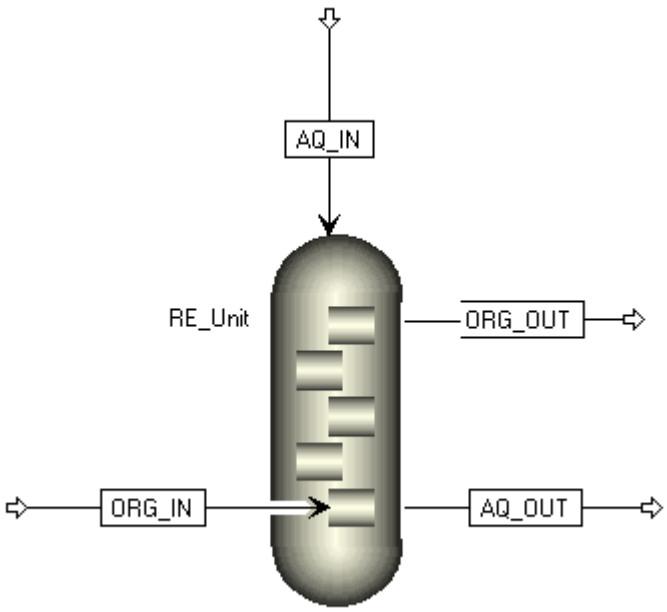

Figure B.1: RE model, including all in- and outflows, in the Aspen Custom Modeler environment.

	Value	Spec
UserNotes		
<ComponentList	Default	
<F	100,0	Fixed
<w("FA")	0,0	Fixed
<w("FRU")	0,1	Fixed
<w("HCL")	0,06	Fixed
<w("HMF")	0,0	Fixed
<w("HUM-FRU")	0,0	Fixed
<w("HUM-HMF")	0,0	Fixed
<w("LA")	0,0	Fixed
<w("MIBK")	0,0	Fixed
<w("NACL")	0,1	Fixed
<w("WATER")	0,74	Fixed

	Value	Spec
UserNotes		
<ComponentList	Default	
<F	400,0	Fixed
<w("FA")	0,0	Fixed
<w("FRU")	0,0	Fixed
<w("HCL")	0,0	Fixed
<w("HMF")	0,0	Fixed
<w("HUM-FRU")	0,0	Fixed
<w("HUM-HMF")	0,0	Fixed
<w("LA")	0,0	Fixed
<w("MIBK")	0,97	Fixed
<w("NACL")	0,0	Fixed
<w("WATER")	0,03	Fixed

Figure B.2: Stream specification input windows (left: aqueous phase, right: organic phase) in the Aspen Custom Modeler environment (shown for MIBK system).

```
Model RETBP

//            operating conditions and general constants            //

Nst as IntegerParameter (description: "maximum number of stages [-]");
Nst: 5;

N_stages([0:Nst+1]) as RealVariable (description: "number of stages [-]");
DEF_NSTAGES_0: N_stages(0)=0;
DEF_NSTAGES_Npiul: N_stages(Nst+1)=Nst+1;

Rcost as RealParameter (description: "universal constant of gas [J/K mol]");
Rcost: 8.314;
pi as RealParameter (description: "pi");
pi: 3.14159;

//molecular weight
MW(ComponentList) as molweight (description: "molecular weight of each component [kg/kmol]");
Call (MW(ComponentList)) = pMolWeights() ComponentList;

//volume and residence time

//fixed volume
//Vol as volume (description: "volume of each stage [m3]", spec:Fixed, value: 0.0002);
//res_time_aq ([0:Nst]) as RealVariable (description: "residence time of aqueous phase [min]");
//res_time_org ([1:Nst+1]) as RealVariable (description: "residence time of organic phase [min]");
//res time aq average as RealVariable (description: "average residence time of aqueous phase [min]");

//fixed average mixer time
Vol as RealVariable (description: "volume of each stage [m3]");
res time aq ([0:Nst]) as RealVariable (description: "residence time of aqueous phase [min]");
res time org ([1:Nst+1]) as RealVariable (description: "residence time of organic phase [min]");
res_time_aq_average as RealParameter (description: "average residence time of aqueous phase [min]");
res_time_aq_average: (2*0.259);

//temperature
T([0:Nst+1]) as temperature (description: "temperature [C]");
DEF_T0: T(0)=140;
for n in [1:Nst+1] do
//comment one of the following
DEF Tn const: T(n)=T(0); //T constant along the stages
//DEF_Tn_decr: T(n)= T(n-1)-2; //T decreases along the stages
endfor

Tr as temperature (description:"reference temperature [C]", spec:Fixed, value: 94.85);

//pressure
P([0:Nst+1]) as pressure (description:"pressure [bar]");
for n in [1:Nst+1] do
//comment one of the following
DEF Pn const: P(n)=P(0); //P constant along the stages
//DEF_Pn_decr: P(n)= P(n-1)-0.001; //P descreases along the stages
endfor

Pvap_top as pressure (description:"vapour pressure of the aqueous mixture [bar]");
Pvap bottom as pressure (description:"vapour pressure of the aqueous mixture [bar]");

//_____________________________fraction, concentration and densities_____________________________//

//aqueous phase
x(ComponentList)([0:Nst]) as molefraction (description: "molar fraction of the aqueous phase
[kmol/kmol]");
wx(ComponentList)([0:Nst]) as massfraction (description: "mass fraction of the aqueous phase [kg/kg]"
);
C aq(ComponentList)([0:Nst]) as conc mole (description: "concentration of the aqueous phase[kmol/m3]"
);
rho_aq([0:Nst]) as dens_mol (description: "total concentration of the aqueous phase [kmol/m3]");
rho_aq_mass([0:Nst]) as dens_mass (description: "total density of the aqueous phase [kg/m3]");

w HUM([0:Nst]) as massfraction (description: "total mass fraction of humins");
x_HUM([0:Nst]) as molefraction (description: "total molar fraction of humins");
C_HUM([0:Nst]) as conc_mole (description:"total molar concentration of humins [kmol/m3]");

//organic phase
y(ComponentList)([1:Nst+1]) as molefraction (description: "molar fraction of the organic phase
[kmol/kmol]");
wy(ComponentList)([1:Nst+1]) as massfraction (description: "mass fraction of the organic phase
[kg/kg]");
C_org(ComponentList)([1:Nst+1]) as conc_mole (description: "concentration of the organic phase
[kmol/m3]");
rho_org([1:Nst+1]) as dens_mol (description: "total concentration of the organic phase [kmol/m3]");
rho_org_mass([1:Nst+1]) as dens_mass (description: "total density of the organic phase [kg/m3]");

//of the flow from mixer to settler
xm(ComponentList)([1:Nst]) as molefraction (description: "molar fraction of the flow going from
```

```
    mixer to settler [kmol/kmol]");
 80
 81 //                concentration acid and pH                //
 82
 83 H3O([0:Nst]) as conc_mole (description: "total concentration of the ion H+ [kmol/m3]");
 84
 85 //                              flow                              //
 86 //aqueous phase
 87 R([0:Nst]) as flow_mol (description: "molar flow of the aqueous phase [kmol/hr]");
 88 R_mass([0:Nst]) as flow_mass (description: "mass flow of the aqueous phase [kg/hr]");
 89 R_vol([0:Nst]) as flow_vol (description: "volumetric flow of the aqueous phase [m3/hr]");
 90
 91 //organic phase
 92 E([1:Nst+1]) as flow_mol (description: "molar flow of the organic phase [kmol/hr]");
 93 E_mass([1:Nst+1]) as flow_mass (description: "mass flow of the organic phase [kg/hr]");
 94 E_vol([1:Nst+1]) as flow_vol (description: "volumetric flow of the organic phase [m3/hr]");
 95
 96 //from mixer to the settler
 97 Rm([1:Nst]) as flow_mol (description: "molar flow of the flow going from the mixer to the settler
    [kmol/hr]");
 98
 99 //initial flow
100 F as flow_mass (description: "mass feed flow [kg/hr]", spec: Fixed, value: 46000);//20kton/year at
    8000 hours
101 S as flow_mass (description: "mass solvent flow [kg/hr]");
102 sf_ratio as RealVariable (description: "solvent to feed ratio [-]", spec:Fixed, value: 2);
103
104 //_____________________physical equilibrium_____________//
105
106 //distribution coefficient
107 Kd([1:Nst]) as RealVariable (description: "distribution coefficient of HMF [kg/kg]");
108 Kd nosalt as RealVariable (description: "distribution coefficient of HMF in a system without salt
    [kg/kg]", spec:Fixed, value: 3.15); //MIBK: 1.21 //2pentanol: 1.73
109 Ks_Kd as RealVariable (description: "Setscheow (or salting) constant for the distribution
    coefficient [M-1]", spec:Fixed, value: 0); //MIBK: 0.15 //2pentanol: 0.088
110
111 //selectivity
112 SelS([1:Nst]) as RealVariable (description: "selectivity of the solvent [kg/kg]");
113 SelS_nosalt as RealVariable (description: "selectivity of the solvent in a system without salt
    [kg/kg]", spec:Fixed, value: 53.31); //MIBK: 28.23 //2pentanol: 10.43
114 Ks SelS as RealVariable (description: "Setscheow (or salting) constant for the selectivity of the
    solvent [M-1]", spec:Fixed, value: 0); //MIBK: 0.17 //2pentanol: 0.18
115
116 //_____________________kinetic parameters by Cesnovar_____________________//
117
118 k0 dehyd as RealParameter (description:"kinetic constant for dehydration of fructose [(mol/L)^x/min]
    = [(kmol/m^3)^x/min]", value:9.29e-3);
119 k0_hyd as RealParameter (description:"kinetic constant for rehydration of HMF [(mol/L)^x/min] =
    [(kmol/m^3)^x/min]", value:1.05e-2);
120 k0_decFRU as RealParameter (description:"kinetic constant for decomposition of fructose
    [(mol/L)^x/min] = [(kmol/m^3)^x/min]", value:4.45e-3);
121 k0_decHMF as RealParameter (description:"kinetic constant for decomposition of HMF [(mol/L)^x/min] =
    [(kmol/m^3)^x/min]", value:1.77e-3);
122
123 p1 as RealParameter (description:"exponent kinetic H+ in dehydration of fructose", value:1.76);
124 p2 as RealParameter (description:"exponent kinetic H+ in decomposition of fructose", value:1.59);
125 r1 as RealParameter (description:"exponent kinetic H+ in rehydration HMF", value:1.46);
126 r2 as RealParameter (description:"exponent kinetic H+ in decomposition HMF", value:1.35);
127 m1 as RealParameter (description:"exponent kinetic FRU in dehydration of fructose", value:1.02);
128 m2 as RealParameter (description:"exponent kinetic FRU in decomposition of fructose", value:1.36);
129 n1 as RealParameter (description:"exponent kinetic HMF in rehydration of HMF", value:0.96);
130 n2 as RealParameter (description:"exponent kinetic HMF in dehydration of HMF", value:1.02);
131
132 EA_dehyd as RealParameter (description:"activation energy dehydration of fructose [J/mol]", value:
    150800);
133 EA hyd as RealParameter (description:"activation energy rehydration of HMF [J/mol]", value:104800);
134 EA_decFRU as RealParameter (description:"activation energy decomposition of fructose [J/mol]", value:
    124000);
135 EA_decHMF as RealParameter (description:"activation energy decompoisition of HMF [J/mol]", value:
    128000);
136
137 //_____________________reaction_____________________________//
138
139 Rkin_dehyd([1:Nst]) as RealVariable (description: "kinetic expression of dehydration of fructose to
    HMF [kmol/(m3*hr)]");
140 Rkin_hyd([1:Nst]) as RealVariable (description: "kinetic expression of rehydration of HMF to LA and
    FA [kmol/(m3*hr)]");
141 Rkin_decHMF([1:Nst]) as RealVariable (description: "kinetic expression of degradation of fructose
    [kmol/(m3*hr)]");
142 Rkin decFRU([1:Nst]) as RealVariable (description: "kinetic expression of degradation of HMF
    [kmol/(m3*hr)]");
143
144 Rxn(ComponentList)([1:Nst]) as RealVariable (description: "reaction for each component
    [kmol/(m3*hr)]");
145
```

```
146  //_____________conversion, selectivity and yields_____________//
147
148  p conv([1:Nst+1]) as RealVariable (description: "conversion");
149
150  p_sel_rxn([1:Nst+1]) as RealVariable (description: "overall selectivity");
151  sum_Rxn_HMF([0:Nst+1]) as RealVariable;
152  sum_Rxn_FRU([0:Nst+1]) as RealVariable;
153
154  p_yield([0:Nst+1]) as RealVariable (description: "yield");
155
156  p_sel_dehyd([1:Nst+1]) as RealVariable (description: "selectivity on fructose");
157  p_sel_hyd([1:Nst+1]) as RealVariable (description: "selectivity on hydration rxn");
158  p_sel_decHMF([1:Nst+1]) as RealVariable (description: "selectivity on degradation of HMF rxn");
159  p_sel_nonreactHMF([1:Nst+1]) as RealVariable (description: "selectivity: not reacted HMF");
160
161  sum_Rxn_dehyd([0:Nst+1]) as RealVariable (description: "sum of reaction extent of dehydration
     reaction [kmol/m3*hr]");
162  sum_Rxn_hyd([0:Nst+1]) as RealVariable (description: "sum of reaction extent of rehydration reaction
     [kmol/m3*hr]");
163  sum_Rxn_decHMF([0:Nst+1]) as RealVariable (description: "sum of reaction extent of degradation of
     HMF reaction [kmol/m3*hr]");
164
165  EQ_SUM_RXN_HMF0: sum_Rxn_HMF(0) = 0 ;
166  EQ_SUM_RXN_FRU0: sum_Rxn_FRU(0) = 0 ;
167  EQ_SUM_RXN_DEHYD0: sum_Rxn_dehyd(0) = 0 ;
168  EQ_SUM_RXN_HYD0: sum_Rxn_hyd(0) = 0 ;
169  EQ_SUM_RXN_DECHMF0: sum_Rxn_decHMF(0) = 0 ;
170
171  //_____________extraction factor and yields_____________//
172
173  ExtF([1:Nst]) as RealVariable (description: "extraction factor [-]");
174
175
176  //____________________check_____________________//
177
178  //check on molar fraction
179  check_x([0:Nst]) as RealVariable (description: "check if the sum of x equals 1 [-]");
180  check_y([1:Nst+1]) as RealVariable (description: "check if the sum of y equals 1 [-]");
181  check_xm([1:Nst]) as RealVariable (description: "check if the sum of xm equals 1 [-]");
182
183  //check on mass fraction
184  check_wx([0:Nst]) as RealVariable (description: "check if the sum of wx equals 1 [-]");
185  check_wy([1:Nst+1]) as RealVariable (description: "check if the sum of wy equals 1 [-]");
186
187  //check on mass
188  check_mass([1:Nst]) as RealVariable (description: "check if the mass is conserved [kg/hr]");
189  check_tot_mass as RealVariable (description: "check if the total mass is conserved [kg/hr]");
190
191
192  //____________________value at 0 and N+1____________________//
193
194  //residence time
195  DEF_RESTIME_AQ_0: res_time_aq(0) = 0;
196  DEF_RESTIME_ORG_Npiu1: res_time_org(Nst+1) = 0;
197  DEF_RESTIME_AQ_AVERAGE: res_time_aq_average = res_time_aq(Nst) / Nst;
198
199  //mass fraction - aqueous phase
200  DEF_W_0_HMF: wx("HMF",0) = 0.000001;
201  DEF_W_0_FRU: wx("FRU",0) = 0.36; //w=0.09 --> 0.5M// w=0.018 --> 0.1M//w=0.36 --> 2M
202  DEF_W_0_NaCl: wx("NaCl",0) = 0.1;
203  DEF_W_0_TBP: wx("TBP",0) = 0.0;
204  DEF_W_0_WATER: wx("WATER",0) = 1 - sigma(wx(ComponentList - "water",0));
205  DEF_W_0_HUMHMF: wx("HUM-HMF",0) = 0.0;
206  DEF_W_0_HUMFRU: wx("HUM-FRU",0) = 0.0;
207  DEF_W_0_LA: wx("LA",0) = 0.0;
208  DEF_W_0_FA: wx("FA",0) = 0.0;
209
210  //catalyst concentration
211  catalyst_constant as RealParameter (description: "catalyst weight fraction/M in aqueous feed");
212  catalyst_constant: 0.03485;
213
214  cat_c0 as RealParameter (description: "catalyst concentration [M]");
215  cat_c0: 2;
216
217  DEF_W_0_HCL: wx("HCl",0) = cat_c0 * catalyst_constant;
218
219
220  //0.01749 for 0.5M
221  //w=0.0018 corresponding to nearly H+ = 0.045M
222  //w=0.01 corresponding to nearly H+ = 0.26M
223  //w=0.02 corresponding to nearly H+ = 0.52M
224  //w=0.04 corresponding to nearly H+ = 1M
225  //w=0.06 corresponding to nearly H+ = 1.52M
226  //w=0.075 corresponding to nearly H+ = 2M
227
```

```
228   //mass fraction - organic phase
229   DEF W Npiu1 HMF: wy("HMF",Nst+1) = 0.0;
230   DEF W Npiu1 FRU: wy("FRU",Nst+1) = 0.0;
231   DEF_W_Npiu1_NaCl: wy("NaCl",Nst+1) = 0.0;
232   DEF_W_Npiu1_TBP: wy("TBP",Nst+1) = 1.0;
233   DEF_W_Npiu1_WATER: wy("WATER",Nst+1) = 0.0;
234   DEF W Npiu1 HUMHMF: wy("HUM-HMF",Nst+1) = 0.0;
235   DEF_W_Npiu1_HUMFRU: wy("HUM-FRU",Nst+1) = 0.0;
236   DEF_W_Npiu1_LA: wy("LA",Nst+1) = 0.0;
237   DEF_W_Npiu1_FA: wy("FA",Nst+1) = 0.0;
238   DEF_W_Npiu1_HCL: wy("HCl",Nst+1) = 0.0;
239
240   //density
241   Call (rho_aq_mass(0)) = pDens_Mass_Liq(T(0), P(0), x(ComponentList,0)) ComponentList;
242   Call (rho_org_mass(Nst+1)) = pDens_Mass_Liq(T(Nst+1), P(Nst+1), y(ComponentList,Nst+1)) ComponentList;
243
244   Call (rho aq(0)) = pDens Mol Liq(T(0), P(0), x(ComponentList,0)) ComponentList;
245   Call (rho_org(Nst+1)) = pDens_Mol_Liq(T(Nst+1), P(Nst+1), y(ComponentList,Nst+1)) ComponentList;
246
247   //from mass fraction to molar fraction
248   DEF_X_0: x(ComponentList,0) * rho_aq(0) * MW(ComponentList) = wx(ComponentList,0) * rho_aq_mass(0);
249   DEF Y Npiu1: y(ComponentList,Nst+1) * rho org(Nst+1) * MW(COmponentList) = wy(ComponentList,Nst+1)*
      rho_org_mass(Nst+1);
250
251   //concentration
252   DEF_C_0: C_aq(ComponentList,0) = x(ComponentList,0) * rho_aq(0);
253   DEF C Npiu1: C org(ComponentList,Nst+1) = y(ComponentList,Nst+1) * rho org(Nst+1);
254
255   //humins
256   DEF_CHUM_0: C_HUM(0) = 0;
257   DEF WHUM 0: w HUM(0) = 0;
258   DEF XHUM 0: x HUM(0) = 0;
259
260   //mass flow
261   DEF_RMASS_0: R_mass(0) = F;
262   DEF EMASS Npiu1: E mass(Nst+1) = S;
263   DEF_SF: S = SF_ratio * F;
264
265   //molar flow
266   DEF_R_0: R(0) * rho_aq_mass(0) = R_mass(0) * rho_aq(0);
267   DEF E Npiu1: E(Nst+1) * rho org mass(Nst+1) = E mass(Nst+1) * rho org(Nst+1);
268
269   //volumetric flow
270   DEF_RVOL_0: R_vol(0) * rho_aq_mass(0) = R_mass(0);
271   DEF_EVOL_Npiu1: E_vol(Nst+1) * rho_org_mass(Nst+1) = E_mass(Nst+1);
272
273   //check on molar fraction
274   EQ_CHECKX_0: check_x(0) = sigma(x(ComponentList,0));
275   EQ_CHECKY_Npiu1: check_y(Nst+1) = sigma(y(ComponentList,Nst+1));
276
277   //check on mass fraction
278   EQ_CHECKWX_0: check_wx(0) = sigma(wx(ComponentList,0));
279   EQ_CHECKWY_Npiu1: check_wy(Nst+1) = sigma(wy(ComponentList,Nst+1));
280
281   //check on mass
282   EQ CHECK TOTMASS: check tot mass = R mass(0) - R mass(Nst) + E mass(Nst+1) - E mass(1);
283
284   //pressure
285   Call (Pvap_top) = pVap_Pressure(T(0), x(ComponentList)(0)) ComponentList;
286   Call (Pvap_bottom) = pVap_Pressure(T(Nst), x(ComponentList)(Nst)) ComponentList;
287   DEF P0: P(0) = Pvap top + 0.5;
288
289   //H3O
290   DEF_H3O_0: H3O(0) = C_aq("HCl")(0);
291
292   ////////////////////////////////////////FORLOOP////////////////////////////////////////////////////////////
      //
293
294   for n in [1:Nst] do
295
296   DEF_NSTAGES: N_stages(n) = n;
297
298   //__________________residence time_____________________________//
299
300   DEF RESTIME AQ: ( res time aq(n) - res time aq(n-1) ) * R vol(n) = Vol * 60;
301   DEF_RESTIME_ORG: ( res_time_org(n) - res_time_org(n+1) ) * E_vol(n) = Vol * 60;
302
303   //_____________________density, concentration, mass_____________________//
304
305   //density
306   Call (rho_aq_mass(n)) = pDens_Mass_Liq(T(n), P(n), x(ComponentList,n)) ComponentList;
307   Call (rho_org_mass(n)) = pDens_Mass_Liq(T(n), P(n), y(ComponentList,n)) ComponentList;
308
309   Call (rho_aq(n)) = pDens_Mol_Liq(T(n), P(n), x(ComponentList,n)) ComponentList;
310   Call (rho_org(n)) = pDens_Mol_Liq(T(n), P(n), y(ComponentList,n)) ComponentList;
```

```
311
312   //from mass fraction to molar fraction
313   DEF X: x(ComponentList,n) * rho aq(n) * MW(COmponentList) = wx(ComponentList,n) * rho aq mass(n);
314   DEF_Y: y(ComponentList,n) * rho_org(n) * MW(COmponentList) = wy(ComponentList,n) * rho_org_mass(n);
315
316   //concentration
317   DEF CAQ: C aq(ComponentList,n) = x(ComponentList,n) * rho aq(n);
318   DEF_CORG: C_org(ComponentList,n) = y(ComponentList,n) * rho_org(n);
319
320   //molar flow
321   DEF_R: R(n) * rho_aq_mass(n) = R_mass(n) * rho_aq(n);
322   DEF E: E(n) * rho org mass(n) = E mass(n) * rho org(n);
323
324   //volumetric flow
325   DEF_RVOL: R_vol(n) * rho_aq_mass(n) = R_mass(n);
326   DEF_EVOL: E_vol(n) * rho_org_mass(n) = E_mass(n);
327
328   //humins
329   DEF_CHUM: C_HUM(n) = C_aq("HUM-FRU")(n) + C_aq("HUM-HMF")(n);
330   DEF_WHUM: w_HUM(n) = wx("HUM-FRU")(n) + wx("HUM-HMF")(n);
331   DEF_XHUM: x_HUM(n) = x("HUM-FRU")(n) + x("HUM-HMF")(n);
332
333   //acid concentration
334   EQ_H3O: H3O(n) = C_aq("HCl")(n);
335
336   //_____________________________kinetic expressions_____________________________//
337
338   DEF_RKIN_DEHYD: Rkin_dehyd(n) = 60*k0_dehyd * (exp((-EA_dehyd/(Rcost*(Tr+273.15)))*(((Tr+273.15)/(T(n
      )+273.15))-1))) * ((C_aq("FRU")(n))^m1) * ((H3O(n))^p1);
339   DEF_RKIN_HYD: Rkin_hyd(n) = 60*k0_hyd * (exp((-EA_hyd/(Rcost*(Tr+273.15)))*(((Tr+273.15)/(T(n)+273.15
      ))-1))) * ((C aq("HMF")(n))^n1) * ((H3O(n))^r1);
340   DEF RKIN DECHMF: Rkin decHMF(n) = 60*k0 decHMF * (exp((-EA decHMF/(Rcost*(Tr+273.15)))*(((Tr+273.15
      )/(T(n)+273.15))-1))) * ((C_aq("HMF")(n))^n2) * ((H3O(n))^r2);
341   DEF_RKIN_DECFRU: Rkin_decFRU(n) = 60*k0_decFRU * (exp((-EA_decFRU/(Rcost*(Tr+273.15)))*(((Tr+273.15
      )/(T(n)+273.15))-1))) * ((C_aq("FRU")(n))^m2) * ((H3O(n))^p2);
342
343   EQ_RXN_FRU: Rxn("FRU")(n) = -Rkin_dehyd(n) - Rkin_decFRU(n);
344   EQ_RXN_HMF: Rxn("HMF")(n) = +Rkin_dehyd(n) - Rkin_hyd(n) - Rkin_decHMF(n);
345   EQ_RXN_HUMHMF: Rxn("HUM-HMF")(n) = Rkin_decHMF(n);
346   EQ_RXN_HUMFRU: Rxn("HUM-FRU")(n) = Rkin_decFRU(n);
347   EQ_RXN_HCL: Rxn("HCl")(n) = 0;
348   EQ_RXN_LA: Rxn("LA")(n) = Rkin_hyd(n);
349   EQ_RXN_FA: Rxn("FA")(n) = Rkin_hyd(n);
350   EQ_RXN_WATER: Rxn("water")(n) = 3*Rkin_dehyd(n) - 2*Rkin_hyd(n);
351   EQ_RXN_TBP: Rxn("TBP")(n) = 0;
352   EQ_RXN_NACL: Rxn("NaCl")(n) = 0;
353
354   //_____________________________check_____________________//
355
356   //check on molar fraction
357   EQ_CHECKX: check x(n) = sigma(x(ComponentList,n));
358   EQ_CHECKY: check_y(n) = sigma(y(ComponentList,n));
359
360   //check on mass fraction
361   EQ_CHECKWX: check_wx(n) = sigma(wx(ComponentList,n));
362   EQ_CHECKWYn: check wy(n) = sigma(wy(ComponentList,n));
363
364   //check on mass
365   EQ_CHECK_MASS: check_mass(n) = - R_mass(n) + R_mass(n-1) + E_mass(n+1) - E_mass(n);
366
367   //                    molar balance                          //
368
369   EQ_MOLBAL_MIXER: R(n-1) * x(ComponentList,n-1) + E(n+1) * y(ComponentList,n+1) - Rm(n) * xm(
      ComponentList,n) + Vol*Rxn(ComponentList)(n)= 0;
370   EQ_MOLBAL_SETTLER: - R(n) * x(ComponentList,n) - E(n) * y(ComponentList,n) + Rm(n) * xm(ComponentList
      ,n) = 0;
371
372   //_____________________physical equilibrium_____________//
373
374   DEF KD: Kd(n) = Kd nosalt * ( 10^( Ks Kd * C aq("NaCl",n) ) );
375   DEF_SELS: SelS(n) = SelS_nosalt * ( 10^( Ks_SelS * C_aq("NaCl",n) ) );
376
377   EQUIL_HMF: wy("HMF",n) = Kd(n) * wx("HMF",n);
378   EQUIL_WATER: wy("water",n) * SelS(n) = Kd(n) * wx("water",n);
379
380   EQUIL_TBP: x("TBP",n) = 0.0;
381
382   EQUIL_NACL: y("NaCl",n) = 0.0;
383   EQUIL_FRU: y("FRU",n) = 0.0;
384   EQUIL_HUMHMF: y("HUM-HMF",n) = 0.0;
385   EQUIL_HUMFRU: y("HUM-FRU",n) = 0.0;
386   EQUIL_LA: y("LA",n) = 0.0;
387   EQUIL_FA: y("FA",n) = 0.0;
388   EQUIL_HCL: y("HCl",n) = 0.0;
389
```

```
390   //_________________SUM = 1_________________//
391   //comment one of the following
392
393   EQ_SUMX: sigma(x(ComponentList,n)) = 1;
394   EQ_SUMY: sigma(y(ComponentList,n)) = 1;
395   EQ_SUMXM: sigma(xm(ComponentList,n)) = 1;
396   /*
397   EQ_SUMWX: sigma(wx(ComponentList,n)) = 1;
398   EQ_SUMWY: sigma(wy(ComponentList,n)) = 1;
399   EQ_SUMXM: sigma(xm(ComponentList,n)) = 1;
400   */
401
402   //_____________conversion selectivity and yields_____________//
403
404   EQ_SUM_RXN_HMF: sum_Rxn_HMF(n) = sum_Rxn_HMF(n-1) + Rxn("HMF",n) ;
405   EQ_SUM_RXN_FRU: sum_Rxn_FRU(n) = sum_Rxn_FRU(n-1) + Rxn("FRU",n) ;
406   EQ_SEL_RXN: p_sel_rxn(n) * (-sum_Rxn_FRU(n)) = sum_Rxn_HMF(n);
407
408   EQ_SUM_RXN_DEHYD: sum_Rxn_dehyd(n) = sum_Rxn_dehyd(n-1) + Rkin_dehyd(n) ;
409   EQ_SUM_RXN_HYD: sum_Rxn_hyd(n) = sum_Rxn_hyd(n-1) + Rkin_hyd(n) ;
410   EQ_SUM_RXN_DECHMF: sum_Rxn_decHMF(n) = sum_Rxn_decHMF(n-1) + Rkin_decHMF(n) ;
411   EQ_SEL_DEHYD: p_sel_dehyd(n) * (-sum_Rxn_FRU(n)) = sum_Rxn_dehyd(n);
412   EQ_SEL_HYD: p_sel_hyd(n) * (sum_Rxn_dehyd(n)) = sum_Rxn_hyd(n);
413   EQ_SEL_DECHMF: p_sel_decHMF(n) * (sum_Rxn_dehyd(n)) = sum_Rxn_decHMF(n);
414   EQ_SEL_NOTREACTHMF: p_sel_nonreactHMF(n) = 1 - p_sel_hyd(n) - p_sel_decHMF(n);
415   DEF_CONV: p_conv(n) * (R(0) * x("FRU",0)) = ((R(0) * x("FRU",0)) - (R(n) * x("FRU",n)));
416   DEF_YIELD: p_yield(n) * (R(0) * x("FRU",0)) = (sum_Rxn_HMF(n) * Vol);
417
418   //_________________extraction factor___________//
419
420   DEF_EXTF: ExtF(n) * R_mass(n) = Kd(n) * E_mass(n);
421
422   endfor
423
424   End
```

C

Matlab code

Matlab (Version R2018a) was used to compute the composition of the reaction mixture based on the kinetic model developed by A. Češnovar [29]. Additionally, it was used to get initial estimates on the relationship between back-extraction and energy requirements.

Kinetic model

```
function Cmax
clc
warning off
% TList=[80 100 120 140 160 180 200];
% FRUList=[0.5 0.75 1.0 1.25 1.5 1.75 2.0 2.25 2.5 2.75 3.0 3.25 3.5 3.75 4.0 4.25
4.5 4.75 5.0];
% HClList=FRUList;
% TList=[140 200];
% FRUList=[0.5 1.0 1.5 2.0 5.0];
% HClList=FRUList;
TList=[200];
FRUList=[2.0];
HClList=[2.0];
RhoPars=[0.14395 0.0112 649.727 0.05107];

for x=1:length(TList)
for y=1:length(FRUList)
for z=1:length(HClList)
RhoSOL(x,y,z)=(RhoPars(1)/RhoPars(2)^(1+(1-(TList(x)+273.15)/RhoPars(3))^RhoPars
(4)))*(1+0.0164*HClList(z)+0.0654*FRUList(y));
Water0=(RhoSOL(x,y,z)-HClList(z)*36.46-FRUList(y)*180.16)/18.02;
c0(x,y,z,:)=[FRUList(y);0;0;0;0;0;Water0];
end
end
end

function dcdt=mix(t,c)
    R=8.314;
    Tr=94.85+273.15;
    Temp=TList(x)+273.15;
    HCl=HClList(z);
    dcdt=zeros(7,1);
    %fructose
    dcdt(1)=(-(9.29e-3*exp((-150800/(R*Tr)*(Tr/Temp-1)))*(c(1)^1.02)*(HCl^1.76))
-(4.45e-3*exp((-124000/(R*Tr)*(Tr/Temp-1)))*(c(1)^1.36)*(HCl^1.59)));
    %HMF
    dcdt(2)=((9.29e-3*exp((-150800/(R*Tr)*(Tr/Temp-1)))*(c(1)^1.02)*(HCl^1.76))
-(1.77e-3*exp((-128000/(R*Tr)*(Tr/Temp-1)))*(c(2)^1.02)*(HCl^1.35))-(1.05e-2*exp
((-104800/(R*Tr)*(Tr/Temp-1)))*(c(2)^0.96)*(HCl^1.46)));
    %fructose humins
    dcdt(3)=((4.45e-3*exp((-124000/(R*Tr)*(Tr/Temp-1)))*(c(1)^1.36)*(HCl^1.59)));
    %HMF humins
    dcdt(4)=((1.77e-3*exp((-128000/(R*Tr)*(Tr/Temp-1)))*(c(2)^1.02)*(HCl^1.35)));
    %LA
    dcdt(5)=((1.05e-2*exp((-104800/(R*Tr)*(Tr/Temp-1)))*(c(2)^0.96)*(HCl^1.46)));
    %FA
    dcdt(6)=((1.05e-2*exp((-104800/(R*Tr)*(Tr/Temp-1)))*(c(2)^0.96)*(HCl^1.46)));
    %water
    dcdt(7)=(-3*(9.29e-3*exp((-150800/(R*Tr)*(Tr/Temp-1))))*(c(1)^1.02)*(HCl^1.76)
+2*(1.05e-2*exp((-104800/(R*Tr)*(Tr/Temp-1)))*(c(2)^0.96)*(HCl^1.46)));
end

for x=1:length(TList)
```

```
for y=1:length(FRUList)
for z=1:length(HClList)
tlim=0.005;
[T,C]=ode23s(@mix,[0 tlim],c0(x,y,z,:));

if min(C(:,7))<0
    C(:,2)=zeros(length(C(:,2)),1);
end

for i=2:length(C(:,2))
   if C(i,2)>C(i-1,2)
       Cmax=C(i,2);
       Conversion=1-C(i,1)/FRUList(y);
       Selectivity=Cmax/(FRUList(y)*Conversion);
       Yield=Cmax/FRUList(y);
   end
end

figure;
plot(T,C,'LineWidth',2)
xlabel('Time (min)')
ylabel('Concentration (mol/L)')
xlim([0 tlim])
grid on
hold on
legend('Fructose','HMF','Fructose-Humins','HMF-Humins','Levulinic Acid','Formic↙
Acid','Water','Location','northeast')
title(['T=' num2str(TList(x)) '[HCl]=' num2str(HClList(z)) '[FRU]=' num2str(FRUList↙
(y))])
ylim([0 FRUList(y)])

Cstore(x,y,z)=Cmax;
Xstore(x,y,z)=Conversion;
Sstore(x,y,z)=Selectivity;
Ystore(x,y,z)=Yield;
HMFstore(x,y,z)=Cstore(x,y,z)/RhoSOL(x,y,z)*126.11;
end
end
end

MaxHMF=real(max(max(max(HMFstore))))

%Xstore
%Sstore
%Ystore

end
```

Back extraction estimator

```
function BE_Calculator
clear all

F=1000; %Arbitrary Feed Flow Rate
Feed=[0.02 0.05 0.93]; %HMF WATER TBP

%Simulated Data
Hexane=[0:0.05:1]; %xHEXANE
TBP=1-Hexane;      %xTBP
D=[0.297 0.297 0.297 0.324 0.361 0.400 0.485 0.581 0.750 1.000 1.273 1.778 2.571 ↙
3.636 5.375 9.000 15.667 24.000 53.341 113.739 277.933];    %Distribution↙
Coefficient to Water

%Parameter Fitting
function fit=fit(parameters)
for h=1:length(D)
Y(h)=parameters(1)*exp(parameters(2)*TBP(h))+parameters(3);
end
%Least Squares Minimizer
fit=0;
for i=1:length(D)
fit=fit+(Y(i)-D(i))^2;
end
end

%Initial Guess
parameters0=[280.0 -15.0 0.3];
%Run Minimizer
parameters=fminunc(@fit,parameters0);
clc

%Plot Fitted Function
for j=1:length(D)
Fit(j)=parameters(1)*exp(parameters(2)*TBP(j))+parameters(3);
end

figure;
plot(TBP,D,'x','MarkerSize',10,'LineWidth',2)
grid on
hold on
plot(TBP,Fit)
legend('Simulation','Fit','Location','east')
xlabel('x_{TBP}')
ylabel('D_{HMF}')

%Process Parameters
Hwater=2257;
Hhexane=335;

Nsteps=99;
HEXTBPmin=1;
HEXTBPmax=5;
WFRATIOmin=0.01;
```

```
WFRATIOmax=1;
Nstages=[1:1:100];
Check=10;

%Loop (z=stages,n=HEXTBPratio,m=WATERFEEDratio)
for z=1:length(Nstages)
STAGES=Nstages(z);
for n=1:Nsteps+1
HEXTBP(n)=HEXTBPmin+(n-1)*(HEXTBPmax-HEXTBPmin)/Nsteps;
mHEX(n)=HEXTBP(n)*Feed(3)*F; %Mass Hexane
for m=1:Nsteps+1
EHEX(n,m)=mHEX(n)*Hhexane; %Energy Hexane
mFEED(n,m)=mHEX(n)+Feed(3)*F; %Mass Feed
xTBP(n,m)=Feed(3)*F/mFEED(n,m); %TBP Mass Fraction
WFRATIO(m)=WFRATIOmin+(m-1)*(WFRATIOmax-WFRATIOmin)/Nsteps;
mWATER(n,m)=WFRATIO(m)*mFEED(n,m); %Mass Water
EWATER(n,m)=mWATER(n,m)*Hwater; %Energy Water
Dlocal(n,m)=parameters(1)*exp(parameters(2)*xTBP(n,m))+parameters(3); %Calculate
Dependent Distribution Coefficient
E(n,m)=Dlocal(n,m)*mWATER(n,m)/mFEED(n,m); %Extraction Factor
FracHMF(n,m)=1-((E(n,m)-1)/(E(n,m)^(STAGES+1)-1)); %Fraction HMF Extracted
mHMF(n,m)=FracHMF(n,m)*Feed(1)*F; %Mass HMF
EEXP=(EHEX+EWATER)./(mHMF*1000); %Total Energy/Mass HMF
end
end

Emin(z)=min(min(EEXP)); %Minimum Energy Requirement at Given Conditions

%Visualize for Specified Number of Stages
if STAGES==Check
figure;
surf(HEXTBP,WFRATIO,FracHMF,'EdgeColor','none','FaceColor','interp')
colormap('jet')
colorbar
zlabel('HMF Fraction Extracted')
xlabel('Hexane/TBP Ratio')
ylabel('Water/Mixture Ratio')
figure;
surf(HEXTBP,WFRATIO,EEXP,'EdgeColor','none','FaceColor','interp')
colormap('jet')
colorbar
caxis([Emin(z) Emin(z)+100])
zlabel('Energy (MJ/kg HMF)')
xlabel('Hexane/TBP Ratio')
ylabel('Water/Mixture Ratio')
end
end

%Plot MER as Function of Nstages
figure;
plot(Nstages,Emin)
grid on
xlabel('N_{stages}')
```

```
ylabel('Energy (MJ/kg HMF)')
hold on
plot([1 Nstages(end)],[53.1 53.1],'--')
plot([1 Nstages(end)],[34.5 34.5],'--')
legend('TBP','2-Pentanol','MIBK','Location','northeast')

%Plot Benefit of Additional Stages
for x=1:Nstages(end-1)
StageGain(1,x)=(Emin(x+1)-Emin(x))/Emin(x)*100;
StageGain(2,x)=x+1;
end
figure;
plot(StageGain(2,:),StageGain(1,:))
xlabel('Stage Number')
ylabel('Gain (%)')
xlim([0 40])
grid on
hold on
Limit=-1;
plot([0 40],[Limit Limit],'--')
legend('Relative Gain of Stage','Limit','Location','southeast')

end
```

D

Process model user-guide

This is a reference guide on how to use the HMF process design model. The model, created in Microsoft Excel, contains the following tabs:

1. User interface
2. Process calculation
3. Economics
4. Sustainability
5. Cost scenario database
6. Solvent scenario database
7. Material data
8. Reference sheet

User interface

The user interface (Figure D.1) is arguably the most important feature the model provides. An input section (1) with either drop-down menus or numerical inputs gives a user enough possibilities to explore different configurations, without over-complicating specific details. The output section (2) gives a quick overview of both the economic and sustainability results. These results are colour-coded to further help with analysis, with positive results being displayed in green and negative results in red. Lastly, two figures indicate which solvent scenario is selected and what this means in terms of minimum steam requirements (3).

Figure D.1: User interface tab of the process design model.

Process calculation

The process calculation tab (Figure D.2) consists of two main parts. First the organic stream composition is calculated (from the RE unit) (1). The values which are subsequently used to calculate compositions after back-extraction (2) depend on the base calculation model selected by the user (either kinetic of ACM RE) and the solvent scenario. A minimizer is used to determine the optimum ratio of TBP and anti-solvent and the final results are presented on the user interface.

Economics

On the economic tab, the main feature to review is the OPEX table, listing all individual contributions (Figure D.3). Further details include CAPEX and cash flow calculations. It is expected that a user has most of the required economics information available directly on the user interface tab.

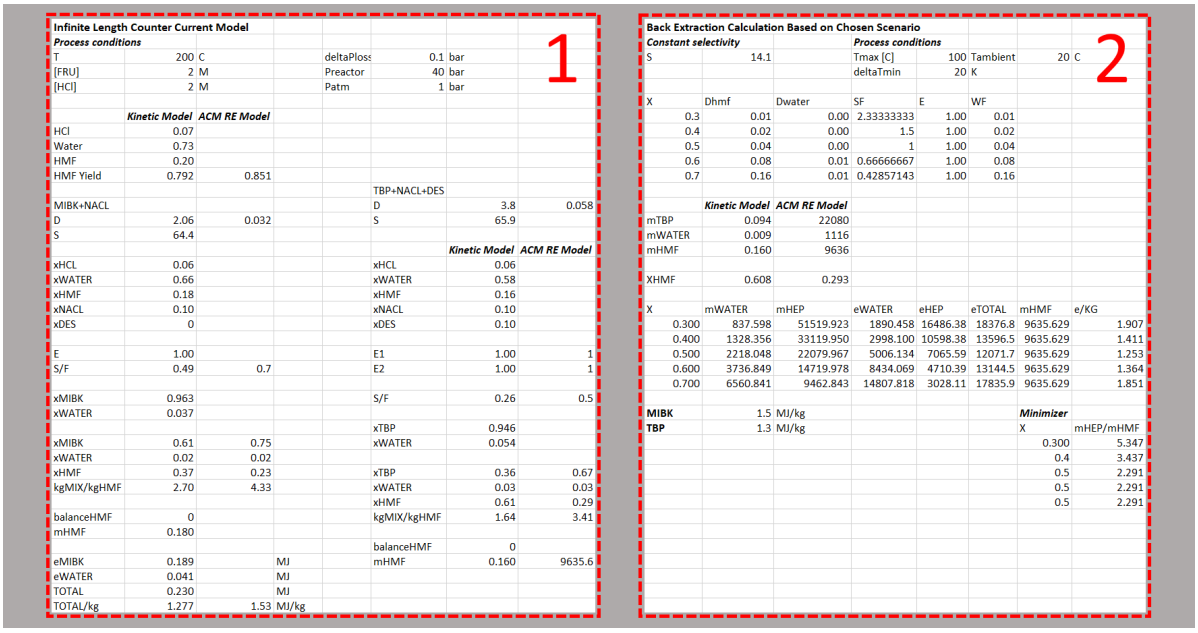

Infinite Length Counter Current Model — 1

Process conditions						
T	200	C		deltaPloss	0.1	bar
[FRU]	2	M		Preactor	40	bar
[HCl]	2	M		Patm	1	bar
	Kinetic Model	***ACM RE Model***				
HCl	0.07					
Water	0.73					
HMF	0.20					
HMF Yield	0.792	0.851				
				TBP+NACL+DES		
MIBK+NACL				D	3.8	0.058
D	2.06	0.032		S	65.9	
S	64.4					
				Kinetic Model	***ACM RE Model***	
xHCL	0.06			xHCL	0.06	
xWATER	0.66			xWATER	0.58	
xHMF	0.18			xHMF	0.16	
xNACL	0.10			xNACL	0.10	
xDES	0			xDES	0.10	
E	1.00			E1	1.00	1
S/F	0.49	0.7		E2	1.00	1
xMIBK	0.963			S/F	0.26	0.5
xWATER	0.037					
				xTBP	0.946	
xMIBK	0.61	0.75		xWATER	0.054	
xWATER	0.02	0.02				
xHMF	0.37	0.23		xTBP	0.36	0.67
kgMIX/kgHMF	2.70	4.33		xWATER	0.03	0.03
				xHMF	0.61	0.29
balanceHMF	0			kgMIX/kgHMF	1.64	3.41
mHMF	0.180					
				balanceHMF	0	
eMIBK	0.189		MJ	mHMF	0.160	9635.6
eWATER	0.041		MJ			
TOTAL	0.230		MJ			
TOTAL/kg	1.277	1.53	MJ/kg			

Back Extraction Calculation Based on Chosen Scenario — 2

Constant selectivity			*Process conditions*				
S	14.1		Tmax [C]	100	Tamblent	20	C
			deltaTmin	20	K		
X	Dhmf	Dwater	SF	E	WF		
0.3	0.01	0.00	2.33333333	1.00	0.01		
0.4	0.02	0.00	1.5	1.00	0.02		
0.5	0.04	0.00	1	1.00	0.04		
0.6	0.08	0.01	0.66666667	1.00	0.08		
0.7	0.16	0.01	0.42857143	1.00	0.16		
	Kinetic Model	***ACM RE Model***					
mTBP	0.094	22080					
mWATER	0.009	1116					
mHMF	0.160	9636					
XHMF	0.608	0.293					

X	mWATER	mHEP	eWATER	eHEP	eTOTAL	mHMF	e/KG
0.300	837.598	51519.923	1890.458	16486.38	18376.8	9635.629	1.907
0.400	1328.356	33119.950	2998.100	10598.38	13596.5	9635.629	1.411
0.500	2218.048	22079.967	5006.134	7065.59	12071.7	9635.629	1.253
0.600	3736.849	14719.978	8434.069	4710.39	13144.5	9635.629	1.364
0.700	6560.841	9462.843	14807.818	3028.11	17835.9	9635.629	1.851

MIBK	1.5	MJ/kg	***Minimizer***	
TBP	1.3	MJ/kg	X	mHEP/mHMF
			0.300	5.347
			0.4	3.437
			0.5	2.291
			0.5	2.291
			0.5	2.291

Figure D.2: Process calculation tab of the process design model.

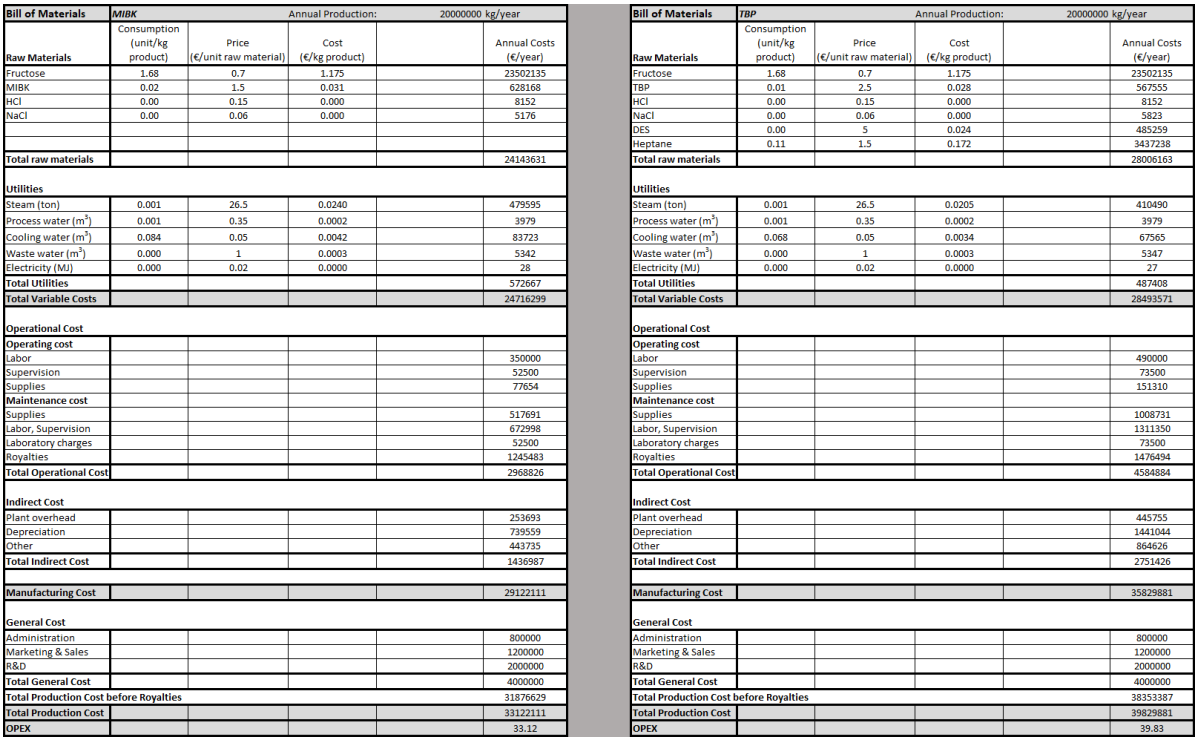

Bill of Materials — *MIBK* — Annual Production: 20000000 kg/year

Raw Materials	Consumption (unit/kg product)	Price (€/unit raw material)	Cost (€/kg product)		Annual Costs (€/year)
Fructose	1.68	0.7	1.175		23502135
MIBK	0.02	1.5	0.031		628168
HCl	0.00	0.15	0.000		8152
NaCl	0.00	0.06	0.000		5176
Total raw materials					24143631
Utilities					
Steam (ton)	0.001	26.5	0.0240		479595
Process water (m^3)	0.001	0.35	0.0002		3979
Cooling water (m^3)	0.084	0.05	0.0042		83723
Waste water (m^3)	0.000	1	0.0003		5342
Electricity (MJ)	0.000	0.02	0.0000		28
Total Utilities					572667
Total Variable Costs					24716299
Operational Cost					
Operating cost					
Labor					350000
Supervision					52500
Supplies					77654
Maintenance cost					
Supplies					517691
Labor, Supervision					672998
Laboratory charges					52500
Royalties					1245483
Total Operational Cost					2968826
Indirect Cost					
Plant overhead					253693
Depreciation					739559
Other					443735
Total Indirect Cost					1436987
Manufacturing Cost					29122111
General Cost					
Administration					800000
Marketing & Sales					1200000
R&D					2000000
Total General Cost					4000000
Total Production Cost before Royalties					31876629
Total Production Cost					33122111
OPEX					33.12

Bill of Materials — *TBP* — Annual Production: 20000000 kg/year

Raw Materials	Consumption (unit/kg product)	Price (€/unit raw material)	Cost (€/kg product)		Annual Costs (€/year)
Fructose	1.68	0.7	1.175		23502135
TBP	0.01	2.5	0.028		567555
HCl	0.00	0.15	0.000		8152
NaCl	0.00	0.06	0.000		5823
DES	0.00	5	0.024		485259
Heptane	0.11	1.5	0.172		3437238
Total raw materials					28006163
Utilities					
Steam (ton)	0.001	26.5	0.0205		410490
Process water (m^3)	0.001	0.35	0.0002		3979
Cooling water (m^3)	0.068	0.05	0.0034		67565
Waste water (m^3)	0.000	1	0.0003		5347
Electricity (MJ)	0.000	0.02	0.0000		27
Total Utilities					487408
Total Variable Costs					28493571
Operational Cost					
Operating cost					
Labor					490000
Supervision					73500
Supplies					151310
Maintenance cost					
Supplies					1008731
Labor, Supervision					1311350
Laboratory charges					73500
Royalties					1476494
Total Operational Cost					4584884
Indirect Cost					
Plant overhead					445755
Depreciation					1441044
Other					864626
Total Indirect Cost					2751426
Manufacturing Cost					35829881
General Cost					
Administration					800000
Marketing & Sales					1200000
R&D					2000000
Total General Cost					4000000
Total Production Cost before Royalties					38353387
Total Production Cost					39829881
OPEX					39.83

Figure D.3: Part of the economics tab of the process design model.

Sustainability

On the sustainability tab, the main feature to review are the LCA tables, listing all individual contributions (Figure D.4). Used reference IDs can also be found on this tab. It is expected that a user has most of the required sustainability information available directly on the user interface tab.

1. Cradle-to-gate MIBK

	Input (unit/kg product)	Distance (km)	Emission factor (kg CO2 eq/unit)	unit	Carbon footprint kg CO2 eq/kg HMF
Fructose	1.68		0.85	kg	**1.43**
Water	0.57		0.0003	kg	**0.00**
MIBK	0.02		6.30	kg	**0.13**
HCl	0.003		0.48	kg	**0.00**
NaCl	0.004		0.24	kg	**0.00**
Electricity	0.00		0.12	MJ	**0.00**
Cooling water	83.5		0.0003	kg	**0.03**
Steam	2.04		0.23	MJ	**0.47**
Shipping	0.00	0	0.01	ton.km	**0.00**
Road transport	0.00	0	0.06	ton.km	**0.00**
Pipe line	0.000	0	0.01	ton.km	**0.00**
Waste water	0.27		0.0008	kg	**0.00**
Other waste	0.00		0	kg	**0.00**
		Total			**2.05**

2. Cradle-to-gate TBP

	Input (unit/kg product)	Distance (km)	Emission factor (kg CO2 eq/unit)	unit	Carbon footprint kg CO2 eq/kg HMF
Fructose	1.68		0.85	kg	**1.43**
Water	0.57		0.0003	kg	**0.00**
TBP	0.01		4.00	kg	**0.05**
HCl	0.003		0.48	kg	**0.00**
NaCl	0.005		0.24	kg	**0.00**
DES	0.005		2.80	kg	**0.01**
Heptane	0.11		0.6	kg	**0.07**
Electricity	0.00		0.12	MJ	**0.00**
Cooling water	67.4		0.0003	kg	**0.02**
Steam	1.75		0.23	MJ	**0.40**
Shipping	0.000	0	0.01	ton.km	**0.00**
Road transport	0.000	0	0.06	ton.km	**0.00**
Pipe line	0.000	0	0.01	ton.km	**0.00**
Waste water	0.27		0.0008	kg	**0.00**
Other waste	0.00		0	kg	**0.00**
		Total			**1.98**

Figure D.4: Part of the sustainability tab of the process design model.

Cost scenario database

The cost scenario tab (Figure D.5) is used to enter new cost scenarios. The active set is displayed and the projected cost of fructose and steam are given for the next twenty years. Furthermore, base cost values and their reference IDs are found on this tab.

Base Values								
Materials			***Reference***	***Reference Date***		***Utilities***			***Reference***
Fructose	0.7	euro/kg	[5]	30/10/2019		Steam	26.5	euro/ton	[13]
NaCl	0.06	euro/kg	[6]	January 2015		Process water	0.35	euro/m3	
HCl	0.15	euro/kg	[7]	04/12/2019		Cooling water	0.05	euro/m3	
DES	5	euro/kg	[8],[9]	2010, 2019		Waste water	1	euro/m3	
Heptane	1.5	euro/kg	[10]	04/12/2019		Electricity	0.07	euro/kWh	
MIBK	1.5	euro/kg	[11]	14/02/2017			0.02	euro/MJ	
TBP	2.5	euro/kg	[12]	04/12/2019					
Period	20	years							
Scenario ID	***Full Descriptor***		***Short Descriptor***	***Fructose change***	***Fructose coefficient***	***Steam change***	***Steam coefficient***		
C1	Stable cost prices		Stable	0	1	0	1		
C2	Fructose price increase, 1000 euro/ton in 20 years		Fru1000;20Y	0.3	1.017993718	0	1		
C3	Gas/Steam price increase, double in 20 years		GasDouble;20Y	0	1	26.5	1.035264924		
C4	Fructose price decrease, 300 euro/ton in 20 years		Fru300;20Y	-0.4	0.95851996	0	1		
C5	Gas/Steam price decrease, half in 20 years		GasHalf;20Y	0	1	-13.25	0.965936329		
Active set	***Fructose coefficient***		***Steam coefficient***						
C1	1		1						
Year	***Fructose price***		***Steam price***						
1	0.7		26.5						
2	0.7		26.5						
3	0.7		26.5						
4	0.7		26.5						
5	0.7		26.5						
6	0.7		26.5						
7	0.7		26.5						
8	0.7		26.5						
9	0.7		26.5						
10	0.7		26.5						
11	0.7		26.5						
12	0.7		26.5						
13	0.7		26.5						
14	0.7		26.5						
15	0.7		26.5						
16	0.7		26.5						
17	0.7		26.5						
18	0.7		26.5						
19	0.7		26.5						
20	0.7		26.5						

Figure D.5: Cost scenario database tab of the process design model.

Solvent scenario database

The solvent scenario tab (Figure D.6) is used to enter new solvent scenarios. The active set is displayed. Furthermore, base distribution coefficients (no anti-solvent present), determined experimentally by Saidah Altway are found on this tab.

Base Values									
	0.3	***0.4***	***0.5***	***0.6***	***0.7***				
x=0	0.001	0.001	0.001	0.001	0.001				
x=1	2.2	1.9	1.7	1.5	1.4				
Scenario ID	***Full Descriptor***	***Short Descriptor***	***0.3***	***0.4***	***0.5***	***0.6***	***0.7***	***Active***	***Index***
S1	Linear	Lin1	0.66	0.76	0.85	0.90	0.98	No	0
S2	Exponential	Exp1	0.01	0.02	0.04	0.08	0.16	Yes	9
S3	Average of linear and exponential	Mean1	0.33	0.39	0.45	0.49	0.57	No	9
S4	Break-even kinetic model	Break1	0.01	0.05	0.08	0.11	0.14	No	9
S5	Break-even RE model	Break2	0.00	0.03	0.06	0.10	0.13	No	9
S6	Zero heptane solubilty	Zero1	0.00	0.00	0.00	0.00	0.00	No	9
S7	Random	Rand1	0.36	0.43	0.52	0.57	0.65	No	9
S8	Random	Rand2	0.24	0.26	0.33	0.37	0.45	No	9
S9	Random	Rand3	0.37	0.40	0.49	0.53	0.61	No	9
S10	Random	Rand4	0.13	0.16	0.25	0.29	0.37	No	9
Active Set									
X									
0.3	0.010								
0.4	0.020								
0.5	0.041								
0.6	0.080								
0.7	0.159								

Figure D.6: Solvent scenario database tab of the process design model.

Material data

In the material data tab (Figure D.7), all key data needed for calculations, are stored. If a new solvent or anti-solvent would be added in the future, key data would need to be entered here.

	MW	**Cp**	**Hvap**	**Density**
	g/mol	***kJ/kg.K***	***kJ/kg***	***kg/m3***
Fructose	180.2			
HMF	126.1			
Heptane	100.2	2.24	320	684
Water	18.0	4.18	2257	997
MIBK	100.2	2.12	405	802
TBP	266.3	1.40	308	973

Figure D.7: Material data tab of the process design model.

Reference sheet

The final tab of the model is used to store references. New references can be added by inserting them at the bottom of the list, with a corresponding reference ID.